

DEVELOPMENT AND APPLICATION OF A
MICROCOMPUTER BASED DATA ACQUISITION
SYSTEM FOR AN ION CYCLOTRON RESONANCE
MASS SPECTROMETER

BY

THOMAS JAMES BUCKLEY

A DISSERTATION PRESENTED TO THE GRADUATE COUNCIL
OF THE UNIVERSITY OF FLORIDA IN
PARTIAL FULFILLMENT OF THE REQUIREMENTS
FOR THE DEGREE OF DOCTOR OF PHILOSOPHY

UNIVERSITY OF FLORIDA

1982

To
mom and dad

ACKNOWLEDGMENTS

The feats accomplished in graduate school are not done by one alone. It is only with the help of others that problems are solved and the journey becomes bearable. I give thanks to my research director John R. Eyler for his continuing encouragement, guidance, and friendship. I greatly appreciate Bob Doyle for his cheerful humor and insights into the art of analog electronics. I am indebted to Lee Morgenthaler and Ron Daubach for their help in familiarizing me with the lab and life as a graduate student. For his help in taming the computers, I wish good luck to Doni Grande during his adventures in graduate school.

Many thanks go to the guys who know how, the electronics shop: Russ Pierce, Steve Miles, Walt Johnston, Bud and Bill Crosby, Mel Courtney, Bill Axson, and Jim Chamblee; the machine shops: Ed Whitehead, Chester Eastman, Art Grant, and Dailey Burch; the storeroom: Morris Mixon and Floyd Goar; and Rudy Strohschein of the glass shop. I am deeply indebted to the ladies who keep the place running: Joanne Bratcher, Wanda Douglas, Julia Bolden, Jeanne Karably, Mildred Neal, Jill Rench, and Carol Drum.

I would like to acknowledge Dawit Teclemariam for his help in obtaining the methyl iodide and trifluoromethyl iodide results and Dr. Robert Hanrahan for his assistance in interpreting them. I give my thanks to Pierre Ausloos and Sharon Lias for the use of the facilities at the National Bureau of Standards and their lessons in ion chemistry.

To all the Piss Ants and FOPA's, I'll miss everyone of you. A special thanks goes to my constant companion and inspiration, Andrea Fladager, for her help in preparing this manuscript and maintaining my sanity. And to the rest of those too numerous to mention, thanks for everything.

TABLE OF CONTENTS

CHAPTER		PAGE
	ACKNOWLEDGMENTS.....	iii
	KEY TO IMPORTANT ABBREVIATIONS.....	vii
	ABSTRACT.....	viii
1	INTRODUCTION.....	1
	Development of ICR Spectrometry.....	1
	Computers.....	5
	Preview of Chapters to Follow.....	6
2	THEORY.....	8
	Ion Motion.....	8
	Ion Detection.....	11
	Signal and Noise.....	15
	Ion Kinetics.....	18
3	SYSTEM HARDWARE.....	20
	Introduction.....	20
	Single Microcomputer System.....	20
	Dual Microcomputer system.....	24
4	SOFTWARE.....	56
	Introduction.....	56
	Program Initialization.....	56
	Functional Description of Program.....	57
	Data Analysis.....	71
5	INSTRUMENT CALIBRATION.....	72
	Introduction.....	72
	Experimental.....	74
	Results.....	75
	Discussion.....	79
	Conclusion.....	84

6	$C_5H_5^+$ ION STUDIES.....	85
	Introduction.....	85
	Experimental.....	87
	Results.....	89
	Discussion.....	89
	Conclusion.....	96
7	ION CHEMISTRY OF CH_3I and CF_3I	97
	Introduction.....	97
	Experimental.....	98
	Results.....	99
	Discussion.....	102
	Conclusion.....	109

APPENDICIES

A	BASIC PROGRAM.....	110
B	ASSEMBLY LANGUAGE PROGRAMS.....	120
	Apple Program.....	120
	KIM Programs.....	126
	REFERENCES.....	140
	BIOGRAPHICAL SKETCH.....	147

KEY TO IMPORTANT ABBREVIATIONS

A/D	- Analog to digital converter.
BCD	- Binary coded decimal.
CPU	- Central processing unit.
D/A	- Digital to analog converter.
fticr	- Fourier transform ion cyclotron resonance mass spectrometer.
icr	- Ion cyclotron resonance mass spectrometer.
I/O	- Computer input and output.
I.P.	- Ionization potential.
IRQ	- Processor maskable interrupt request.
m.o.	- Marginal oscillator.
NMI	- Processor non-maskable interrupt request.
PCAH	- Polycyclic aromatic hydrocarbon.
PIA	- Peripheral interface adapter.
RAM	- Random access memory.
r.f.	- Radio frequency radiation.
ROM	- Read only memory.

Abstract of Dissertation Presented to the Graduate Council
of the University of Florida in Partial Fulfillment of the
Requirements for the Degree of Doctor of Philosophy

DEVELOPMENT AND APPLICATION OF A
MICROCOMPUTER BASED DATA ACQUISITION
SYSTEM FOR AN ION CYCLOTRON RESONANCE
MASS SPECTROMETER

By

THOMAS JAMES BUCKLEY

December 1982

Chairman: Dr. John R. Eyler
Major Department: Chemistry

A dual microcomputer based data acquisition system for an ion cyclotron resonance mass spectrometer with a marginal oscillator detector is described. The system uses an Apple II microcomputer acting as the master processor and a KIM-1 microcomputer serving as the slave. The two microcomputers communicate through a common S-100 bus and its control logic. A unique experiment interface panel, accessible by either microcomputer, is also described. The hardware and software for this system is presented and discussed in detail. A single microcomputer system based on an Apple II microcomputer controlling a capacitance bridge detector is also presented.

The dual microcomputer system was used to study the ion chemistry of CH_3I , CF_3I , and a mixture of the two. In the pure CH_3I experiments,

reactions of the electron impact fragments, I^+ and CH_3^+ , with the neutral parent molecule occurred at the collision rate. Experiments with CF_3I showed reactions of the fragment ions, I^+ and CF_3^+ , occur at rates slower than the corresponding reactions in the CH_3I system. Reactions of CF_3I^+ with the neutral parent lead to $CF_3ICF_3^+$, $CF_3I_2^+$, and $(CF_3I)_2^+$. The observed reactions in a mixture of CF_3I and CH_3I indicate charge transfer reactions dominate the reaction chemistry. Ionic species containing hydrogen and fluorine were not seen; however, neutral cross products are speculated. These experiments demonstrated the effective use of a marginal oscillator detector at high masses ($m/e > 300$).

The single microcomputer system was used to study two isomers of $C_5H_5^+$. Rate constants for the more reactive of the two isomers were determined for reactions with diacetylene, norbornadiene, styrene, and other molecules. Some product ions observed from these reactions have been reported in sooting flames. The less reactive of the two isomers was investigated with respect to its thermochemistry. The proton affinity of the C_5H_4 neutral forming this ion was experimentally determined to be 227.9 kcal/mole. The reactive isomer is most likely a linear structure, while the unreactive is a cyclopropenyl cation with an ethylene side chain.

CHAPTER 1 INTRODUCTION

Ion cyclotron resonance (icr) mass spectrometry began its useful life as a tool for use by the physical chemist in studying ion-molecule reactions. Due to the limited resolution and mass range of earlier instruments its use by the analytical chemist was not widespread. However, following significant advances in detection theory, electronics, and digital computers, the use of this instrument is expanding rapidly. The following text describes the development of the instrument to the present, examines the role of computers in instrumentation, and introduces the chapters to follow.

Development of ICR Spectrometry

Work in icr mass spectrometry has been extensive enough to warrant the publication of a few reviews on the subject. A comprehensive survey of the work in the field up to 1973 has been presented by Hartmann [1], while Wanczek recently reviewed the instrumentation and theory from then to the present [2]. In 1971 Beauchamp presented a description of the applications of icr spectrometry to physical chemistry [3]. These applications include determination of ion-molecule collision frequencies, reaction rate constants, reaction pathways and product distributions, energy dependence of rate constants, and thermochemical properties such as gas phase acidities and proton affinities. Most of the chemical studies to date using icr spectrometry involve one or more of these areas.

Earlier versions of the icr spectrometer involved a drift cell with three regions (ion source, analyzer, and ion collector) for ion monitoring. An illustration of the cell and an explanation of how it worked has been given by Beauchamp [3]. The cell required constant production and detection of the ions as they drifted from the source to the ion collector. Ions absorbed energy from a radio frequency (r.f.) field causing the resonant ion to collide with one of the cell walls where the resulting ion current was measured as in the original omegatron [4]. The highest performance, however, is expected from a detector which does not eject resonant ions from the ion cell [5].

The use of a r.f. detector which monitored the power absorbed by resonant ions without removing them from the cell improved performance [6]. The operation of the icr was further enhanced by use of modulation techniques which varied one of the parameters affecting power absorption. This allowed phase sensitive detectors, monitoring the modulation frequency, to improve the signal to noise ratio. Types of modulation included pulsing electron energy above and below the ionization potential of the ion [7] and pulsing the electron current by controlling the grid of a triode gun, thus changing the ion population itself [8]. Other techniques involved the changing of the cyclotron frequency of the ion by pulsing the trapping potential [9] or magnetic field [10].

Maximum resolution for the drift cell is still limited, however, by the residence time of the ion in the analyzer region. This problem was solved by the longer residence times made possible by trapped ion cells [11]. The original application of this cell generated ions by a pulsed electron beam, then probed them some time later by pulsed magnetic field

modulation while detecting their power absorption with a marginal oscillator detector. In the mode of operation commonly used with these cells, the ions are probed by a pulsed r.f. detector. A more detailed explanation of the behavior of ions in a trapped ion cell is given in Chapter 2.

After detection, a quench pulse, collapsing one of the trapping potentials, cleared the cell of all ions before the next pulse cycle. Recent developments have used the unquenched mode of operation where a steady state abundance of ions, formed by continuous electron impact and lost by wall collisions, makes possible the study of slow equilibrium reactions [12]. The trapped ion cell and pulsed operation allowed better definition of reaction time. As before, the ion signal was modulated by pulsing the trapping potentials [13], but eventually this gave way to a pulsed marginal oscillator (m.o.) detector [14].

The marginal oscillator is a tuned detector; thus only one ion can be seen at a time. Mass sweeps are usually accomplished by a slow magnetic field scan which brings the ions into resonance at the frequency of the m.o. detector. Broad band detector circuits capable of fast frequency sweeps and simultaneous observation of many ions eventually were constructed.

One type of broad band detection scheme which evolved from the trapped ion cell, pulsed timing techniques, and digital computers is Fourier transform ionic Fourier transform (fticr). The principle of extracting frequency domain spectra from time domain signals has long been understood, but it wasn't until the development the fast Fourier transform algorithm by Cooley and Tukey that such routine analysis became practical [15]. Analogies and similarities in instrumentation and theory between fticr

and Fourier transform nuclear magnetic resonance have been noted [16]. Data systems for the later and some specialized electronics led to the development of the first fticr [17].

Since the introduction of fticr, theories of its operation and limitations have flourished. The effects of digitizing errors and truncation of the free induction decay have been examined [18], and problems with peak height errors have been corrected by zero filling of the digitized transient [19] and by accounting for excitation level differences produced by frequency swept excitation [20]. Convolution based techniques for phase correcting the calculated frequency domain spectra of fticr signals have been proposed [21] and verified in experiments [22]. The line shapes at low pressures have also been expressed mathematically [23].

Mass resolution, which has always been a limitation of icr spectrometry in the past, can reach 95 percent of its optimal value in fticr experiments by acquiring data during the first three half lives of a transient signal [24]. The maximum resolution of fticr experiments can be made arbitrarily high by going to arbitrarily low pressures [21]. The highest recorded resolution using a 1.2 T conventional electromagnet is 760,000 for benzene (m/e 78) at about 5×10^{-9} torr [25]. Instruments using a 4.7 T superconducting magnet have trapped ions for up to 13.5 hours and obtained a resolution of 1,500,000 for m/e 166 at similar pressures [26].

Wilkins and Gross have surveyed the use of Fourier transform icr spectrometry as an analytical technique and attribute its advance in this field to its high resolution, high sensitivity, and sufficiently accurate mass measurement [27]. Using a three parameter empirical

formula, mass accuracies of a few parts per million have been obtained over limited mass ranges [28]. Ftior has been used as a detector for gas chromatography [29], chemical ionization [30], and to study fragments from collision induced dissociation [31].

Other broad band techniques surfaced after the invention of ftior. One such method, rapid scan icr, requires the use of a computer to digitize and analyse the transient signal obtained by sweeping across the frequencies of ions of interest [32]. The rapid scan and ftior spectrometers are close enough in performance to allow the functions of the former to be accomplished by the latter [33]. Another broad band detector, a capacitance bridge, provides the convenience of frequency sweep to obtain mass spectra but does not require the use of a computer to obtain spectra [34,35]. A similar technique had been introduced in 1965 by Wobshall but did not gain wide use until after the development of ftior [36].

Computers

The digital electronic computer has evolved over the years from a system made up of thousands of vacuum tubes, to thousands of discrete transistors, to a few silicon chips with as many as 100,000 transistors on a quarter inch square. With each new generation of computers came a decrease in size, an increase in reliability, an increase in operation speed, and a decrease in cost for the same amount of computing power. Due to the speed at which they could perform complex and tedious calculations, computers were initially used for data analysis. Later, they were used to perform experiments in real time where the events monitored were too fast to record by hand or too agonizingly slow to justify the use of one's valuable time. The computer is noted for the

speed with which it can perform operations, the precision at which it can reproduce its results, and its ability to remember and faithfully execute any task it has been taught without complaining or becoming bored. Its only problem is a tendency to be temperamental and do what one says rather than what one means.

The early years of computerized experiments were dominated by minicomputers based on discrete transistors. The development of medium and large scale integrated circuits has resulted in the microcomputer: a machine with sufficient power for most problems but at an affordable cost. The use of microcomputers in laboratory experiments is not new at the University of Florida. One instrument used a microcomputer for control and data acquisition of photoacoustic experiments [37], while our own lab has collected photodissociation data from our icr [38] and performed fticr experiments [39,40]. Even the fast kinetic technique of pulse radiolysis has been adapted to control by a microcomputer based system [41]. Microcomputers have also been used to control a quadrupole [42], magnetic sector [43], and spark gap mass spectrometers [44].

Preview of Chapters to Follow

More details about the theory of icr ion motion and detection, analysis of kinetic data, and signal to noise considerations are given in Chapter 2. The microcomputer systems designed by the author to perform icr experiments are described in Chapter 3 and 4. Chapter 3 furnishes information about the hardware assembled to acquire and process the icr data. Chapter 4 and the appendices supply operating instructions and a description of the software used to drive the hardware and perform data analysis.

Any new instrument used for scientific investigations must first prove itself before its results can be regarded as a true representation of the event being monitored. Unfortunately, for icr studies there is no a priori way to determine all the factors which relate the electrical response of the detector and measured pressure to the concentration of ions in the cell. By performing an experiment whose reaction rate is well known, however, the instrument can be corrected for various errors. The procedure used to verify the performance of the icr data system described in this work is given in Chapter 5.

The remaining two chapters deal with applications of the computer controlled icr to chemical problems. The $C_5H_5^+$ ion has been shown to have more than one isomer in the gas phase [45] as well as being an ion found in sooting flames. Chapter 6 demonstrates the use of a broad band icr detector in experiments designed to identify one of the $C_5H_5^+$ isomers and to measure the reaction rate of the other with various neutral species of potential importance in flame systems. Chapter 7 details the investigation of ionic processes in CH_3I , CF_3I , and a mixture of the two. These systems have been studied before in relation to their radiation chemistry and/or ion chemistry.

CHAPTER 2 THEORY

Ion Motion

An ion in crossed electric and magnetic fields, as in Figure 2.1, is governed by the Lorentz equation:

$$\vec{F} = q(\vec{E} + \vec{v} \times \vec{B})$$

where \vec{F} is the force exerted on the ion, q is the ion's charge, \vec{v} is its velocity, \times signifies the vector cross product, and \vec{E} and \vec{B} are the electric and magnetic field vectors, respectively [46]. The magnetic field causes the ion to move in a circular orbit in a plane perpendicular to the field with a characteristic angular frequency, ω_C ,

$$\omega_C = \frac{qB}{m} \quad (2.1)$$

for an ion of mass m . The electric field experienced by an ion in a trapped ion cell with flat rectangular sides (see Figure 2.1) has been numerically calculated to correspond closely to a three dimensional quadrupole field [46]. Experiments with hyperbolically shaped walls in an ion cell show little improvement over flat plates, thus confirming the validity of the quadrupole approximation for electric fields [5,47].

The ion oscillates back and forth between the two trapping plates at a frequency, ω_T , given by

$$\omega_T = \left[\frac{4q(V_T - V_0)}{ma^2} \right]^{1/2} \quad (2.2).$$

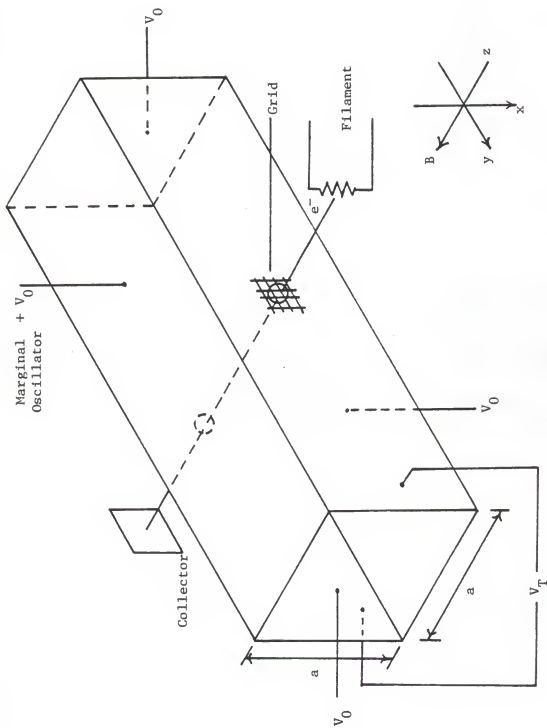


Figure 2.1. Basic diagram of the trapped ion icr cell showing the connections for the marginal oscillator, the ionizing electron source, and the various plate potentials (V 's).

Here, a is the distance between the plate pairs, and V_T and V_0 are the trapping and side plate potentials, respectively [46]. The observed cyclotron frequency of the ion, ω , is

$$\omega = (\omega_C^2 - \omega_T^2)^{1/2}$$

but since $\omega_T \ll \omega_C$ for practical experiments, $\omega = \omega_C$ to a first approximation. Even smaller frequency shifts, on the order of a part per million, due to Coriolis coupling of ion cyclotron motion to rotational degrees of freedom, have been postulated [48].

If the ion is probed by a radio frequency electric field in a plane perpendicular to the magnetic field, it can absorb energy from the field for frequencies near ω . The ions are accelerated to an average kinetic energy, T , of

$$T = \frac{(qEt)^2}{8m} + \frac{m}{2} v_0^2$$

where t is the duration of the r.f. pulse of amplitude E , and v_0 is the initial velocity of the ion [13]. The first term is the energy absorbed by the ion from the r.f. field, while the second term corresponds to the initial kinetic energy of the ion. Due to differences in the phase of the oscillation of various ions of the same charge to mass ratio a particular ion's kinetic energy may vary up to $\pm qEv_0 t/4$ [49].

As the ion accelerates, the size of its cyclotron orbit increases. The radius, r , of the orbit can be calculated from

$$r = \left[\frac{2T}{m\omega} \right]^{1/2}$$

The maximum orbital radius attainable is limited by the physical dimensions of the cell and is equal to one half the separation between the upper and lower plates.

Energy can also be imparted to the ions from a r.f. electric field applied to the trapping plates at a frequency given by Equation 2.2. This principle has been applied to obtain mass spectra from an icr and is used in the ejection of electrons from the cell when negative ions are being trapped [9].

Ion Detection

The motion of an ion has been modelled as a rotating electric monopole between the plates of the icr cell [50]. However, in icr experiments one does not deal with just one ion but rather a macroscopic ensemble of ions in which case the macroscopic rotating electric polarization must be considered. As the ions are excited their initial random phases are driven into coherence. This coherent packet of ions then induces an oscillating image current across the detector.

A generalized circuit diagram for icr detectors is shown in Figure 2.2A and applies for both tuned and broad band detectors. In a tuned circuit, the m.o. detector for example, a parallel tank circuit made up of a capacitor, inductor, and resistor are driven by a constant current source. This produces an instantaneous voltage change, $\Delta V(t)$, across the tank due to power absorption by the ions which is given by the expression

$$\Delta V(t) = \frac{Nq^2 E t R}{2md^2} \sin \omega t$$

where R is the value of the resistor, N is the total number of ions of mass m, and all other variables are as previously defined [51]. From the above expression one can see that the signal voltage is inversely proportional to the ion mass. Amano has shown by a different model that the signal induced in the detector by the motion of the ion is exactly

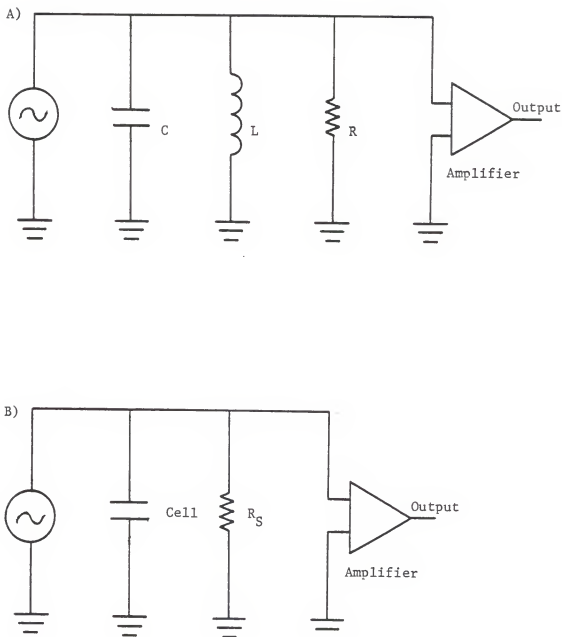


Figure 2.2. A) General circuit diagram for tuned and broad band icr detectors. A radio frequency oscillator drives a capacitor, inductor, and resistor. A change in the number of resonant ions in the icr cell causes a change in the amplified output signal. B) Circuit diagram for the parallel resistor model for icr power absorption detectors. Resonant ions cause a drop in the amplified output signal by shunting power to ground.

out of phase with the driving voltage. Thus the oscillation voltage across the tank decreases [52].

Another theory applied to conventional icr's which use power absorption detectors is illustrated in Figure 2.2B [50]. The power absorbed by the ions from the r.f. generator is modelled by a resistor which shunts the icr cell. When power absorption is not detected the shunt resistance is infinity. The m.o. detector has been modelled this way and yields the same detector response as predicted by the other theories.

Comisarow's rotating electric monopole theory yields two different cases for detectors of the type shown in Figure 2.2A. If the circuit is predominately resistive (or tuned) then the signal voltage behaves as in the m.o. detector: the voltage is inversely proportional to ion mass and in phase with the current; thus the ions absorb power. On the other hand if the detector is predominately capacitive, as in broad band detectors, then the signal voltage is independent of ion mass and the current leads the voltage by 90 degrees. Thus no power is lost in the capacitor, but only through the resistive components of the circuit. McIver et al. have also shown that the equations of motion for the ions are coupled to the circuit equations of the detector and therefore dependent upon the circuit used [53].

The resolving power, R_p , of a mass spectrometer is defined as the mass of the ion divided by the width of the ion signal, m , in terms of mass (commonly full width at half peak height) as shown in the following equation.

$$R_p = \frac{m}{\Delta m} \quad (2.3)$$

For icr spectrometers this quantity is numerically equal to the resolution defined in terms of frequency [23]. Thus for a particular ion mass the ultimate resolution is determined by the width of the mass peak.

At low pressures, the line shapes for trapped ion and drift cells using a m.o. detector are the same and are given by the expression

$$\Delta\omega_{50\%} = \frac{5.566}{T} \quad (2.4)$$

where $\Delta\omega_{50\%}$ is the line width in terms of frequency and T is the data acquisition time in seconds [23]. When using MKS units the resolution is equal to

$$\frac{m}{\Delta m} = \frac{qBT}{5.566m}$$

Fourier transform icr's have a somewhat narrower line width which is given by the expression

$$\Delta\omega_{50\%} = \frac{3.971}{T} \quad (2.5).$$

Even though equations 2.4 and 2.5 differ by only a factor of 1.5, the data acquisition period for the m.o detector is on the order of a few milliseconds, while the fticr detector can acquire data for hundreds of milliseconds, thus greatly increasing the resolution attainable by fticr

High pressures in the icr cell cause the mass peaks to broaden due to collisions. The effect of this pressure broadening takes the same form in drift and trapped ion cells as it does in the fticr experiment and has been expressed analytically [24]. When the collisions are nonreactive then the peaks have a Lorentzian distribution with the half line width at half peak height equal to the elastic collision frequency

[49]. Even when reactive collisions are taking place the ion signals are still Lorentzian but the expression for the peak width is more complicated.

Signal and Noise

While attempting to monitor the signal from the detector one must always contend with the noise that comes with it. Malmstadt et al. have discussed the sources of noise found in any detection circuit [54]. Some sources of noise are inherent characteristics of the electronic components used while others are picked up from the environment, and are therefore avoidable. Johnson, or thermal, noise is produced by random motion of electrons in resistive elements of the circuit. It can be reduced by using lower value resistors wherever possible or by lowering the operating temperature of the circuit. Thermal noise is totally absent at zero Kelvin, but this is hardly a practical operating condition. Random motion of electrons across a junction is called shot noise, produced at junctions of gates in transistors and such is a problem one must live with; at electrical contacts like solder joints, it is a problem which can be reduced by good soldering technique.

Excess noise is considered to be anything above and beyond that of Johnson and shot. There are two classes of this, the first being interference noise. Included here are 60 Hz and harmonics from power supplies and power cords, and radio frequency interference from electric motors, switches, and local broadcast stations. The second is flicker noise, usually referred to as drift. It can be caused by power supply voltage fluctuations, changes in component values, or temperature drifts. Flicker noise is partially due to natural aging of components while other sources can be reduced by placing the electronics in a stable environment.

One final source of noise, quantizing noise, is introduced when one attempts to quantify the analog output of the detector. The magnitude of this noise is dependent upon the instruments used and eyesight of the investigator when quantification is done by hand from a plot of the data. When the data are digitized by an analog to digital converter the finite resolution of the A/D defines the amount of digitizing noise which can be quantified as $\pm 1/2$ bit. Often the analog signal from the detector is such that quantizing noise is insignificant relative to other noises.

If the sources of noise are random and independent of each other the noise adds quadratically. If not, then cross terms must be included when calculating the total noise present.

The signal to noise ratio of icr signals has been given much attention since the development of fticr. Marshall has shown that S/N in fticr is improved for short data acquisition times; however, resolution is enhanced by long times [16]. White et al. have shown the simultaneous increase in S/N and resolution resulting from a reduction in collisions as the pressure is decreased [25].

In icr signal modeling the only source of noise which has been included in S/N calculations is thermal noise. Comisarow has derived an expression for the S/N for RC parallel circuit icr detectors as being

$$\frac{S}{N} = \frac{Nq^2 rBR^{1/2}}{2ma \sqrt{2k_B T \Delta f}}$$

where T is the temperature of resistor R, Δf is the detection bandwidth, k_B is the Boltzmann constant, and all other variables are as previously defined [50]. If two ions of different masses are detected under the same conditions except resonance frequency (but the same

magnetic field strength), then the relative signal to noise ratio is

$$\frac{(S/N)_2}{(S/N)_1} = \frac{m_1}{m_2} \quad (2.6).$$

Thus, if one doubles the mass of the ion being investigated, the S/N drops by a factor of two relative to the lighter ion. This illustrates the difficulty of monitoring heavy ions in an icr.

One need not abandon all hope for studying heavy ions if one has access to a computer. In this case signal averaging may be performed to increase the signal to noise ratio. However, there are certain requirements which must be satisfied for accurate averaging [55]. These requirements are:

1. It must be possible to take repetitive scans such that exactly the same regions of the transient signal are being scanned.
2. Data must be acquired at a fixed sample time interval and initiated by a trigger pulse to insure that the information goes into the same channel as in previous scans.
3. The signal must have only random noise centered around zero volts.
4. The analog to digital converter must represent zero volts as zero counts or be corrected in software.

If these conditions are met then the signal, S , grows linearly with the number of scans, N_0 .

$$S = k_S N_0$$

If the noise, N , is random, with no coherent contributions, then its growth is proportional to the square root of the number of scans.

$$N = k_N N_0^{1/2}$$

This leads to a signal to noise ratio given by

$$\frac{S}{N} = \frac{k_S}{k_N} N_0^{1/2}$$

where the above k's are constants of proportionality.

The conditions mentioned above can easily be accomplished by a computer controlled icr. Thus one can obtain a signal to noise enhancement which is proportional to the square root of the number of averaged passes.

Ion Kinetics

Experimental conditions in an icr spectrometer are such that the concentration of the ions is orders of magnitude less than the concentration of the neutral gas. Thus when the ions are reacting with the neutral gas the observed ion decay signal follows pseudo-first order kinetics. In this case the intensity, I , of the ion at any time, t , is given by the expression

$$I = I_0 e^{-kt}$$

where I_0 is the initial intensity at time zero and k is the ion decay rate. Since the intensity follows an exponential decay, one way the rate can be determined is to plot the natural logarithm of the ion intensity versus time. The plot will give a straight line with a slope of $-k$. Another means of determining the decay rate is to calculate the natural logarithm of I/I_0 for various point pairs where I_0 is now any concentration taken at a time, Δt , before I . The decay rate for this method is given by

$$-k = \frac{1}{\Delta t} \ln \left[\frac{I}{I_0} \right]$$

The decay rates from above are converted to a rate constant by dividing by the neutral gas density. The very low gas pressures allow use of the ideal gas law for this as follows:

$$\frac{n}{V} = \frac{PN_A}{RT}$$

where n/V is the gas density, P is its pressure, R the gas constant, T the absolute temperature, and N_A is Avagadro's number. If the pressure is in torr, T is in Kelvin, and R is in $\text{cm}^3 \cdot \text{torr} / \text{K} \cdot \text{mole}$, then the resulting density is in molecules per cm^3 . Dividing the decay rate by the gas density gives the reaction rate constant in units of $\text{cm}^3 / \text{molecule} \cdot \text{sec}$.

The two methods outlined above for determining the reaction rate constant give slightly different values in practical use. The slope from the semilog plot is usually calculated by a linear regression routine for the best straight line fit through the noisy data. The ratio method is usually repeated for several point pairs separated by a constant interval of time, with the results then averaged. The first method is not sensitive to the order of the noise in the data while the second one is. This accounts for the slightly different values obtained when using the two methods on the same data. The use of linear regression calculations is preferred and gives better results.

CHAPTER 3 SYSTEM HARDWARE

Introduction

Two microcomputer controlled data acquisition systems are described in this chapter. The first to be presented is a single microcomputer setup designed for the National Bureau of Standards (NBS) and used for the $C_5H_5^+$ studies described in Chapter 6. Then a dual microcomputer system, used for the $CH_3I + CF_3I$ experiments described in Chapter 7, and a special experiment interface are discussed in detail. These two microcomputer systems were designed with the idea of future expansion in mind; therefore, comments concerning expansion capabilities will be made when appropriate.

Single Microcomputer System

A microcomputer based data acquisition and analysis system for an existing ion mass spectrometer [56] with a new capacitance bridge detector (CBD) [34] was installed at the National Bureau of Standards by the author. The microcomputer system is based upon a single Apple II (Apple) [57], which utilizes mainly commercial peripherals and controllers, and carries out basic experimental control and data acquisition functions similar to the dual microcomputer system described later in this chapter. Due to the unique nature of the instrument, however, a few special interfaces were built to couple the computer with the mass spectrometer. The Apple-based system was chosen due to past proven performance, completeness of documentation, and low cost.

The microcomputer system, shown in Figure 3.1, is intended primarily for use as a pulsed ion mass spectrometer controller. A 12 inch color monitor provides video display and graphics while expansion of the basic computer performance is furnished by the peripheral connector slots on the microcomputer's motherboard. The software is designed with the understanding that several boards must be in certain slots. A list of the slots and cards expected by the software along with the function performed is given in the following paragraphs.

Slot 1. Mountain Computer's CPS Multifunction Card [58] provides a parallel port for driving a dot matrix printer. The printer supplies hardcopy of experiment parameters and spectra while a 24 hour clock/calender, with battery backup, aids in data logging. A serial port is still available for future endeavors.

Slot 3. Interactive Microware's ADALAB [59] provides an A/D and parallel port for use in the experiment. The 12-bit plus sign A/D digitizes the CBD output while one 8-bit parallel port delivers the detector's pulse sequence. An unused 12-bit plus sign D/A and one 8-bit parallel port are available for expansion.

Slot 4. Solid State Music's IEEE-488 [60] controller communicates with devices which interface through an IEEE-488 bus. Presently it controls a frequency synthesizer [61] which supplies the CBD's ω_1 resonance frequency. The board is capable of controlling up to 16 different devices through one cable.

Slot 6. Apple II disk drive controller with two floppy disk drives for use in system initialization and mass storage of programs and data files.

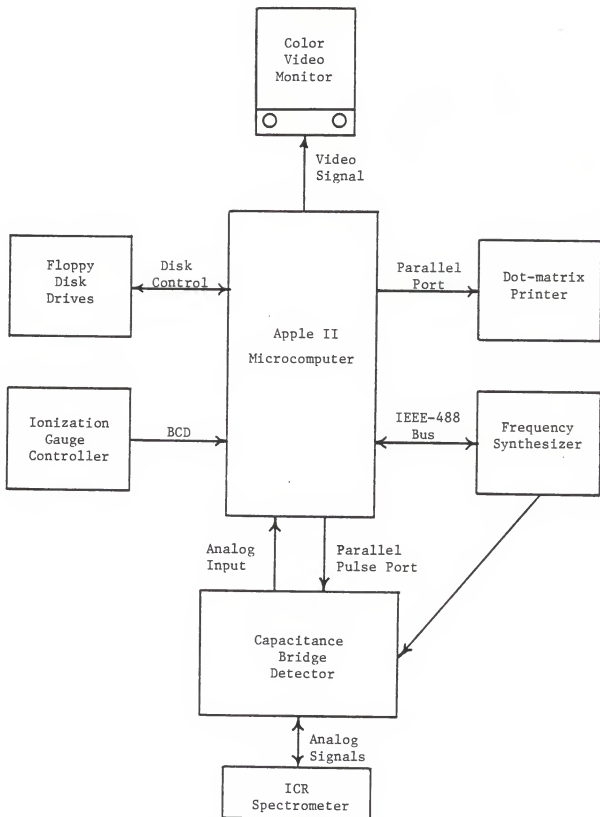


Figure 3.1. Block diagram of the single microcomputer controlled ICR spectrometer at the National Bureau of Standards.

Slot 7. Contains the custom made spectrometer interface for driving the parallel port to the CBD and for accepting binary coded decimal input from an ionization gauge controller. This card is the only component of the data system which is not commercially available.

Not required by the software but available for future development is a 16 K RAM card in slot 0 [62]. This expands the Apple's memory to 64 K of RAM and allows use of languages other than floating point BASIC such as INTEGER BASIC and PASCAL. Two remaining slots, 2 and 5, are unoccupied and can be used for additional devices.

The program for running the system is similar to that described in the next chapter. Modifications to the program take advantage of the synthesizer's frequency sweep capability for obtaining mass spectra and determining product ions through double resonance experiments. Other software changes manipulate the distinct hardware, correct for clock frequency differences, and compensate for single processor control. The use of a single microcomputer requires that it performs all tasks needed to run an experiment. Since it can only perform one task at a time, e.g. pulse the detector or analyze the data, all tasks must be stopped periodically. The output from pulsed detectors, however, have a tendency to drift when they are not being pulsed and must be corrected in software. Surely, a dual or multi-processor system could overcome this problem.

Dual Microcomputer System

The microcomputer system designed for our laboratory evolved through time from a single KIM-1 microcomputer [63] and KIMSI S-100 bus [64] to a dual microcomputer system with numerous peripherals. The complexity of the system was governed by the most difficult experiment it was to perform: Fourier transform mass spectrometry. Our earlier experiments and hardware have been reported earlier [39,40]. Later, the earlier computer system was renovated to a general data acquisition and control instrument capable of several different experiments by modifying the software and changing a few connectors.

A block diagram of the system in its latest configuration for controlling a marginal oscillator detector is shown in Figure 3.2. The earlier spectrometer is the same used by an earlier colleague but modified for computer control [38]. Two microcomputers are arranged in a master-slave configuration with an Apple acting as the master and a KIM serving as the slave. The master microcomputer is responsible for interaction with the user, program development (for both itself and the KIM), graphics, storage of programs and data on disk, and data analysis. The slave microcomputer performs the routine tasks needed to run the earlier experiment. These include system initialization, pulse generation, signal averaging, and system status display. Both microcomputer systems have 6502 microprocessors as their central processing units (CPU's), thus allowing the machine code from one to run on the other.

Communication between the master and the slave is accomplished through a common S-100 bus and its control logic. The Apple microcomputer, being the source of commands, determines the use of the

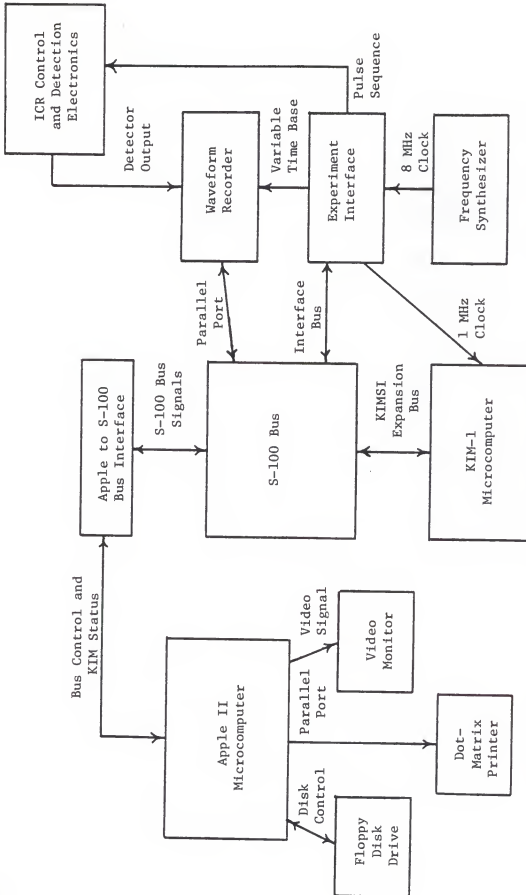


Figure 3.2. Block diagram of a dual microcomputer based control and data acquisition system for an ICR spectrometer.

S-100 bus and halts instruction execution of the KIM when the bus is desired. All data and programs which pass between the two microcomputers are placed in the common 8 K memory block on the S-100 bus. A waveform recorder [65] for fast analog to digital conversion, an experiment interface with analog and digital I/O, and a frequency synthesizer [66] for the system clock and sine wave generation are accessible through the S-100 bus. All components on the S-100 bus, except for non-common memory, and the experiment interface can be used by either processor.

Apple Microcomputer System

The Apple microcomputer used for this system is one of the earlier versions which has a set of memory select headers on the motherboard, otherwise it is the same as the Apple described for the single microcomputer system. A 9 inch black and white TV monitor serves for video display and graphics. In the peripheral slots are the 16 K RAM memory card (slot 0), the multifunction card (slot 1), and the disk drive controller with one floppy disk drive (slot 6), all functioning as previously described. A fast floating point processor board in slot 2 contains the hardware necessary for speeding up the calculation of the transcendental functions called from the languages APPLEFAST 3.3 or PASCAL [67]. The appropriate software must be loaded into the 16 K RAM card before the fast functions can be used. Interfacing with the S-100 bus and ier spectrometer is accomplished through custom logic built on a prototype card in slot 5. Slots 3, 4, and 7 are unoccupied and ready for expansion.

To the microcomputers the world appears as a series of unique addresses, each of which allows access to a particular device or memory

location. Addresses of interest to a programmer, which deal with the custom logic of this system, are shown in Tables 3.1 and 3.2. All addresses and numbers used in this section are in hexadecimal. The Apple addresses listed are determined by the peripheral slot occupied by the custom interface. The DEV address in Table 3.1 for slot 5 is CODX, where the X corresponds to a number from 0 to F. The S-100 addresses in Table 3.2 all begin with an I/O page number. For the Apple using slot 5 the first byte of the address, often referred to as the page number, is C5 while the KIM sees the devices in page F0. This difference is due to the way the I/O page is decoded by the Apple and KIMS1 and must be taken into account when using code written for one microcomputer on the other.

Note that a read or write instruction to a particular address may control two different devices. Write devices are those which accept information from the CPU, such as D/A's and parallel output ports, and are activated by a write instruction. A read device is one which sends information to the CPU, an A/D or parallel input port for examples. The addresses marked as "unused" are decoded by the hardware but not assigned to any particular device. These addresses are ready to aid in any future expansion. Addresses marked as "not available" have not been fully decoded and will require extra logic for expansion.

Access to these addressed devices can be achieved through BASIC, machine language, or the Apple monitor. To send a reset command to the KIM's CPU one would execute the read instruction "PEEK 49362" from BASIC or "LDA \$COD2" from assembly language. Typing "COD0" followed by a carriage return into the Apple monitor will also initiate the above function. Writing to the same address, though, will execute a different command, namely request the S-100 memory. The Apple may send a trigger

Table 3.1. Interface device address map for the Apple . All addresses are in hexadecimal. "Unused" signifies the address is decoded but not in use. "Not available" designates an address which has not been totally decoded.

<u>Apple Address</u>	<u>Read Device</u>	<u>Write Device</u>
(DEV)0	Interface status	S-100 request
1	KIM status	S-100 release
2	KIM reset	S-100 memory request
3	KIM NMI	S-100 memory disable
4	Unused	Enable interface reset
5	Unused	Disable interface reset
6	Unused	Apple memory request
7	Unused	Apple memory disable
8	Unused	Not available
9	Unused	Not available
A	Unused	Not available
B	Unused	Not available
C	Unused	Not available
D	Unused	Not available
E	Unused	Not available
F	Unused	Not available

Table 3.2. Interface device address map for the S-100 bus. All addresses are in hexadecimal. "Unused" signifies the address is decoded but not in use. "Not available" designates an address which has not been totally decoded.

<u>S-100 Address</u>	<u>Read Device</u>	<u>Write Device</u>
(I/O)00	Serial Port A Control	Serial Port A Status
01	Serial Port A Data In	Serial Port A Data Out
02	Serial Port B Control	Serial Port B Status
03	Serial Port B Data In	Serial Port B Data Out
04	Biomatic Data	Biomatic Control
05	Biomatic Status	Parallel Port B
10	Open relay	X-D/A output
11	Close relay	Y-D/A output
12	Reset clock	High clock byte
13	A/D input	Low clock byte
14	Unused	Trigger A
15	Unused	Trigger B
16	Unused	Unused
17	Unused	Unused
18	Not available	Unused
19	Not available	Unused
1A	Not available	Unused
1B	Not available	Unused
1C	Not available	Unused
1D	Not available	Unused
1E	Not available	Unused
1F	Not available	KIM status port
20	PIA-1A data/direction	PIA-1A data/direction
21	PIA-1A control	PIA-1A control
22	PIA-1B data/direction	PIA-1B data/direction
23	PIA-1B control	PIA-1B control
24	PIA-2A data/direction	PIA-2A data/direction
25	PIA-2A control	PIA-2A control
26	PIA-2B data/direction	PIA-2B data/direction
27	PIA-2B control	PIA-2B control
28	PIA-3A data/direction	PIA-3A data/direction
29	PIA-3A control	PIA-3A control
2A	PIA-3B data/direction	PIA-3B data/direction
2B	PIA-3B control	PIA-3B control

pulse (see Table 3.2) out the experiment interface panel (Trigger A) by the write instruction "POKE 50452,0" from BASIC, "STA \$C514" from assembly language, or "C514:0" from the Apple monitor. The KIM can send the same trigger pulse by "STA \$F014" from assembly language only. The Apple or KIM must have control of the S-100 bus before the addresses in Table 3.2 can be used by the corresponding microcomputer. More detail on the function and use of the devices in the tables follows in the remainder of this chapter, Chapter 4, and the appendices.

The Apple to S-100 control logic shown in Figure 3.3 is mounted on a hobby/prototyping board. All Apple interface functions and addresses in Table 3.1 are generated by this board. The eight write activated devices are decoded by the 74LS138. Since the Apple uses the device select line, \overline{DEVS} , the board may be operated from any slot to generate a 500 nsec active low pulse on the appropriate line. Writing to the S-100 request address, DEV0, pulses the $\overline{S1R}$ line. This activates the S-100 bus for use by the Apple and places the KIM's processor in a hold state. Writing to the S-100 release address, DEV1, pulses the $\overline{S1D}$ line causing the S-100 bus to return to the KIM's control and restarts the processor where it stopped.

The Apple and S-100 bus have a common 8 K of RAM addresses from A000 to BFFF. Two memories exist in this area, one in the Apple's dynamic RAM and the other in the S-100's static RAM. The active memory is selected by writing to the memory request and disable addresses. Disabling the Apple 8 K memory leaves the microcomputer with 40 K of RAM and sets the Apple memory enable line, AME, to a logical zero. The S-100 memory enable line, S1ME, goes to a logical one when the Apple is using the S-100 memory; however, the S-100 bus must be requested before the memory is available.

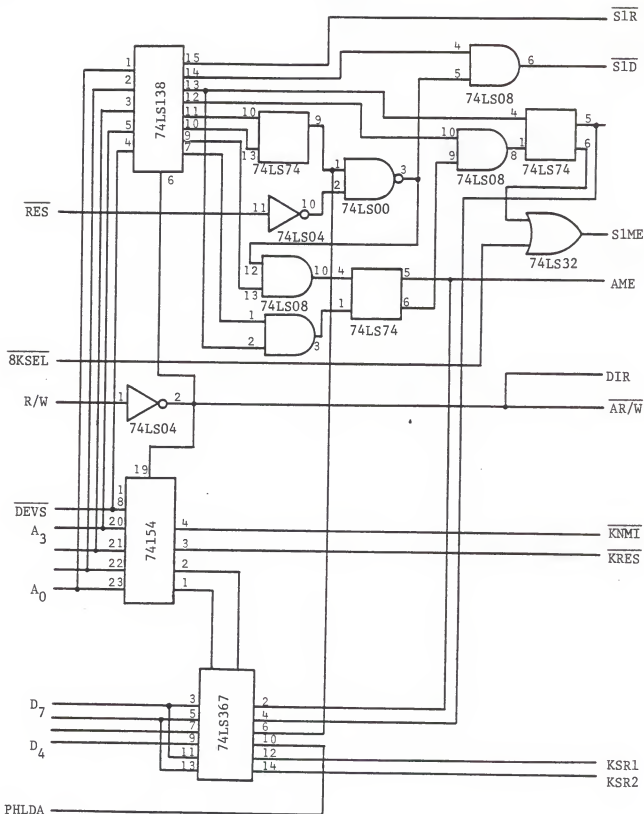


Figure 3.3. Schematic diagram of the Apple to S-100 control logic for device address decoding and status ports.

Both memories may be disabled from use by the Apple but a network of flip-flops, AND, and NAND gates prevents both memories from being used at the same time. This logic also causes one memory to be released if the other is requested.

Writing to the enable and disable interface addresses DEV4 and DEV5 allows the selection of the interface reset feature. When the reset is enabled, pressing the reset key on the Apple keyboard will force the interface to a configuration where the S-100 memory and bus is released and the Apple 8 K memory is activated. Disabling the feature lets the Apple reset itself without changing the configuration of the interface hardware. This is very useful when debugging software in the S-100 memory from the Apple.

A 74154, 4 to 16 line decoder, generates the read activated device addresses. Two of the addresses cause a reset and non-maskable interrupt (NMI) request to be sent to the KIM. These addresses function the same as if someone pushed the corresponding buttons on the KIM. The interface status and KIM status ports are supplied by the 74LS367 hex tristate driver chip. The interface status port tells the configuration of the Apple to S-100 interface through the four most significant bits of the port. Bit 7 represents the Apple 8 K memory status and is a one when the Apple has 48 K of RAM and a zero when there is only 40 K of Apple memory. Bit 6 is a one when the S-100 memory is requested; a zero when it is not. Bit 5 indicates the state of the reset feature and is a one when it is activated. Bit 4 monitors the S-100's processor hold available line, PHLDA, and is a one when the bus is ready for use by the Apple. The four least significant bits of the port are not connected and have no meaning.

The 8 K bytes of memory which overlap between the Apple and S-100 systems are decoded by the logic in Figure 3.4. The three most significant bits of the 16-bit address bus are decoded for the range A000 to BFFF. This signal is then used to disable the memory decoder lines F1-8 and D1-8 from the Apple memory select headers without destroying the contents of the memory. The Apple memory enable line gates the memory select line "on" when necessary. The BUSEN line activates the data bus drivers during phase two of the system clock when S-100 memory or devices are used by the Apple. This coordinates the data bus so it does not interfere with the memory refresh cycles.

The seven 74LS245's in Figure 3.5 drive the data and address buses between the Apple and S-100 bus. The three chips on the left of the figure are mounted with the rest of the Apple's control logic on the prototype board, normally in slot 5, which has just been described. The right four are on the wire wrap interface board occupying one slot of the KIMSI S-100 bus. When the S-100 bus is requested the PHLDA line goes low and activates the 16-bit address. This bus operates in only one direction, from the Apple to the S-100 hardware. The bi-directional data bus from the Apple is driven to the S-100 system where it is converted to a data in and data out bus.

KIM and S-100 Systems

The KIM is the major user of the S-100 bus and its peripherals for experiments. The signal-to-noise ratio of a digitized signal is enhanced by signal averaging. However, this requires a very reproducible timing sequence for each signal recorded and is especially critical in the fticr experiment. The necessary synchronization for the experiment is accomplished by a 8 MHz system master clock provided by the frequency

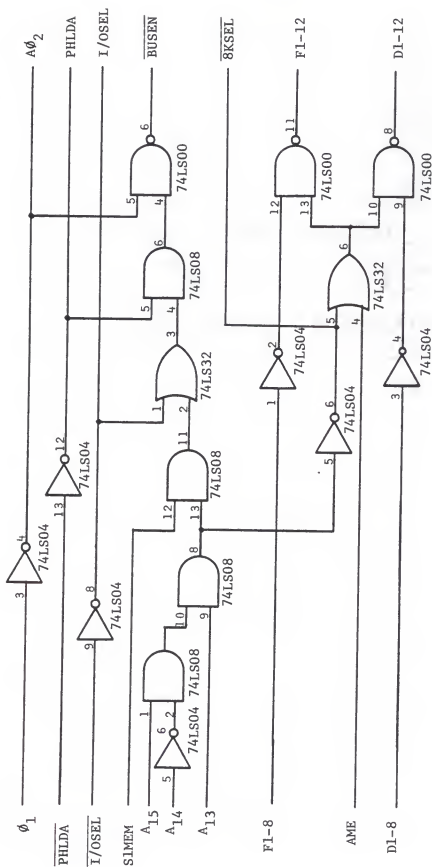


Figure 3.4. Apple 8 K memory decoding logic.

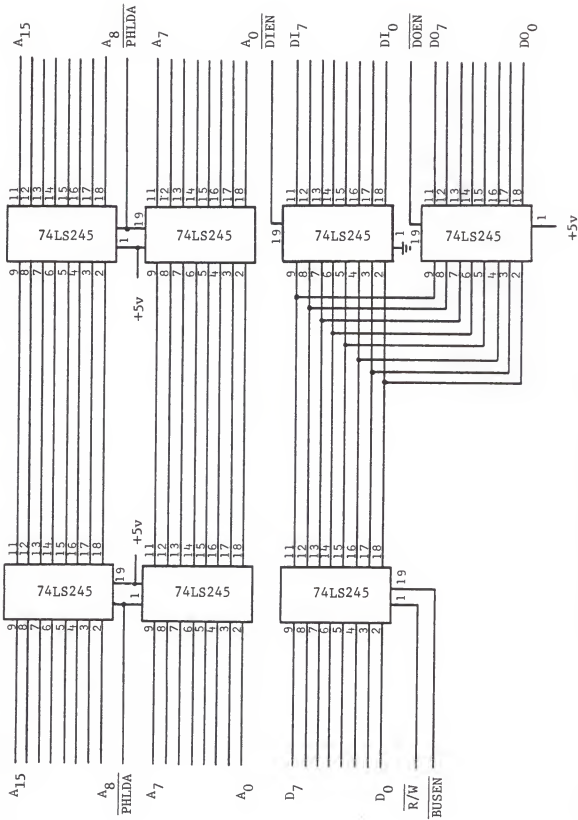


Figure 3.5. Apple to S-100 data bus and address bus drivers.

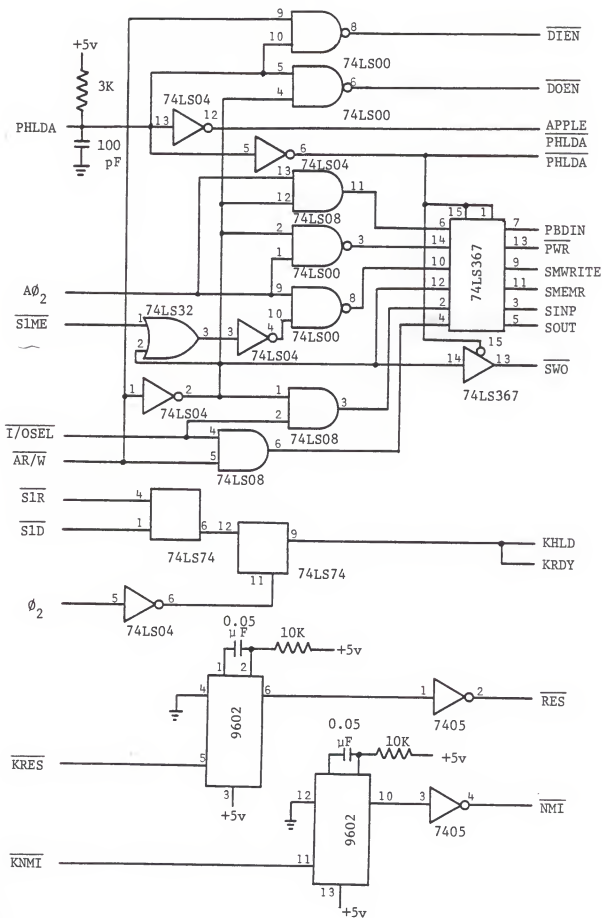
synthesizer's internal clock. This signal is divided by a clock generator circuit on the experiment interface which then supplies a 1 MHz clock directly to the KIM's CPU phase zero input from which all computer timing is derived. A variable sample clock rate used to sample the waveform recorder is derived from the master clock by a divide-by-N circuit on the experiment interface.

Once the Apple address and control lines are driven over to the S-100 system, the logic in Figure 3.6 converts these signals to those needed by the KIM and S-100 bus. Two mono-stable vibrators, 9602's, stretch out the 0.5 μ sec KIM reset and MNI pulses from the Apple into 2 μ sec pulses. The longer pulse is not important for the edge sensitive NMI signal but is imperative for the level sensitive reset line. Open collector inverters drive the lines in a wired-or fashion to the KIM's CPU.

The S-100 request pulse, $\overline{S1R}$, causes the KIM's ready line to drop to a logical zero, thus stopping the CPU while the S-100 release pulse, $\overline{S1D}$, causes it to restart. The pulses are latched by one 74LS74 flip-flop and synchronized with the KIM's phase two clock by a second flip-flop to generate the KIMSI ready and hold signals, KHL D and KR D Y. This insures that the transition only occurs during phase one of the system clock as required by the 6502 CPU chip. When the S-100 bus is free of the KIM's control, the processor hold available line, \overline{PHLDA} , goes high and is driven by a pair of inverters to the Apple and other circuits.

Additional logic gates convert the Apple control signals to S-100 type signals. The most widely used signals are the memory select lines, MWRITE and SMEMR, I/O select lines, SINP and SOUT, and read/write lines, PBDIN, \overline{PWR} , and \overline{SWO} . Selection of the proper S-100 data bus driver, data

Figure 3.6. Schematic diagram of the Apple to S-100 control line decoding logic. The upper half converts the Apple interface signals to standard S-100 signals. The center circuit coordinates the S-100 request and release commands with the KIM's phase two clock. The circuits at the bottom produce the KIM reset and interrupt signals.



in enable ($\overline{\text{DIEN}}$) and data out enable ($\overline{\text{DOEN}}$), is determined by a pair of NAND gates which combine the PHLDA and R/W signals.

The Biomation waveform recorder is controlled and interrogated for data by two parallel input ports and one output port listed in Table 3.1. The control port uses three of the four least significant bits to arm, request output, and toggle the next data point out of the recorder's memory using bits 0, 2, and 3, respectively. Bits number 2, 4, 5, 6, and 7 are not used. Bits 7 and 6 of the status port display the data ready flag and record flag, respectively. The 8-bit data are read from the recorder's memory through the Biomation data port. Data recording is started by arming the Biomation then triggering it from the front panel. For an example of how to use this peripheral check the Biomation operator's manual and the subroutines INIT, BREQ, GETB, and BIODAT in the assembly language program KIM ICR-MO TEXT listed in Appendix B.

Experiment Interface

Most computer systems are designed for controlling only a limited number of instruments, usually one. This often makes the alteration of an experiment difficult since the interfaces were designed only for a particular task. In many cases the hardware is present but the interconnections are integrated into the system such that it is virtually impossible, or at least undesirable, to modify it further. The experiment interface described here provides easy hook-up to many devices through standard types of connectors, while expansion capabilities are present in the form of unused gates and decoded addresses.

A block diagram of the interface is shown in Figure 3.7. A 19 in. rack mount front panel houses a series of BNC connectors, banana jacks,

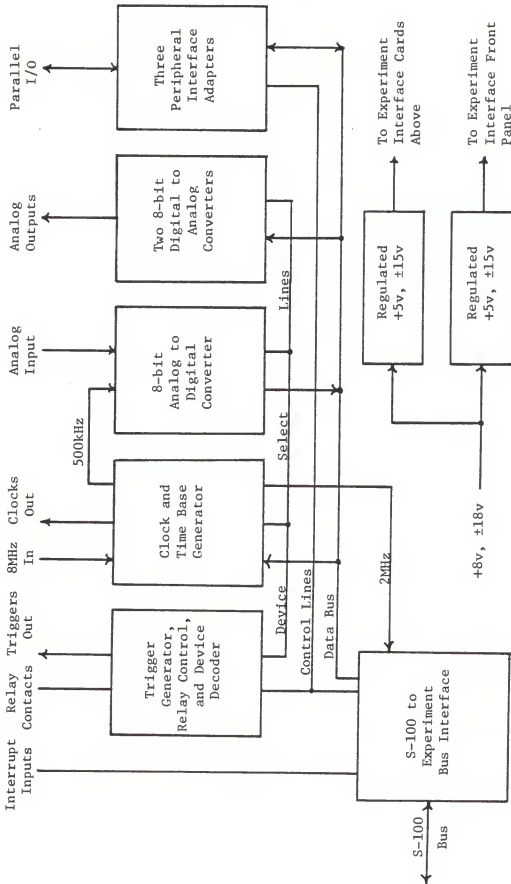


Figure 3.7. Block diagram of the experiment interface showing the interface cards, their interconnections, and power supplies.

buttons, and a switch. The chassis of the interface holds a row of eight 44-pin edge connectors. Five of the slots are in use leaving three ready for expansion with the power lines and data bus connected. Starting on the right while looking from the back, the first board houses several miscellaneous circuits. The second board generates the time base for the computer and waveform recorder. The third holds two 8-bit D/A's, the fourth supplies the 8-bit A/D, and the fifth contains three peripheral interface adapters (PIA's). All boards are inserted such that their components face to the left when seen from the rear, except for the first board due to the large heat sinks on the voltage regulators.

The interface control logic and bus drivers (see Figures 3.8 and 3.9) convert the S-100 bus signals to those used by the custom experiment interface. This involves the integrating of the two S-100 mono-direction buses into a single bi-direction bus. The S-100 I/O control lines, SINP and SOUT, are decoded with four of the address lines to generate the active low signals $\overline{I/O1X}$ and $\overline{I/O2X}$. The four least significant bits of the address bus and five S-100 timing signals are driven to the experiment interface slots. One driver bit is still available for expansion on the 74LS367.

The KIM status port is produced by a 74LS138 and 74LS74 shown in Figure 3.10. Eight addresses are write activated by the decoder but only one is used, I/O1F, leaving seven available for expansion. A write to the flip-flops latches the contents of bits 6 and 7 of the data bus; thus four different statuses can be indicated. A read of this address has no significance and returns garbage.

A 2 MHz clock runs through the interface cable and supplies the corresponding S-100 clock not provided by the KIMSI. For operation of the

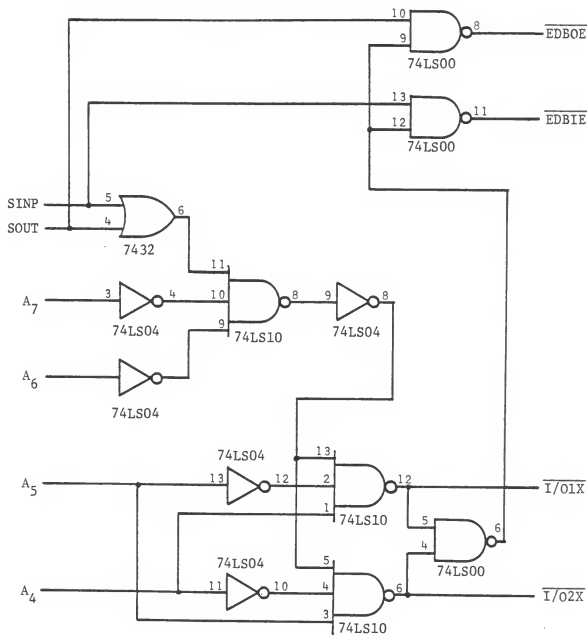


Figure 3.8. Schematic diagram of the experiment interface data bus enable and address decoding logic.

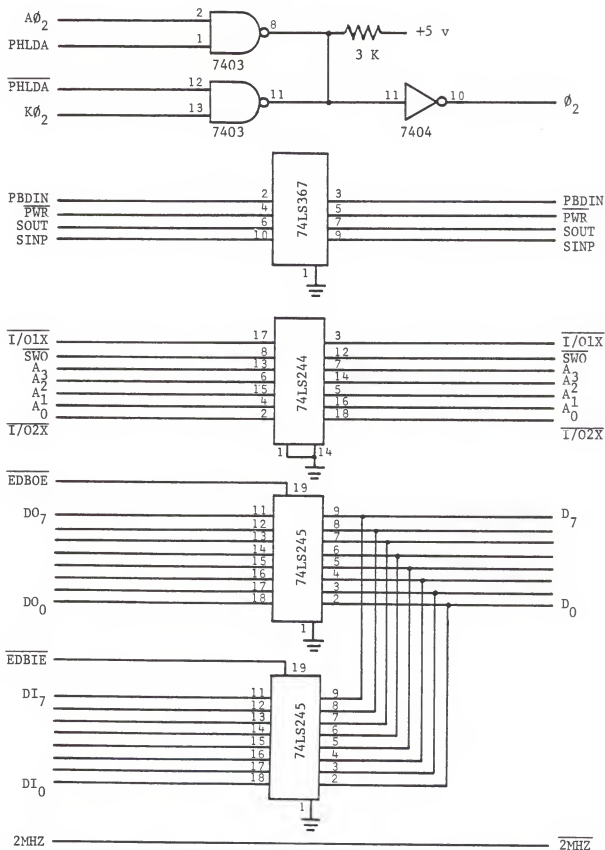


Figure 3.9. Schematic diagram of the experiment interface data bus, control line, and clock drivers.

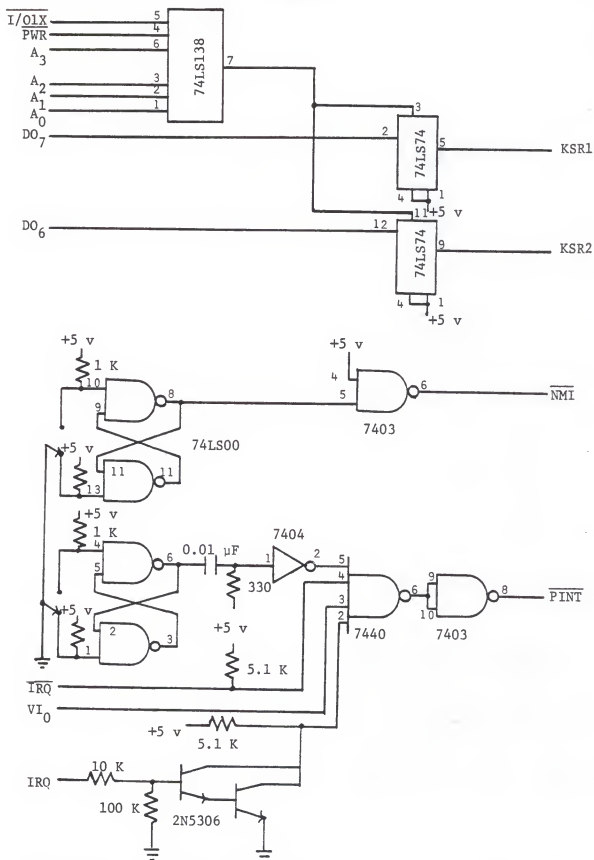


Figure 3.10. Schematic diagram of the KIM status port (upper half) and the KIM interrupt request generators on the experiment interface.

PIA's the phase two clock, ϕ_2 , is selected from either the KIM or Apple depending on which has control of the S-100 bus. Two momentary contact switches are debounced by a pair of NAND gates. One is connected to the KIM's $\overline{\text{NMI}}$ line while the other produces an interrupt request. The 7404 inverter acts as a 2 μsec pulse generator to shorten the relatively long time the IRQ button is pressed by hand. On the experiment interface front panel there is an active high and active low interrupt request bnc. A 5.1 K pull up resistor is used on the active low line while a Darlington transistor makes an active high line. The $\overline{\text{IRQ}}$ lines are combined in a four input NAND gate to form one pulse. Both the $\overline{\text{NMI}}$ and $\overline{\text{IRQ}}$ lines are driven by 7403 open collector gates in a wired-or fashion.

Experiment interface slots

Signals from the experiment interface bus driver run to the boards on the experiment interface main frame. The first board supports the interface power supplies, device decoders, trigger generator, and relay control. The circuits for these functions are shown in Figure 3.11. The interface has two D.C. power supplies; each is capable of furnishing 1 amp at +5 v (for digital circuits), 100 ma at +15 v, and 100 ma at -15 v (for operational amplifiers). One supply, on the first board, handles the power bus for the interface cards while the other, mounted on the chassis, is accessible through the front panel for prototype designs.

The 74LS138 device decoders generate eight read and eight write activated device addresses from the I/O1X line. Six of the write addresses are used, leaving two for expansion, while only four of the read addresses are in use. The decoders produce a 0.5 μsec active low pulse when selected. Two of the write generated pulses are channelled directly to the interface front panel to the TRIGGER A and TRIGGER B bnc connectors. These outputs are capable of driving ten TTL loads.

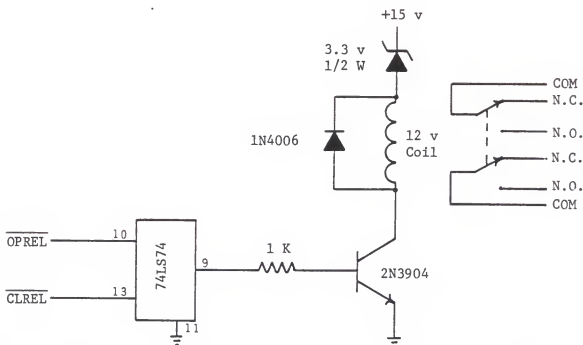
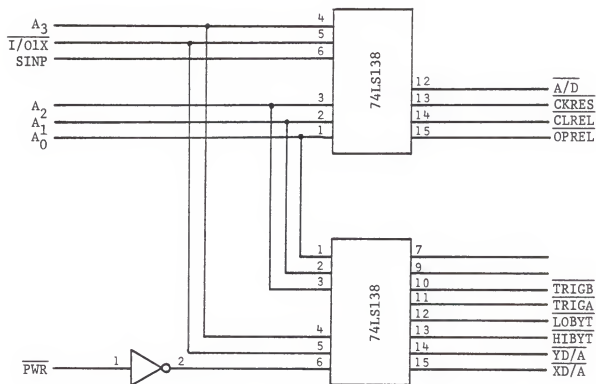
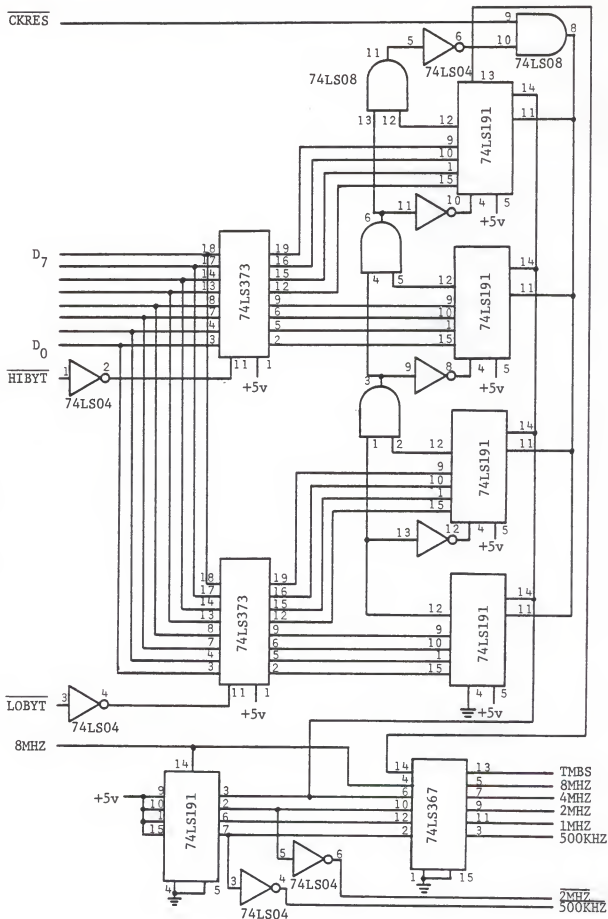


Figure 3.11. Schematic diagram of the experiment interface device decoders (upper half) and the relay control logic (lower half).

A single relay with two parallel contact sets is accessible through the interface front panel. The contacts are isolated from the interface chassis and can control up to 120 v A.C. at 2 amps. The relay logic uses a single 74LS74 flip-flop to regulate the power to the relay coil through a 2N3904 transistor. Reading the address I/O11 powers the relay coils causing the normally open and normally closed circuits to change state. Reading address I/O10 returns the contacts to their normal states.

The system clocks are generated by the logic shown in Figure 3.12. The 8 MHz master clock from the frequency synthesizer is first divided by a 74LS191 counter into 4, 2, 1, and 0.5 MHz. The 4 MHz clock drives the four count down counters synchronously to produce the variable time base. Two 74LS373 8-bit latches hold the 16-bit clock divide value. If the clock is loaded with zero, then the dividing stops and the output stays a logical zero. The clock may be divided by any preset value from 1 to 65535 to generate a 4 MHz to 61.036 Hz active low pulse lasting 125 nsec. This pulse was intended primarily to serve as an external clock for the waveform recorder, however, due to limitations of the recorder, not all the times are usable. Reading from address I/O12 causes, at the end of the read cycle, the clock to reset itself and start counting over again. A series of AND gates and inverters act as fast look ahead logic, insuring reliable operation at 4 MHz. All clock signals are driven from the card by either a 74LS367 line driver or inverter. The inverted signals are the $\overline{500\text{ KHz}}$ to the A/D and the $\overline{2\text{ MHz}}$ to the S-100 bus. All the non-inverted clocks go directly to their corresponding bnc connector on the front panel.

Figure 3.12. Schematic diagram of the experiment interface clock generator logic.



The two D/A's and their associated circuits are shown in Figure 3.13. The 1408 8-bit converters generate a current which is changed to a voltage by an operational amplifier. Two pots for each op amp adjust the output voltage zero and range. The voltage varies linearly with the input from -5.00 v for 00 to 4.96 v for FF. The output is smoothed by a 200 KHz low pass filter. Two 8-bit latches hold the input value so that the output voltage holds steady between conversions.

Analog to digital conversion is performed by a Datal ADC-EH8B2 fast 8-bit converter shown in Figure 3.14. The converter is triggered by the 500 kHz clock and latched with the A/D's end of conversion signal. This keeps the digitized signal synchronized with the KIM. The Apple is not synchronized with the A/D converter; therefore, one should exercise care when using them together. Bipolar analog signals from -5.00 to 4.96 v change the digitized output from 00 to FF, respectively. Input voltage overload protection is accomplished by a pair of back to back 18 v zener diodes. The input impedance of the A/D converter is 4.45 Kohm and should be buffered when connected to any high impedance voltage source.

Three PIA's, shown in Figure 3.15, supply 48 bits of parallel I/O and 12 control lines. The output of PIA-2 runs to the front panel parallel output BNC's to produce an A and B port with their corresponding control lines. PIA's 1 and 3 go to a pair of DB-25 connectors on the back of the chassis. The bits represent a maximum of one TTL load when used as inputs. As outputs the A port can drive one TTL load while the B port can directly drive the base of a transistor switch. The PIA interrupt lines are connected in a wired-or fashion to a single interrupt line; therefore, polling must be used if more than one chip is interrupt active. The 6820 and 6821's PIA's are latched with the phase two clock and operate in the

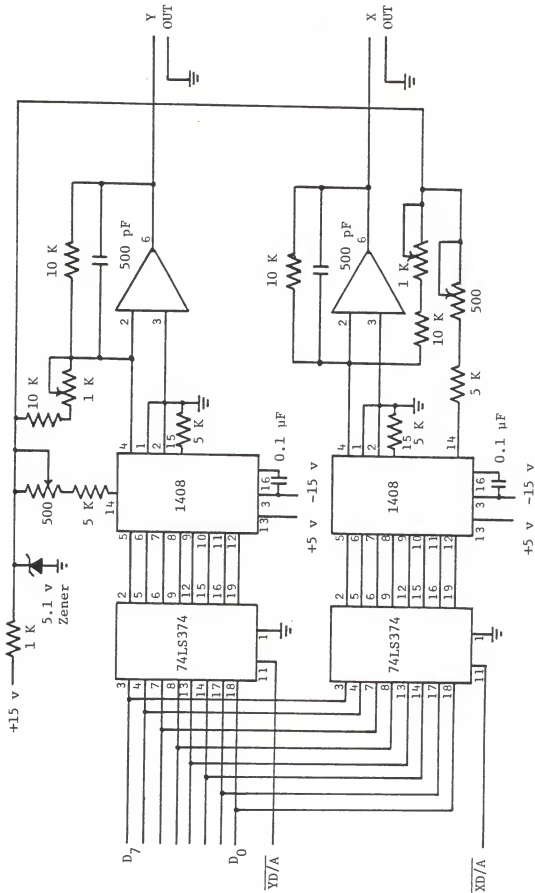


Figure 3.13. Schematic diagram of the experiment interface 8-bit digital to analog converters. The circuit was designed and constructed by Steve Miles.

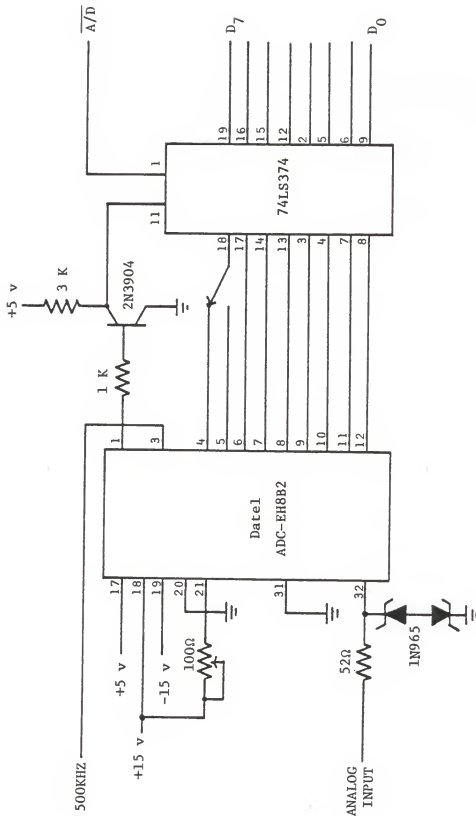


Figure 3.14. Schematic diagram of the 8-bit analog to digital converter circuit on the experiment interface panel.

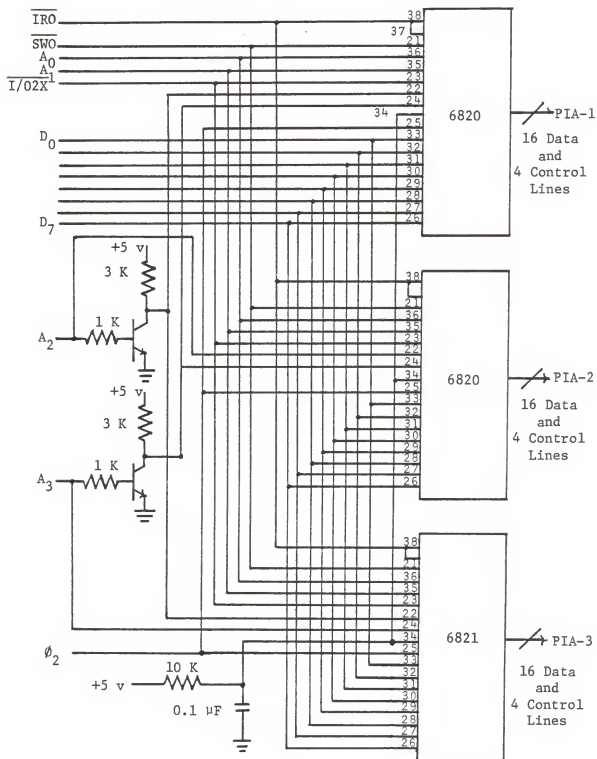


Figure 3.15. Schematic diagram of the three peripheral interface adapters on the experiment interface panel.

I/O2X address range. For programming considerations one should consult the reference manual [68]. Sample PIA initialization procedures are given in subroutine INIT of the KIM ICR-MO TEXT assembly language program listed in Appendix B.

Connections to the marginal oscillator

The pulse sequence for the icr spectrometer is channelled through parallel port B on the front panel of the experiment interface. Six of the eight bits are presently used, leaving two available for expansion purposes such as triggering a dye laser or gating a CO_2 laser. The pulse sequence needed by the icr and m.o. detector is shown in Figure 3.16 along with the corresponding bit supplying the pulse. The grid pulse is sent to the EXT. GRID bnc connector on the icr control panel. The EXT./INT. switch is then set to external allowing the computer to gate the electron beam. The ω_2 line is connected to the external trigger of the ω_2 oscillator. The quench pulse is spliced into the icr cell plate potential control electronics through the quench pulse bnc on the controller front panel after disconnecting the controller's internal clock from the circuit. The reset, detect, and sample and hold (S/H) pulses are sent to the m.o. detector and post detection system with the timing shown.

Once the m.o. detector output is connected to the input of the waveform recorder the system is ready to go, provided the software is all written.

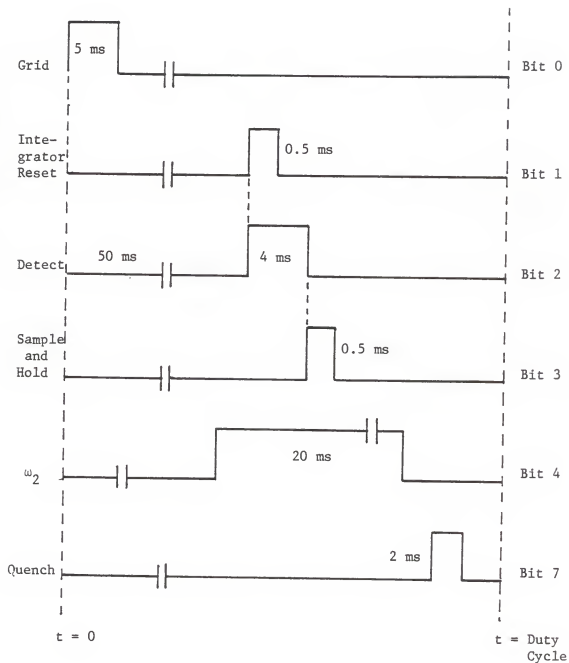


Figure 3.16. Pulse timing sequence for a typical icr experiment using our marginal oscillator detector and cell potential control electronics. The designated bits of PIA-2B on the right control the corresponding signals on the left.

CHAPTER 4 SOFTWARE

Introduction

While hardware gives a computer its physical capabilities it is the software which bestows versatility. This chapter discusses programs written to operate the ICR spectrometer in our laboratory with the microcomputer system previously described. These programs represent only one possible application of the computer system. The full capabilities of the hardware are not even close to being thoroughly taxed, and thus will require additional software in order to satisfy the needs of an innovative scientist or curious student.

The subsequent description outlines in some detail an operational and functional picture of the software. Various tasks are examined such as initialization and control of the hardware and loading of BASIC and machine language code, along with data acquisition, storage, and analysis. The coordination of the master and slave computers through software instructions is also explained.

Program Initialization

The program is started by inserting the "MO Program Disk" and typing the lines

```
<reset>  
COD7:0  
6<ctrl-P>
```

where the < > signifies pressing a particular key on the keyboard,

otherwise a series of keys is pressed. All entry lines except reset end with a RETURN key. This sequence of lines resets the machine to monitor control, configures the Apple to 40 K of RAM memory, and boots the disk. Under control of the "HELLO" program the language APPLEFAST is loaded into the language card, if present, and an EXEC file containing the commands

```
POKE 103,1
POKE 104,64
POKE 16384,0
NEW
POKE 232,0
POKE 233,10
BLOAD ICR SHAPE,A$A00
BLOAD APPLE ICR-MO CODE
RUN ICR-MO
```

is started. The first four set the system pointers such that the BASIC program loads in above page one of the high resolution graphics. This overrides the normal load and frees memory below the graphics for the Apple machine language code and shape table. The next three commands identify to BASIC the location of the shape table, a plus sign used as a data display cursor, and load it into memory. The last two commands load the Apple machine code for communicating with the KIM and then begin loading and executing the BASIC control program, ICR-MO.

Functional Description of Program

The operation of a program by a garden variety homo sapien does not require understanding the internal workings of the routine, thus a functional description of the program is sufficient for performing experiments solely to obtain chemical information. For a detailed description of how the programs work one should see the appendices. Appendix A explains the BASIC program used, while Appendix B covers the assembly language code. The following text provides a brief description of the commands and concepts necessary to run an experiment.

Numbered Command Mode

After initializing the BASIC program, a set of instructions for initializing the KIM appears on the video monitor. These instructions must be entered by hand through the KIM's keyboard. They disable the processor's interrupt request service flag through its status port and set the non-maskable interrupt request vector to the entry point of the KIM's experiment code.

Next a list of numbered commands, as seen in Table 4.1, appear on the video screen and a request for a command number is made. Any one of the ten numbers may be typed at this time in order to perform the specified task. An invalid entry simply causes the computer to ask for another command. A description of the numbered commands follows, however, not in the order given in the table.

The EXIT PROGRAM (1) command provides a graceful way to leave the program and return to the operating system for control. Inadvertent breaks from the program often can be forgiven by typing the string "GO TO 8000". This places one back at the numbered command display and entry without resetting the program variables. When all else fails the disk should be rebooted.

Occasional hardware glitches in the KIM and S-100 system can be corrected by reloading KIM's program with the LOAD KIM PROGRAM (10) command. This restarts the same routine described earlier for initializing the KIM.

The MASS CALCULATION (6) command allows determination of any one of the three $i\alpha r$ resonance parameters when the other two are known. The resonance frequency, magnetic field strength, or mass to charge ratio are determined, neglecting trapping potential effects, by Equation 2.1.

Table 4.1. List of numbered commands.

<u>Number</u>	<u>Command</u>
1	EXIT PROGRAM
2	STORE DATA ON DISK
3	CATALOG DISK
4	UPDATE EXPERIMENT CONDITIONS
5	CHANGE PARAMETERS
6	MASS CALCULATION
7	LOAD PARAMETER FILE
8	SAVE PARAMETER FILE
9	PRINT DATA
10	LOAD KIM PROGRAM

An icr experiment is set up and executed by the program sequence invoked by the command CHANGE PARAMETERS (5). At this time the experiment mode of operation is entered. Due to its significance, this operation mode will be discussed later.

The command of UPDATE EXPERIMENT CONDITIONS (4) allows the recording of many of the variables not controlled by the computer but useful in interpreting the data. The conditions recorded are listed in the lower half of Table 4.2 and can be set to any integer, real, or scientific notation value. During this routine four key commands are operational and are given in Table 4.3B. These key commands function as explained in the section on the experiment mode of operation.

After an experiment has been completed, the data may either be saved on disk or listed on a printer by the appropriate numbered commands (2 and 9 respectively). Data is stored on disk in a text file whose format, first the total number of values, then a list of X,Y pairs, is compatible with the scientific software package [69]. Depending on the experiment performed, determined by the scan modes listed in Table 4.3C, the pairs represent different quantities. Their exact significance will become apparent when the scan modes are described later. For experiment scan modes 1 and 2 the X,Y pairs correspond to the point number and m.o. output level, respectively, while for scan modes 3 and 4 the pairs correspond to the detect delay time, in milliseconds, and the m.o. output level. After saving on disk under any given filename the program prints, if desired, the filename, date, time, description, experiment parameters, and experiment conditions. Printed data, again as X,Y pairs, is preceded by the same list just described but with the filename "NONE."

Table 4.2. List of experiment parameters and conditions along with typical values.

EXPERIMENT PARAMETERS

GRID PULSE WIDTH	5	MSEC
DETECT PULSE DELAY	250	MSEC
STEP	10	MSEC
WIDTH	3	MSEC
W2 PULSE DELAY	0	MSEC
WIDTH	5	MSEC
QUENCH PULSE DELAY	265	MSEC
WIDTH	5	MSEC
DUTY CYCLE TIME	270	MSEC
SCAN MODE	4	
NUMBER OF PASSES	10	

EXPERIMENT CONDITIONS

ELECTRON BEAM :		
GRID POTENTIAL	-75	VOLT
FILAMENT POTENTIAL	-70	VOLT
COLLECTOR POTENTIAL	12	VOLT
COLLECTOR CURRENT	50	NAMP
CELL POTENTIALS: UPPER	-1.25	VOLT
LOWER	-1.25	VOLT
SIDE(F)	1.5	VOLT
SIDE(C)	1.5	VOLT
END1	-1.25	VOLT
END2	-1.25	VOLT
MAGNETIC FIELD STRENGTH	12.1	KG
TEMPERATURE	50	C
R.F. LEVEL	30	MV
W1 FREQUENCY	87.4	KHZ
W2 FREQUENCY	0	KHZ
PRESSURE	1.5E-06	TORR

Table 4.3. List of keyboard commands and scan modes for the CHANGE PARAMETERS and UPDATE EXPERIMENT CONDITIONS routines.

A) KEY^a FUNCTION

ctrl-A	Abort
ctrl-C	Cursor
ctrl-E	Erase
ctrl-G	Graphics
ctrl-K	Rate Constant
ctrl-P	Pulse
ctrl-Q	Quit
ctrl-T	Text
+	Increment value
-	Decrement value

B) KEY^b FUNCTION

--->	Advance cursor
<---	Back-up cursor
RETURN	Change value
ESC	Escape to numbered commands

C) Scan Modes^a

- 1- Continuous scan
- 2- Signal averaged scan
- 3- Detect delay sweep
- 4- Detect delay sweep with baseline correction

a) For use in CHANGE PARAMETERS routine only.

b) For use in CHANGE PARAMETERS and UPDATE EXPERIMENT CONDITIONS routines.

The experiment parameters and conditions can be saved on disk, as a text file, for any particular set up desired by the LOAD PARAMETER FILE (8) command. Any disk filename may be specified but if none is entered, by just pressing the RETURN key, then the default filename, EXP PARAMETERS, is used. This file is loaded automatically during program initialization to put the program into a non-zero state. The LOAD PARAMETER FILE (7) command loads any parameter file generated earlier by the save command. Again, if no filename is given the default value is used.

Parameter filenames, data filenames, or any information from the disk's directory may be examined by the CATALOG DISK (3) command. This generates a catalog of the active disk on the video monitor.

Experiment Mode

The program sequence started by the CHANGE PARAMETERS numbered command provides a means for performing pulsed icr data acquisition along with some data analysis. The routine starts by displaying the list of experiment parameters shown in the top half of Table 4.2. A flashing greater than sign (>), the parameter pointer, appears before one of the numbers. All parameter changes occur to the number next to the pointer. It also indicates the program is ready for the single key instructions listed in Tables 4.3 A and B. A logical key stroke for each command aids in their memorization. A description of each key and its corresponding function is given below.

Abort (ctrl-A). Used to terminate a pulse sequence in progress. This provides an early exit from a pulse sequence while leaving the data recorded up to that point in memory. After aborting the current pulse

sequence, the KIM is placed in a continuous operation mode even though the data are not being recorded by the Apple.

Cursor (ctrl-C). Allows movement of a cursor, plus sign, across the data previously recorded. The cursor position is controlled by the two hand controllers: paddle zero for coarse movement and paddle one for fine movement. Displayed below the plot are the cursor position parameters: point number, X-value, and intensity.

Erase (ctrl-E). Clears the high resolution screen, regardless of whether the graphics is currently being displayed or not.

Graphics (ctrl-G). Switches the graphics display on. Changes may still be made on the text screen and parameters but they are not visible.

Rate constant (ctrl-K). Allows determination of decay rates from data previously collected during a detect delay sweep (scan modes 3 and 4). Calculations are performed by the ratio method described in Chapter 2. Specifying the first and last data points to be used in the calculation allows evaluation of the decay constant from a portion of the data. Data may be corrected for non-zero decay curve tails when determining decay constants by specifying an appropriate offset value.

Pulse (ctrl-P). Initiates a pulse sequence with the designated parameters and switches automatically to graphics display. Any key command may be entered and executed during a pulse sequence except for a quit, escape, cursor, rate constant, or another pulse command. When single key commands are given, pulse sequences in progress are delayed between points then continued with the updated parameters, if any. The parameter pointer stops flashing during a pulse sequence.

Quit (ctrl-Q). Causes an exit from the program and a return to DOS keyboard control. This key operates the same as the EXIT PROGRAM command (number 1 in Table 4.1).

Text (ctrl-T). Switches the screen from graphics to text display. When an experiment is in progress the text remains on the video screen as experiments are performed and plotted on the high resolution graphics screen.

Plus (+). Increments the value of the experiment parameter currently indicated by the pointer. When the upper limit is reached the parameter remains at the maximum value. The maximum value is determined by the limits set in the "experiment parameter limit check" routine (see program lines 4000 to 4180 in Appendix A).

Minus (-). Decrements the value of the experiment parameter currently indicated by the pointer. When the lower limit is reached the parameter remains at the minimum value. The lower limit is determined the same way as described in the previous paragraph.

Advance (-->). Shifts the parameter pointer down one line. The pointer returns to the top of the list if the key is pressed when the pointer is at the bottom of the list.

Back-up (<--). Shifts the parameter pointer up one line. The pointer returns to the bottom of the list if the key is pressed when the pointer is at the top of the list.

Change (Return). Modifies the value next to the parameter pointer. Changes are checked against the parameter's upper and lower limits, then corrected as necessary.

Escape (ESC). Causes exit from the experiment mode of operation and return to the numbered command mode.

The experiment parameters controlled by the computer are the pulse times, duty cycle, scan mode, and number of passes (when signal averaging). Four different types of experiments (scan modes) can be performed by the computer and are given in Table 4.3C. The experiment is selected by the scan mode value.

Continuous scan (1). The pulse sequence repeats with all parameters held constant. The detect pulse delay parameter equals the detect delay time. The maximum number of points on the screen and in memory is 280. The screen is cleared when full and the previous data are replaced with the incoming data. This scan mode is most commonly used when tuning the icr for a particular ion.

Signal averaged scan (2). Experiments, such as magnetic field and double resonance sweeps, are signal averaged for the specified number of passes during one sweep, then displayed on the screen. The screen is filled with 280 points representing 280 experiments averaged N times each (where N is the number of passes averaged) then the pulse execution is terminated and data saved in memory.

Detect delay sweep (3). The grid pulse is enabled and the m.o. output signal is averaged for the specified number of passes at a given detect pulse delay time. This detect pulse delay time is swept from zero to the maximum detect pulse delay time displayed on the screen in increments of the displayed step size.

Detect delay sweep with baseline correction (4). Ion signal and baseline are averaged, in turn, for the specified number of passes. The detect delay is swept as in scan mode 3. The baseline is linear least squares fitted, then subtracted from the ion signal.

The grid pulse starts at time zero and can vary in width from 0 to 25 msec. Its value may be incremented by 0.5 msec steps within the above limits using the + and - key commands.

The detect pulse is controlled by three times: detect width, delay, and step. The width can vary from 1.5 to 25 msec in 0.5 msec steps. The detect delay and step size have two different meanings depending on the scan mode. If a continuous or signal averaged scan, modes 1 and 2, is selected, then the screen shows the delay time used in the experiment. This delay time can vary from zero to the quench delay minus the detect pulse width. The step value is used as the amount of increase or decrease when the detect delay time is changed by the + or - keys. During a detect delay sweep, modes 3 and 4, the actual detect delay time varies from zero to the detect pulse delay time displayed on the screen. The detect pulse delay time is swept between the above limits by incrementing its value by the detect pulse step size.

The ω_2 pulse width and delay times are controlled by their corresponding parameters. The values are not bound by any limits. The quench pulse width can vary from 0 to 10 msec while the quench pulse delay must be less than or equal to the duty cycle time minus the quench pulse width. The duty cycle time determines the maximum time for pulse generation and must be greater than or equal to the quench pulse width plus quench pulse delay. The maximum duty cycle time is currently set at 16 seconds.

When a signal averaging scan is in progress, the number of passes taken for each point is set by the corresponding parameter and may vary from 1 to 255.

Pulse Timing Parameters

An 8-bit pulse routine, whose operation is described in Appendix B, provides the Apple or KIM microcomputer with the ability to produce accurate and variable pulse sequences needed for various experiments. A single 8-bit parallel port produces eight separate pulses which are independent of each other but change synchronously.

The pulses generated are active high, that is, a logical one when "on" and a logical zero when "off". Each pulse corresponds to a particular bit in the pulse hardware port. Two parameters are needed for each pulse bit, an "on" time and an "off" time; therefore, 16 parameters are needed to specify pulses for all eight bits. One additional parameter, the duty cycle time, is needed to specify the maximum time for pulse generation. All parameters are 16 bits in length and thus require double precision values (two 8-bit bytes).

The pulse parameters mentioned above are in units of 0.5 msec; consequently, the shortest pulse lasts 0.5 msec, the longest lasts 32568 msec. Any pulse size between these limits is possible but only in 0.5 msec increments.

Several different signal types can be generated by this routine. A typical pulse is when the bit goes high then low some time later. The pulse may go high immediately then low as in Figure 4.1A, or first delay and then go "on" and "off" as in Figure 4.1B. For these pulses the "on" time is greater than or equal to zero, and the "off" time is greater than the "on" time but less than or equal to the duty cycle time. This will generate a pulse equal in length to the difference between "on" and "off" times. The pulse is generated each time the program is executed.

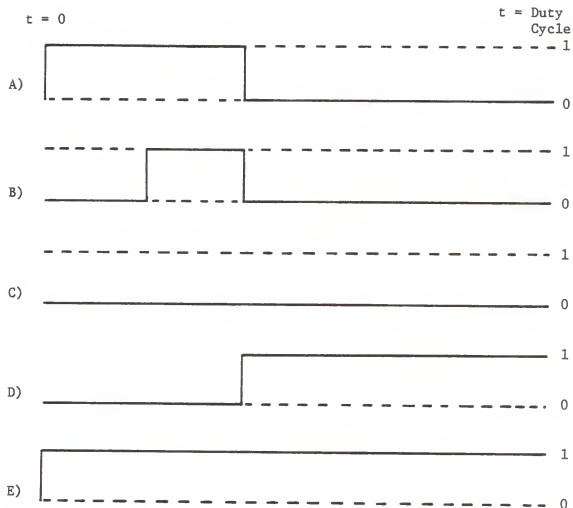


Figure 4.1. Some of the pulse shapes which can be produced by the 8-bit pulse routine. The bits are switched between a logical 1 and 0 by setting the "on" and "off" times to the appropriate values: A) "on" time equal to zero and the "off" time less than the duty cycle; B) "on" time greater than zero and the "off" time less than the duty cycle; C) "on" time greater than the "off" time; D) "on" time greater than zero and the "off" time greater than the duty cycle; E) "on" time equal to zero and the "off" time greater than the duty cycle.

A pulse port bit can be always "off" as in Figure 4.1C. This can be generated in three different ways: "on" time equal to "off" time, "off" time less than "on" time, or "on" time greater than duty cycle time. The preferred way is to set the "off" time equal to zero, then the "on" time can be any value.

The pulse port bit may remain "on" at end of the duty cycle as in Figure 4.1D. This is accomplished by making the "on" time less than or equal to the duty cycle time, while the "off" time is greater than the duty cycle time. A pulse bit can be kept high at all time, as in Figure 4.1E, by setting the "on" time equal to zero and the "off" time greater than the duty cycle. After the first pass through the routine the bit will go high and remain in that state.

KIM Status Display

Since a computer which is working properly often looks like one which is not, the slave microcomputer is instructed to flash its vital signs periodically. The KIM displays its status in three bytes on the KIM's 6-digit LED front panel display. The first byte on the left displays the scan mode status of the computer. There are three possible values: 00 for end of signal averaged scan, 01 for continuous scan, and 02 for signal averaging in progress. The display's middle byte changes value by one each time a pass through the KIM ICR-M0 program is completed. When a continuous scan is in progress the display value increments, but during an averaging scan the value begins at the number of passes then decreases to zero. The right byte displays the data read from the 8-bit A/D during the last pass. A hexadecimal 00 is the lowest value and FF is the highest.

Data Analysis

Most of the data are analyzed through the use of three commercial scientific routines when possible [69]. A curve fitter is used to perform linear least squares calculations, while a scientific plotter enables the combining of several different data sets for visual comparison. The program VIDICHART is particularly useful when comparing mass spectra to each other. For specific details about operating these routines one should consult the manuals. Hard copy of plotted data is obtained from a dot matrix printer controlled by a graphics screen dump routine [70].

CHAPTER 5 INSTRUMENT CALIBRATION

Introduction

Due to the low gas densities involved in icr studies, the most difficult quantity to measure, if accurate ion-molecule rate constants are to be determined, is pressure. All experiments were carried out with gas pressures in the 10^{-7} to 10^{-4} torr range, thus allowing the use of an ionization gauge for pressure measurement. Since this transducer works by ionizing the gas and then measuring the resulting ion current, the gauge sensitivity depends upon gas characteristics, particularly the cross-section for ionization. Unfortunately, the sensitivity is not directly related to some known quantity such as the ionization potential or polarizability of the gas; thus, the gauge must be calibrated for each sample used. If the ion trapping cell is not near the ionization gauge, as in our instrument, then the geometry of the vacuum system must also be accounted for in the evaluation of the true pressure by determining a system correction factor.

If one lets P_i and S be the pressure reading and sensitivity of the ionization gauge, and F the system correction factor, then the pressure of the gas at the cell, P_c , is given by the following equation:

$$P_c = P_i * S * F .$$

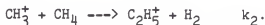
The sensitivity can be determined by calibrating the ionization gauge against a pressure gauge whose output is independent of the species

used, such as a capacitance manometer. The system correction factor is evaluated by comparing reaction rates from our icr spectrometer with well-established rates for a known reaction and then adjusting the results by the appropriate constant.

One of the most highly studied chemical systems in ion-molecule reaction kinetics must be the ions produced in methane gas. The only reactions which occur at an appreciable rate ($k > 10^{-11}$ cm³/sec) are those of the primary ions, CH₃⁺ and CH₄⁺, with the neutral parent [71]:



and



The rate constants measured by a variety of methods (such as drift tube, icr, and other mass spectrometers) for these two reactions are in good agreement resulting in average values of $k_1 = 11 \pm 1 \times 10^{-10}$ and $k_2 = 9 \pm 1 \times 10^{-10}$ cm³/sec [72]. If only icr results are considered one obtains averages of $k_1 = 11.5 \pm 0.4 \times 10^{-10}$ and $k_2 = 9.9 \pm 1.6 \times 10^{-10}$ cm³/sec (all errors reported are 95% confidence limits) [73].

Due to the abundance of earlier work on ion-molecule reactions in methane gas, the rate constants for reactions in this system were used for calibrating the instrument. The following text describes the procedures used for determining ionization gauge sensitivity, system correction factor, and reaction rate constants. The ion-molecule reaction rates for several other chemical systems, reported in the literature, also are determined to illustrate the validity of the corrections applied.

Experimental

Gauge Sensitivity Experiments

The ionization gauge was calibrated against a single-sided capacitance manometer [74] in the mid 10^{-6} to 10^{-4} torr range. To aid in reading the manometer, a digital voltmeter was connected to the analog output of the manometer control unit. Experiments were performed by first pumping out the vacuum chamber to a low background pressure, then reading both pressure gauges. Next, a sample gas was leaked into the vacuum system followed by the reading of both gauges again when the pressure had stabilized. This procedure was repeated for several different sample pressures in the range specified above.

Ion Decay Determination

Ion decay experiments were performed in the 10^{-6} to 10^{-7} torr pressure range. Ions were formed by electron impact with 30 to 70 eV electrons and trapped in the ion cell, then the signal intensity was monitored as a function of the detect pulse delay time by the data system previously described. The cyclotron frequency for most experiments was set for ion resonance at 1.2 T, except for methane which was run at 0.8 T due to the upper frequency limit of the marginal oscillator. For a typical experiment the cell trapping plates were at +1 v, the upper, lower, and end plates were at -1 v, the grid was pulsed for 5 ms, and a 4 ms detect pulse gated the 30 mv peak-to-peak marginal oscillator irradiating frequency. After each experiment ions were removed from the cell with a 5 ms quench pulse. Ion signals were averaged from 10 to 25 times at each detect pulse delay time, then stored on disk. Gaseous samples in glass bulbs were routinely purified by repeated freeze-pump-thaw cycles in our experiments.

Results

Gauge Sensitivity Experiments

The appropriate background readings were subtracted from the sample pressure for both the ionization and manometer readings to give pressure changes. Linear variations were assumed when correcting for drifts in the capacitance manometer background measurements. Plots of the capacitance manometer vs ionization gauge pressure readings for a few selected gases are shown in Figure 5.1. Slopes of the lines were determined by linear least squares analysis and are listed under sensitivity in Table 5.1. Linear correlation coefficients for all fits were better than 0.996, thus indicating good linear behavior over the pressure range.

Methane Experiments

Three typical ion decay curves for the reaction of the methane parent ion with neutral methane gas are shown in Figure 5.2. The curves were normalized to the same extrapolated intensity at time equal to zero. Plots of the natural logarithm of ion intensity versus time yielded straight lines verifying the application of pseudo-first order reaction kinetics. Slopes of the lines were determined by linear least square analysis. When the pressure read from the ionization gauge is corrected for the gauge sensitivity using curves as in Figure 5.1 to obtain the values in Table 5.1, and one assumes a neutral gas temperature of 323 K [75], then the reaction rate constant can be calculated by the method described at the end of Chapter 2. The evaluation of the CH_4^+ reaction rate at six different pressures gives an average of $18.9 \pm 1.7 \times 10^{-10} \text{ cm}^3/\text{sec}$. Similar analysis of four

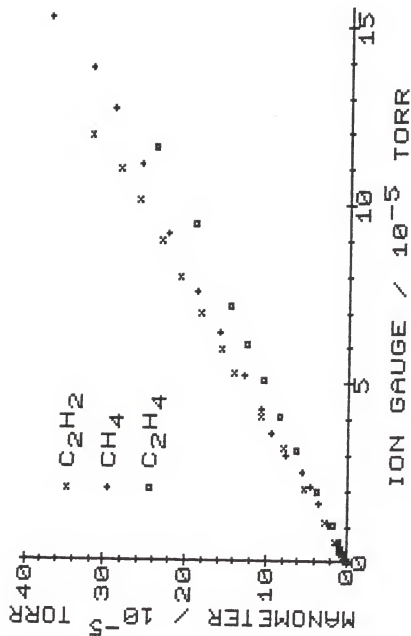


Figure 5.1. Ionization gauge sensitivity plots for three different gasses. The pressure read from the capacitance manometer, displayed on the vertical axis, is compared to the ionization gauge pressure reading, displayed on the horizontal axis.

Table 5.1. Results of system calibration experiments for selected ion-molecule reactions. All rate constants are in cm^3/sec with 95% confidence intervals. The temperature is assumed to be 323 K. The corrected rate constants (k_{corr}) were evaluated using a system correction factor of 1.67 ± 0.21 obtained for methane.

System	Sensitivity	$k_{\text{obs}} / 10^{-10}$	k_{corr}	k_{ref}	Reference	Remarks
$\text{CH}_4^+ + \text{CH}_4$	2.36 ± 0.04	18.9 ± 1.7	11.4 ± 2.5	11.5 ± 0.4	[73]	icr only
				11.3 ± 0.8	[73]	Mean of all
				10.5 ± 1.0	[76]	Mean of 15
				11 ± 1	[77]	
$\text{CH}_3^+ + \text{CH}_4$		16.8 ± 1.2	10.1 ± 2.0	9.9 ± 1.6	[73]	icr only
				9.9 ± 1.8	[73]	Mean of 16
				10.2 ± 2.1	[76]	Mean of 13
				9 ± 1	[72]	
$\text{C}_2\text{H}_2^+ + \text{C}_2\text{H}_2$	2.60 ± 0.02	16.8 ± 2.1	10.1 ± 2.5	11.8 ± 1.9	[73]	Mean of 10
				10.4 ± 3.1	[76]	Mean of 3
$\text{C}_2\text{H}_3^+ + \text{C}_2\text{H}_4$	2.04 ± 0.02	20.3 ± 2.0	12.2 ± 2.7	14.1 ± 3.7	[73]	Mean of 3
				12.1 ± 5.4	[76]	Mean of 2
$\text{C}_2\text{H}_4^+ + \text{C}_2\text{H}_4$		12.4 ± 2.6	7.4 ± 2.5	7.2 ± 1.3	[73]	Mean of 20
				6.6 ± 3.0	[76]	Mean of 7
				8.0 ± 0.1	[78]	Recent icr
$\text{C}_6\text{H}_6^+ + \text{C}_6\text{H}_6$	1.19 ± 0.04	0.23 ± 0.15	0.14 ± 0.11	0.12	[79]	
$\text{C}_3\text{H}_3^+ + \text{C}_3\text{H}_3\text{Cl}$	2.0 [80]	0.047 ± 0.011	0.028 ± 0.010	0.0	[81]	

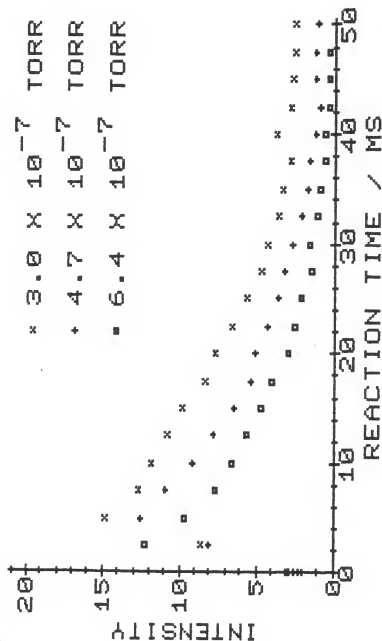


Figure 5.2. Typical ion decay signals for CH_4^+ in methane gas at three different pressures. Ions were formed by a 5 msec pulse of 50 eV electrons and detected at a magnetic field strength of 0.82 T by a marginal oscillator set for a resonance frequency of 784.88 kHz and gated at each reaction time for 2.5 msec. Each point is an average of 16 scans. All curves were normalized to the same intensity at time equal to zero.

CH_3^+ ion decay signals in methane results in an average of $16.8 \pm 1.2 \times 10^{-10} \text{ cm}^3/\text{sec}$.

These two reaction rates are obviously much higher than the rates determined by icr studies described earlier, thus indicating a significant system correction factor. The ratio of the CH_4^+ reaction rate to the CH_3^+ rate determined in this study is 1.13 and compares well with the ratio of 1.16 determined from an average of icr experiments [73]. A relative rate of 1.2 from the two reactions determined on another icr is in good agreement with our results [82]. If one assumes the average icr literature results as being the true value then one obtains a multiplicative system correction factor of 1.64 ± 0.20 for the CH_4^+ reaction and 1.70 ± 0.40 for the CH_3^+ results or an average of 1.67 ± 0.21 (error limits were determined by use of the CH_4^+ results). Using this value one calculates a corrected rate constant, k_{corr} , of $k_1 = 11.4 \pm 2.5 \times 10^{-10} \text{ cm}^3/\text{sec}$ and $k_2 = 10.1 \pm 2.0 \times 10^{-10} \text{ cm}^3/\text{sec}$.

Reactions in acetylene, ethylene, benzene, and chlorocyclopropane were also investigated for comparison with previous studies. Pressures read from the ionization gauge were corrected for gauge sensitivity to the gas and then the reaction rate constants were determined in a manner analogous to that used in the methane system. Using the system correction factor obtained from the methane calibration reactions one gets the rate constants k_{corr} in Table 5.1.

Discussion

Several measured quantities involved in the determination of reaction rate constants introduce error into the results. One important factor is reaction time, but this quantity is computer controlled and accurate to within a part per million, thus not a significant source of error. Another factor is the resolution of the digitizer. In this system the 8-bit A/D can distinguish changes of 0.4% in signal intensity, a value much smaller than the noise in the observed ion signal. As can be seen from the plots in Figure 5.2, a few percent precision can be obtained by signal averaging. Pressure measurement inaccuracies are by far the most significant source of errors due in part to the inability to measure accurately the pressure and also due to pressure fluctuations caused by pumping speed changes, leak valve variations, and gas reservoir pressure changes. Another possible source of error is the sensitivity of the ionization gauge measured in the 10^{-6} to 10^{-4} torr pressure range which must be assumed the same for the 10^{-7} torr range.

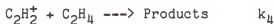
The system correction factor of 1.67 ± 0.21 seems reasonable in light of the location of the ionization gauge, closer to the oil diffusion pump than the cell, and the gas sample inlet to the high vacuum chamber being directly below the cell. This system correction factor indicates a higher pressure at the cell than at the gauge, which is consistent with the facts just presented.

Average rate constants, k_{corr} , for the reactions investigated in this study are presented in Table 5.1 with 95% confidence limits calculated by propagation of errors from the pressure correction factor, ion signal decay rate, gauge sensitivity, and uncertainty in the methane

literature values. The errors are such that all values overlap for the methane system indicating good agreement with the literature. In the acetylene system the reaction of the parent ion with the neutral forms a condensation product which can fragment into various ions and neutrals:



As before, the rate of $k_3 = 10.1 \pm 2.5 \times 10^{-10} \text{ cm}^3/\text{sec}$ compares well with the literature values. A similar case exists for the reaction of C_2H_2^+ and C_2H_4^+ ions in ethylene



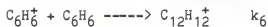
and



Only a few rates have been reported for k_4 while considerable attention has been given to the determination of k_5 . Again, as can be seen in Table 5.1, the results from this study are consistent with the literature values.

There are two possible mechanisms for removal of ions from the cell. The first, which supplies chemical information, is the reaction of the ions with the neutral background gas to generate another ion and often another neutral. The second mechanism, ions diffusing to the cell walls where they are neutralized, complicates the analysis of the data. One can experimentally determine the ion loss rate by looking at a non-reactive or very slowly reacting chemical system so the diffusive losses from the cell are dominant.

The parent ion in benzene is known to react slowly to form a condensation product by



with a rate constant of $1.2 \times 10^{-11} \text{ cm}^3/\text{sec}$ for ions formed by 30 eV electron impact [79]. The rate constant determined may be complicated due to the reformation of $C_6H_6^+$ ions by charge transfer from fragments [83]. The electron impact studies on benzene showed that 57% of the ions formed are the parent [79]. The only ions which can transfer charge to the neutral benzene are $C_4H_4^+$, $C_4H_2^+$, and $C_2H_2^+$ (ionization potentials were taken from Rosenstock et al. [84]) but they initially comprise only 17% of the total ion population at the pressures in these experiments. Our experiments with benzene at a pressure of 1.2×10^{-6} torr, Figure 5.3, show that 74% of the peak parent ion signal remains 500 ms after formation. Assuming no loss from the trapping cell and correcting for the ionization gauge and system correction factor, then the reaction rate constant for the ion decay is $1.4 \pm 1.1 \times 10^{-11} \text{ cm}^3/\text{sec}$. This compares well with the rates reported in the literature.

The slowest ion decay signal, also shown in Figure 5.3, is observed for the reaction of cyclic $C_3H_3^+$ with propargyl chloride:



The calculated reaction rate from this study is $k_7 = 2.8 \pm 1.0 \times 10^{-12} \text{ cm}^3/\text{sec}$. A previous study of this ion reported that no reaction occurs with propargyl chloride [81]. The value obtained does, however, set an upper limit on the ion loss rate which in turn establishes the ion decay detection limit for this instrument. Since almost all experiments involve observation of the ion for times less than 500 ms, cell loss may be neglected.

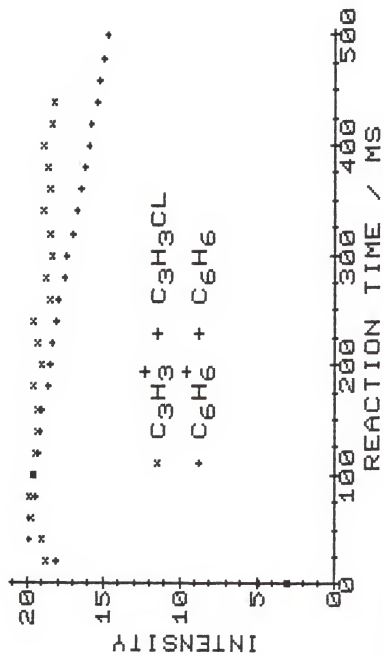


Figure 5.3. Ion decay signals for two different chemical systems showing good trapping efficiency at long times.

Conclusion

The trapping efficiency of the ion cell is sufficient to justify the neglect of non-reactive ion loss processes when determining most rate constants (k 's $> 10^{-11}$). Sensitivity of the ion gauge to gas composition is linear in the pressure range of interest but pressure measurements are by far the most inaccurate quantity measured and must be improved to increase the accuracy of the reaction rates obtained. Our instrument appears to be seeing a representative picture of the reactions of interest as indicated by the agreement of results from this study with previous results.

CHAPTER 6 $C_5H_5^+$ ION STUDIES

Introduction

Soot Formation

The combustion of hydrocarbons in the presence of oxygen is an important process presently being given considerable attention. This process results in the liberation of heat and the formation of various byproducts. Under certain circumstances, however, byproducts such as soot may be undesirable. The mechanism responsible for the formation of soot in fuel rich flames is not very well known but has been the subject of much investigation. A recent review by Calcote discusses this problem in detail [85].

During combustion, the fuel and oxidizer are changed into various neutral molecules, free radicals, and ions by pyrolysis [86], oxidation [87], and chemi-ionization mechanisms [88]. These primary species are low molecular weight and short chain or small cyclic molecules and ions. The reaction of the various fragments with one another and the initial fuel and oxidizer leads to formation of monocyclic and polycyclic aromatic hydrocarbons, PCAH's. This transformation is referred to as "nucleation" and is one of the least understood parts of soot formation. Two schools of thought differ on the major cause of soot nucleation. One emphasizes the role of ions [88], while the other highlights the importance of neutral free radicals [89].

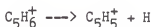
The entire process of soot formation proceeds very rapidly, on the order of milliseconds, even in reduced pressure flames. Kinetic arguments favor the ion-molecule reaction mechanism, due in part to the very fast reaction rates possible for some ions. Another reason is that isomeric rearrangement of ions is known to proceed very rapidly [90]. This is very important in explaining the formation of cyclic aromatic compounds in sooting flames, since cyclization is expected to proceed only slowly for neutral free radicals. At least some thermodynamic arguments tend to favor the ion-molecule mechanism for soot nucleation and also cast doubt on the feasibility of a neutral reaction mechanism to lead to the formation of very large cyclic molecules [85].

A better understanding of the structures and reactivities of ions during nucleation of small molecules to soot should help clarify the mechanism of soot formation. One ion observed in sooting flames, which has been suggested as an intermediate ion leading to soot, is $C_5H_5^+$ [85]. Certainly more studies dealing with the structure and reactivity of this ion would help in the understanding of soot formation and ion chemistry in general.

Thermochemistry of $C_5H_5^+$ Ions

The number of atoms in the $C_5H_5^+$ ion is such that several different linear and cyclic isomers are possible. These isomers cannot be differentiated directly by mass spectrometry and thus can only be inferred from properties such as measured heats of formation and chemical reactivities. Evidence has been reported for the existence of more than one stable isomer but conclusive data as to which isomers exist is still elusive [45].

The appearance potentials of $C_5H_5^+$ ions from a large number of alkylbenzenes and chloro-alkylbenzenes have been measured [91]. Results of this work indicate that in these compounds the $C_5H_5^+$ generated has a heat of formation less than or equal to 284 ± 6 kcal/mole. An earlier study measured the appearance potential of $C_5H_5^+$ from $HC=CCH=CHCH_3$ and calculated a heat of formation of 277 kcal/mole for the ion formed in the reaction



[92]. The linear ionic structure is assumed to result from the fragmentation of this ion, thus leading to a heat of formation of about 280 kcal/mole for linear $C_5H_5^+$ isomers.

Another possible isomer of the $C_5H_5^+$ ion is a five membered ring (cyclopentadiene cation). Using the most recent ionization potential of 8.41 eV for the neutral parent radical [93] and accepting a value of 60.9 kcal/mole for the heat of formation of the neutral [94] leads one to $\Delta H_f = 255$ kcal/mole for the cyclic cation. A separate study reported the appearance energy of $C_5H_5^+$ from $C_6H_5CH_2^+$ (3.55 eV) resulting in a heat of formation of 242 kcal/mole [95]. This lower value suggests the existence of another, more stable, isomer for the $C_5H_5^+$ ion.

Experimental

All experiments were performed at NBS using the single micro-computer controlled ion mass spectrometer described in the single microcomputer section in Chapter 3. Norbornadiene was used to generate two different isomers of $C_5H_5^+$. The internal energy of the ions was controlled via charge transfer reactions to norbornadiene involving CO (I.P. = 14.0 eV [84]). A typical experiment used 1×10^{-6} torr of

norbornadiene with 1 to 2×10^{-6} torr of a reactant gas with CO then added to a total pressure of about 1.5×10^{-5} torr. This procedure insured that most of the hydrocarbon ions were produced by charge transfer and not by direct electron impact of norbornadiene, and also increased the concentration of $C_5H_5^+$ in the icr cell compared to what might be obtained by direct electron impact. The CO^+ ions were produced by electron impact on CO of 25 to 55 eV electrons gated for 5 msec with 40 namp of current seen at the collector plate. $C_5H_5^+$ ions also were prepared by charge transfer from CO^+ to p-chlorotoluene and benzylchloride under the conditions stated above.

Proton transfer reactions of one of the $C_5H_5^+$ isomers were observed under conditions similar to those mentioned above, except that the ions were produced from charge transfer reactions with Ar^+ ($I.P.(Ar) = 15.6$ eV). All experiments were performed at a magnetic field strength of 13 kG and a gas temperature of 61 °C as measured by an iron-constantan thermocouple mounted to the icr cell.

Ion-molecule reaction pathways were determined from double resonance experiments where the reactant ion was ejected out of the cell while a mass sweep was performed through the possible product ions. The double resonance oscillator was gated on, then off, while averaging signals for each ion at a particular frequency. The averaged signal from the oscillator "off" experiments was then subtracted from the "on" data. Product ions appeared as negative going peaks at their characteristic cyclotron frequency.

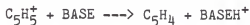
Results

Kinetics and Products

The two different isomers of $C_5H_5^+$ from norbornadiene are evident in the decay curve shown in Figure 6.1. Table 6.1 lists the calculated rate constants and reaction products observed for the "reactive" $C_5H_5^+$ isomer. The rate constants reported were determined by subtracting the unreactive ion signal from the decay curve then running a linear least squares analysis on a semi-log plot of the reactive part of the data. Due to the fast reaction of $C_5H_5^+$ with norbornadiene, rate constants less than $1 \times 10^{-10} \text{ cm}^3/\text{sec}$ with the added reaction gas could not be determined with any useful precision.

Proton Affinities

Four proton transfer reactions of the "unreactive" $C_5H_5^+$ with different bases were performed to bracket the proton affinity of the C_5H_4 neutral produced in the reaction

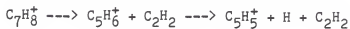


The results of the proton transfer reactions are given in Table 6.2 and indicate a proton affinity of $227.9 \pm 0.3 \text{ kcal/mole}$ for the C_5H_4 neutral [96].

Discussion

Reaction Products and Kinetics

Isotope studies on carbon-13 labeled norbornadiene indicate the main route for $C_5H_5^+$ formation is the following [97].



Two $C_5H_5^+$ structures are produced from norbornadiene [45] but only one,

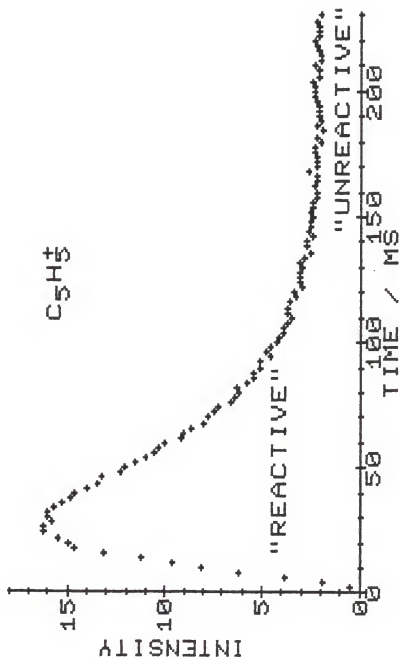


Figure 6.1. Ion decay signal showing the "reactive" and "unreactive" $C_5H_5^+$ isomers. This decay curve is an average of 12 scans at each point taken from a mixture of norbornadiene (1.2×10^{-6} torr) and carbon monoxide (1.0×10^{-5} torr). The ions were trapped at a magnetic field strength of 1.3 T and detected with a capacitance bridge detector gated for 3 msec at a resonance frequency of 309.48 kHz (80 mv p-p).

Table 6.1. Experimental rate constants and reaction products for the "reactive" $C_5H_5^+$ isomer reacting with several neutral molecules.

Reaction			k (cm ³ /sec) / 10 ⁻¹⁰
$C_5H_5^+$	+	C_2D_2 ---->	0.6
	+	C_2H_2 ---->	< 0.1
	+	$HC\equiv CC\equiv CH$ ----> $C_9H_7^+$	2.6 ± 0.7^a
	+	$H_2C=C=CHCH_3$ ----> $C_9H_9^+ + H_2$	2.5 ± 1.0
	+	$H_2C=CHCH=CH_2$ ---->	1.6
	+	C_6H_6 ---->	< 0.1
	+	C_7H_8 (norbornadiene) ----> Products	12.1 ± 1.2
		----> $C_7H_7^+ + C_5H_6$	b
		----> $C_{10}H_9^+ + C_2H_4$	
		----> $C_{10}H_{11}^+ + C_2H_2$	
	+	$C_6H_5CD_3$ ---->	1.2 ± 0.2
	+	$C_6H_5CH=CH_2$ ----> Products	0.9 ± 0.3
		----> $C_8H_9^+ + C_5H_4$	b
		----> $C_{13}H_{13}^+$	
		----> $C_{13}H_{12}^+ + H$	
	+	C_8H_{18} (isooctane) ---->	< 0.1
	+	$C_6H_5i-C_3H_7$ ---->	5.0 ± 1.7
	+	$C_6H_5CH_2Cl$ ----> $C_7H_7^+ + C_5H_5Cl$	3.6 ± 1.3
	+	$p-ClC_6H_5CH_3$ ----> $C_7H_7^+ + C_5H_5Cl$	4.3 ± 0.6

a) 95% confidence intervals given when more than one determination of the rate constant was made.

b) Major reaction pathway.

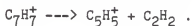
Table 6.2. Results from observations of $C_5H_5^+$ (unreactive structure) formed in norbornadiene with a few additive molecules.

Additive Molecule	Proton Affinity ^a (kcal/mole)	Ionization ^b Potential (eV)	Mode of Reaction	k_{exp} (cm^3/sec)
$(CH_3)_3N$	225.9	7.82	No Reaction	$<10^{-11}$
Azulene	227.6	7.4	No Reaction	$<10^{-11}$
$(n-C_3H_7)_2NH$	228.3	7.84	Proton Transfer	$\approx 10^{-10}$
$(C_2H_5)_3N$	233.0	7.5	Proton Transfer	$>10^{-9}$

a) Proton affinities taken from Aue and Bowers [98].

b) Ionization potentials taken from Rosenstock et al. [84].

the "reactive", is seen when aromatic six-membered rings are used as precursor molecules [97]. In this case the $C_5H_5^+$ is formed from the benzyl or tropylium $C_7H_7^+$ structure by the reaction



Our results agree with the investigation mentioned above in that only the "reactive" isomer was observed when p-chlorotoluene and benzyl-chlorotoluene were used as the source of $C_5H_5^+$ (see results at the bottom of Table 6.1).

The reaction products shown in Table 6.1 indicate most reactions proceed by condensation followed by fragmentation. Many of the products have been seen in flames and have a low hydrogen to carbon atom ratio as found in PACH's. Reaction of $C_5H_5^+$ with the larger neutrals indicates that ions of high molecular weight can be formed quickly by ion-molecule reactions. Benzene and acetylene do not react at an appreciable rate with the $C_5H_5^+$ ion, yet diacetylene and aromatics with side chains do. This suggests soot nucleation may proceed by adding a few large molecules rather than through addition of many smaller ones.

As can be seen from Table 6.1, the rates of many of the reactions reported in this study appear to be occurring at a fraction of the collision rate (which is about $1 \times 10^{-9} \text{ cm}^3/\text{sec}$ for most reactions listed). Little previous work dealing with this ion is reported in the literature. The only literature value known to the author for a reaction similar to those examined in this study is



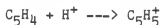
with a rate constant of $7 \times 10^{-11} \text{ cm}^3/\text{sec}$ [76]. This rate compares

reasonably well with our value of $1.2 \pm 0.2 \times 10^{-10}$ cm³/sec determined for partially deuterated toluene reacting with $C_5H_5^+$ from norbornadiene.

The initial steps of soot formation have been computer simulated and demonstrate that large ions evolve rapidly enough to account for the appearance of soot even when using a modest reaction rate constant of 2×10^{-11} cm³/sec for all reactions [88]. Our rates show reactions of $C_5H_5^+$ an order of magnitude faster than those used in the simulation while producing various ions found in flames.

$C_5H_5^+$ Thermochemistry

The proton affinity of C_5H_5 determined in our experiments corresponds to the energy released in the reaction

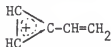


where $C_5H_5^+$ is the unreactive species. Using our value for the proton affinity of C_5H_4 and a heat of formation of 365.7 kcal/mole for H^+ [84] leads to a difference between the heats of formation of "unreactive" $C_5H_5^+$ and C_5H_4 of

$$\Delta H_f(C_5H_5^+) - \Delta H_f(C_5H_4) = 137.8 \text{ kcal/mole.}$$

The $C_5H_5^+$ cannot be the cyclopentadiene cation because the ionization potentials are such that this species would transfer charge to all the bases in Table 6.1.

Assuming that the "unreactive" $C_5H_5^+$ is not the higher energy linear ion, and accepting that it is not the cyclopentadiene ion, then the most likely structure is that below [99].



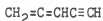
Since McCrery and Freiser formed an ion with a heat of formation of 242 kcal/mole [95], and the next most stable structure (cyclopentadiene cation) has an estimated heat of formation equal to 255 kcal/mole, we will assume that they were forming this ion. If this ion transferred a proton, then the only molecule that could be formed without rearrangement is the following.



The estimated heat of formation of this molecule is about 130 kcal/mole (calculated below) leading to

$$[\Delta H_f(\text{C}_5\text{H}_5^+) - \Delta H_f(\text{C}_5\text{H}_4)] = 112 \text{ kcal/mole}.$$

If rearrangement occurs during proton transfer, a square planar structure may result; however, this is not expected due to the amount of strain present in the molecule. Other C_5H_4 molecules which might result if rearrangement occurs during proton transfer are



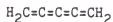
$$[\Delta H_f(\text{C}_5\text{H}_5^+) - \Delta H_f(\text{C}_5\text{H}_4)] = 131 \text{ kcal/mole}$$

or



$$[\Delta H_f(\text{C}_5\text{H}_5^+) - \Delta H_f(\text{C}_5\text{H}_4)] = 140 \text{ kcal/mole}$$

or



$$[\Delta H_f(\text{C}_5\text{H}_5^+) - \Delta H_f(\text{C}_5\text{H}_4)] = 150 \text{ kcal/mole}$$

None of the heats of formation for these neutrals are known and all have been estimated by using the technique of "macro-incrementation" [100].

Instead of adding up the contributions of the bonds as in Benson estimations [101], one estimates the heat of formation using "groups" from molecules of known ΔH_f , choosing molecules having the same structural features (or strain). For example,



$$130 \text{ (est.)} = 96.4 \text{ [102]} + 45.6 \text{ [103]} - 12.45 \text{ [103]}$$

Using this method, an estimate of the heat of formation of the radical corresponding to the "unreactive" C_5H_5^+ ion is 123 kcal/mole. Therefore, we can estimate an ionization potential of about 5.2 eV for this radical, and the observation that the ion does not transfer charge to the amines with ionization potentials of 7.4 to 7.8 eV is consistent with our proton affinity data.

Conclusion

The C_5H_5^+ ion does react rapidly with some of the species found in flames to produce much larger ions which are also seen. The reactions are fast enough to account for the rapid generation of soot in fuel rich flames. These ions, however, are near ground state in energy unlike a significant number of species found in flames. These excited ions may be expected to be even more reactive due their added internal energy.

The "unreactive" C_5H_5^+ ion is most likely the vinylcyclopropenyl structure shown earlier. On the basis of thermodynamic arguments, it can be inferred that this ion deprotonates to give a linear C_5H_4 neutral. The "reactive" C_5H_5^+ could be the cyclopentadiene ion or have a linear structure. However, more experiments are necessary to determine its structure more conclusively.

CHAPTER 7 ION CHEMISTRY OF CH_3I AND CF_3I

Introduction

Ion chemistry

The radiation chemistry of gas phase CH_3I [104,105] , CF_3I [106,107,108], and mixtures of the two [109] have been investigated in recent years. In the CF_3I system, the initial absorption of radiation by CF_3I generates the ionic species CF_3^+ , I^+ , and CF_3I^+ [106]. These ions are believed to produce I_2 via the I radical formed by charge transfer of I^+ to CF_3I , or ion-molecule reactions which generate I_2^+ or I_2 [108]. Free radical scavenger studies support the role of ions in the formation of I_2 from the radiolysis of CF_3I [107]. Iodine seen in the radiolysis of CH_3I [104] and mixtures of CH_3I and CF_3I [109], may be produced through a similar ionic mechanism. End product analysis of irradiated CF_3I and CH_3I mixtures shows a variety of cross product species, CH_3F and CF_3H for examples, and there has been speculation that ion-molecule reactions might be involved in forming some of them [109].

The ion chemistry of CH_3I has been reported previously [110,111], as well as deuterated studies which probed the mechanism of the reactions [112]. The ion chemistry of CF_3I has also been published but with some conflicting results [113,114]. Both the CH_3I and CF_3I work show the production of I^+ as a fragment from ionization, while one of the CF_3I studies reports the formation of I_2^+ [113]. The ion chemistry of the mixture has not been reported to date, yet such a study would shed light on the role of ions in the radiolysis of this system.

Detector limitations

Due to inherent characteristics of the icr m.o. detector used in these studies (see Chapter 2 for details), high mass signals are weak compared to low mass signals under similar conditions. This makes the detection of ions containing more than one iodine difficult at best. The detector sensitivity is inversely proportional to ion mass; thus the S/N ratio at m/e 265 ($CF_3ICF_3^+$) is about four times less than that at m/e 69 (CF_3^+) as determined by use of Equation 2.6. Signal averaging is necessary to pull the signal out of the noise yet one must average 16 of the high mass experiments just to reach the same S/N ratio as one at the low mass. The S/N problem is compounded when low intensity ions are observed in the high mass range.

While the ions are losing intensity at high masses one must also contend with a loss of resolution. A zero pressure resolution for m/e 69 at 12 kG magnetic field strength is 1500 (calculated from Equation 2.3), whereas a maximum of only 392 is possible for m/e 265. Resolution is not a problem in the icr study of CF_3I since the possible products are widely separated in the mass spectrum. However for the CH_3I system, the gain or loss of one hydrogen may be difficult to see. High pressures collisions broaden the peaks, further degrading the resolution by spreading the peak out and decreasing its maximum intensity.

Experimental

Chemicals were purified and supplied by Mr. Dawit Teclemariam and degassed by repeated freeze-pump-thaw cycles. Ionization gauge sensitivities for CH_3I , CF_3I , and a 1:1 mixture were determined in the same fashion as described in the instrument calibration section of

Chapter 5. Values of 1.51 ± 0.09 , 2.19 ± 0.17 , and 1.82 ± 0.19 respectively were obtained (95% confidence intervals given). These sensitivities are such that the 1:1 mixture value equals, within experimental error, half the sum of the component values. All experiments were performed on the dual microcomputer based data system previously described in Chapters 3 and 4. Marginal oscillator signals were averaged from 7 to 30 times for each experiment. Double resonance experiments were performed by sweeping across the frequency of the ion of interest with a function generator and averaging the output of the m.o. detector with the computer. Chemically coupled ions are indicated by a negative-going peak in the spectrum [115].

All fragment ions were formed by 70 eV electron impact on reactant gases in the 3×10^{-7} to 5×10^{-5} torr pressure range. In a typical experiment the electron beam was pulsed for 5 msec while measuring currents of 30 to 600 namp at the collector plate. The trapping, side, and end plates of the icr cell were at +1, -1, and -1 v respectively.

Results

Pure CH_3I

The parent ion, CH_3I^+ , and two fragment ions, CH_3^+ and I^+ , are produced by electron impact of the CH_3I neutral. The product ions $\text{CH}_3\text{ICH}_3^+$ and CH_3I_2^+ were both seen but the condensation dimer $(\text{CH}_3\text{I})_2^+$ could not be detected over the pressure range used in these experiments. Ion decay signals were analyzed by linear least squares analysis of semi-log plots. The results of the experiments on CH_3I are given in Table 7.1. Figure 7.1 shows the presence of CH_2I^+ as a shoulder on the CH_3I^+ mass peak; however, due to the limited resolution of the instrument at this mass, quantitative results could not be obtained for the ion.

Table 7.1. Experimental rate constants for ions observed in pure CH_3I . For comparison, the collision rate constants calculated from the Langevin [116], k_L , and average dipole orientation [117], k_{ADO} , theories are given. All reported error limits are 95% confidence intervals.

All k 's are in $\text{cm}^3/\text{sec} \times 10^{-10}$					
Reaction		k_{exp}	k_{ref}	k_L	k_{ADO}
CH_3^+	$+\text{CH}_3\text{I} \rightarrow \text{CH}_3 + \text{CH}_3\text{I}^+$	19.2 ± 1.2		17.6^a	24.8^b
I^+	$+\text{CH}_3\text{I} \rightarrow \text{I} + \text{CH}_3\text{I}^+$	9.7 ± 2.8		7.9	11.2
CH_3I^+	$+\text{Products}$	0.34 ± 0.12		7.7	10.8
	$\rightarrow \text{I} + \text{CH}_3\text{ICH}_3^+$	0.24	0.237 ± 0.005 [120]		ICRDR ^c
	$\rightarrow \text{CH}_3 + \text{CH}_3\text{I}_2^+$	0.15			ICRDR
$\text{CH}_3\text{ICH}_3^+$	$+\text{Products}$	0.09 ± 0.02		7.5	10.5

a) The polarizability of CH_3I used in the Langevin collision rate calculation is 7.65×10^{-24} [118].

b) The dipole moment of CH_3I used in the ADO collision rate calculation is 1.647 D [118].

c) ICRDR signifies the reaction channel was verified by icr double resonance experiments.

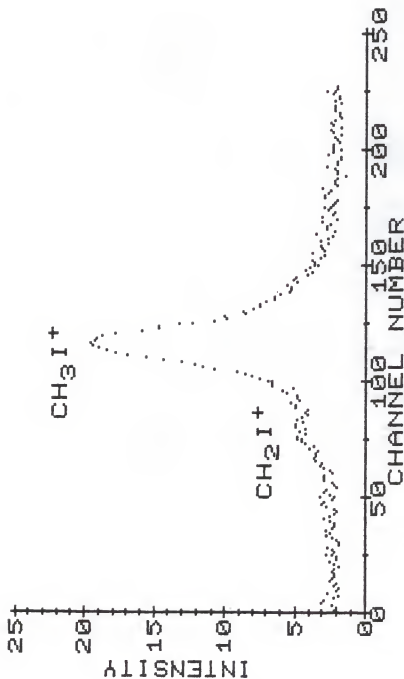


Figure 7.1. Mass spectrum of CH_2I^+ and CH_3I^+ at a pressure of 1.8×10^{-6} torr. The spectrum was obtained from a 500 G magnetic field sweep made in 2.5 min and centered at 12.15 kG. The ions were detected with a marginal oscillator detector at a delay time of 20 msec. Each point is the average of eight passes taken during a single sweep of the magnet.

Pure CF₃I

Ionization by electron impact of trifluoromethyl iodide generated the parent ion and two fragments: I⁺ and CF₃⁺. These species reacted to form various products: CF₂I⁺, I₂⁺, CF₃ICF₃⁺, CF₃I₂⁺, and (CF₃I)₂⁺ in order of decreasing intensity. The latter was seen at very high pressures (5 X 10⁻⁵ torr) and high collector currents (600 namp) as a very broad and weak peak. The results of the experiments are given in Table 7.2.

CH₃I + CF₃I Mixture

The ion chemistry of the mixture looks very much like the ion chemistry of CH₃I. Fragment ions from electron impact of both CH₃I and CF₃I are seen in the mass spectrum of the mixture. The product ions CF₂I⁺, CH₃ICH₃⁺, I₂⁺, and CH₃I₂⁺ appear in the mass spectrum of the mixture. The results of reactions characteristic of the mixture are given in Table 7.3.

DiscussionPure CH₃I

Only a limited number of rate constants have been reported in the literature for the CH₃I system. One reaction studied previously is



resulting in measured rate constants of 0.12 X 10⁻¹⁰ [119] and 0.06 X 10⁻¹⁰ cm³/sec [110]. A more recent value of 0.237 X 10⁻¹⁰ [120] compares well with 0.24 X 10⁻¹⁰ cm³/sec from this study. The previous studies were done by forming the CH₃I⁺ ion with 10 to 11 eV photons [119] or electrons [110] thus generating an ion with little excess

Table 7.2. Experimental rate constants for ions observed in pure CF_3I . For comparison, the collision rate constants calculated from the Langevin, k_L , and average dipole orientation, k_{ADO} , theories are given. All reported error limits are 95% confidence intervals.

Reaction		All k 's are in $\text{cm}^3/\text{sec} \times 10^{-10}$				Comments
		k_{exp}	k_{ref}	k_L	k_{ADO}	
CF_3^+	+ CF_3I ----> Products	2.4 ± 1.0		9.2^a	10.6^b	ICRDR ^c
	----> CF_4 + CF_2I^+	1.2	1.68 [113]			
I^+	+ ----> Products	3.1 ± 0.2		7.5	8.6	ICRDR
	----> I_2^+ + CF_3	1.1	0.79 [113]			
	----> CF_3I^+ + I		3.9 [114]			
CF_3I^+	+ ----> Products	0.74 ± 0.55		7.1	8.2	ICRDR
	----> $\text{CF}_3\text{ICF}_3^+$ + I	0.50 ± 0.18				
	----> CF_3I^+ + CF_3	0.30 ± 0.10	0.03 [113]			
	----> $(\text{CF}_3\text{I})_2^+$	0.18	0.22 [113]			
CF_2I^+	+ ----> Products	0.14		6.8	7.8	
I_2^+	+ ----> Products	0.15		6.2	7.2	
$\text{CF}_3\text{ICF}_3^+$	+ ----> Products	0.29 ± 0.12		6.2	7.1	
CF_3I_2^+	+ ----> Products	0.19 ± 0.08		6.2	7.1	
$(\text{CF}_3\text{I})_2^+$	+ ----> Products	0.14		5.7	6.6	

a) The polarizability of CF_3I was estimated from observed trends in the polarizability of other molecules found in the NBS tables [118] and determined to be $7.87 \times 10^{-24} \text{ cm}^3/\text{molecule}$.

b) The dipole moment of CF_3I used in the ADO collision rate calculations is 0.92 D [118].

c) ICRDR signifies the reaction channel was verified by ion double resonance experiments.

Table 7.3. Experimental rate constants for ions observed in the $\text{CH}_3\text{I} + \text{CF}_3\text{I}$ mixture. For comparison, the collision rate constants calculated from the Langevin, k_L , and average dipole orientation, k_{ADO} , theories are given. All reported error limits are 95% confidence intervals.

Reaction	All k 's are in $\text{cm}^3/\text{sec} \times 10^{-10}$				Comments
	k_{exp}	k_L	k_{ADO}		
$\text{CH}_3^+ + \text{CF}_3\text{I} \longrightarrow \text{CH}_3\text{F} + \text{CF}_2\text{I}^+$	<1	17.6^a	20.2		
$\text{CF}_3\text{I}^+ + \text{CH}_3\text{I} \longrightarrow \text{CF}_3\text{I} + \text{CH}_3\text{I}^+$	6.7	7.1	10.1		ICRDR ^b
$\text{CF}_3^+ + \text{CH}_3\text{I} \longrightarrow \text{CF}_3\text{H} + \text{CH}_2\text{I}^+$	3.0 ± 1.2	9.5	13.4		

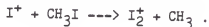
a) See Table 7.1 and 7.2 for the dipole moments and polarizabilities of CH_3I and CF_3I used in the collision rate calculations.

b) ICRDR signifies the reaction channel was verified by icr double resonance experiments.

internal energy; yet their results are in good agreement with those from our experiments, in which the ions were formed by impact with 70 eV electrons. A reaction of $\text{CH}_3\text{ICH}_3^+$ with CH_3I was observed to occur slowly with a rate constant of $9 \pm 2 \times 10^{-12} \text{ cm}^3/\text{sec}$. Unfortunately, the products of this reaction were not determined.

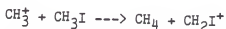
The CH_3I_2^+ detected in this study has been reported in only one earlier investigation [111]. This is due in part to the limited mass range of the icr of Beauchamp et al. [110]. The photoionization experiments concentrated on the formation of the association product and may have missed this low intensity fragment from the association process [119]. Double resonance experiments verified the production of $\text{CH}_3\text{ICH}_3^+$ and CH_3I_2^+ from the parent ion.

The I^+ fragment ion reacts ($k = 9.7 \pm 2.8 \times 10^{-10} \text{ cm}^3/\text{sec}$) via charge transfer with the neutral parent molecule at the collision rate. This is expected due to the difference in ionization potentials of the two species; $\text{I} = 10.451 \text{ eV}$ and $\text{CH}_3\text{I} = 9.54 \text{ eV}$ [84]. This also explains the absence of I_2^+ , seen in the CF_3I system, since it would most likely be produced by the reaction



This reaction channel evidently cannot compete with the fast charge transfer reaction.

The CH_3^+ fragment ion is believed to react rapidly via the reaction



as suggested earlier [110]. However, the reported ionization potential of 9.83 eV for the methyl radical [84] indicates charge transfer is also

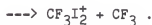
possible between the fragment ion and neutral parent molecule. The rate constant obtained ($19.2 \pm 1.2 \times 10^{-10}$ cm³/sec) has no literature value for comparison. However, the reaction appears to proceed at the collision rate. The low intensity of CH_2I^+ relative to CH_3I^+ seen in Figure 7.1 suggests that the charge transfer reaction is dominant. This is in contrast to isotope studies on reactions of CD_3^+ with CH_3I which indicate both reactions do occur but the reaction producing methane is of primary importance [112]. This reaction, which could explain the formation of methane in the radiolysis of CH_3I , has been postulated by Teclemariam and Hanrahan [109].

Pure CF_3I

The parent ion produced from CF_3I reacts to form a variety of products. Analogous to the CH_3I system, $\text{CF}_3\text{ICF}_3^+$ and CF_3I_2^+ are produced through the reactions



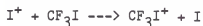
and



These reactions occur at the same or slightly faster rate than in the CH_3I system. Earlier work did not report the formation of $\text{CF}_3\text{ICF}_3^+$ yet did report ions of heavier mass (CF_3I_2^+ and $\text{CF}_3\text{I}_2\text{CF}_3^+$) [113]. A low pressure study (1.7×10^{-7} torr maximum) on CF_3I failed to identify any ions of mass greater than CF_3I^+ [114]. This is to be expected due to the small rate constants involved for many of the reactions forming the heavy product ions. The formation of the $(\text{CF}_3\text{I})_2^+$ dimer is observed at 5×10^{-5} torr, unlike the corresponding dimer ion in pure CH_3I . The association reactions in methyl iodide show an increase in rate when

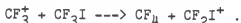
deuterium is substituted for the hydrogens in the methyl iodide molecule [120]. This isotope effect is attributed to a decrease in the vibrational frequency of the C-H bond and the resulting increase in the density of vibrational states. When fluorine atoms take the place of hydrogens in methyl iodide one would expect an enormous change in vibrational frequency along with a greatly increased density of states. This makes the fluorinated compound better suited to partition the energy of association internally, thus stabilizing the ion without the help of a third body.

The fragment ion I^+ reacts to form I_2^+ as demonstrated by icr double resonance experiments. The charge transfer reaction:



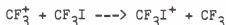
was reported earlier [113].

Analogous to the methyl iodide ion chemistry the fragment CF_3^+ reacts to form CF_2I^+ via the reaction:



Previous work in a time of flight mass spectrometer with a high pressure source did not detect a decay mechanism for the CF_2I^+ ion [113]. The difference between this observation and the above reaction seen in an icr, was explained in terms of energy differences for the reacting ions. It was suggested that the ions in the icr retain some excess energy, while those in the high pressure source mass spectrometer were presumably thermalized. Our experiments do show a slow reaction with a rate constant of $1.4 \times 10^{-11} \text{ cm}^3/\text{sec}$. However, any excess internal energy in the ion should be removed through the numerous non-reactive

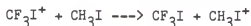
collisions suffered before reaction occurs. The total loss of CF_3^+ cannot be accounted for by the above reaction alone, yet the charge transfer reaction



proposed in an earlier study [113] is too endothermic to be seen in an icr experiment. This is due to the difference in ionization potentials of CF_3I (10.23 eV) and CF_3 (9.25 eV) [84].

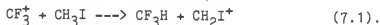
$\text{CH}_3\text{I} + \text{CF}_3\text{I}$ Mixture

The CH_3I ion chemistry appears to dominate in the ion chemistry of the mixture. This is due in part to the loss of CF_3I^+ through charge transfer in the reaction



which is thermodynamically favored due to the difference in ionization potentials between CH_3I (9.54 eV) and CF_3I (10.23 eV). The slower reactions of CF_3I^+ which produce the species CF_3I_2^+ , $\text{CF}_3\text{ICF}_3^+$, and $(\text{CF}_3\text{I})_2^+$ cannot compete with this reaction channel. The above charge transfer reaction was verified by icr double resonance experiments.

The CH_3^+ ion generated from electron impact of methyl iodide does not react with the neutral CF_3I molecule since its decay rate in the mixture can be accounted for by the reactions seen in the pure CH_3I system. The CF_3^+ ion, however, does react with the CH_3I molecule with a rate constant of $3.0 \pm 1.2 \times 10^{-10} \text{ cm}^3/\text{sec}$. The equation for this reaction is assumed to be

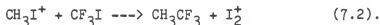


Unfortunately, no previous work has been reported for comparison of rate constants for the mixture.

The iodine ions produced in the mixture appear, not surprisingly, to undergo the same reactions observed in the two pure systems. The production of I_2^+ can be explained by



or by



There seems to be an absence of cross product ions containing hydrogens and fluorines but neutral cross product species do seem probable.

Conclusion

The ion chemistry of pure CH_3I and pure CF_3I are similar in many respects including the production of CH_4 , CH_2I^+ , and their fluorinated analogs. The ion chemistry of the mixture resembles the chemistry of the CH_3I system due to charge transfer from CF_3I^+ to CH_3I . The mixture does not show the presence of ionic cross product species, but the ion molecule reactions determined in this study do indicate the formation of neutral cross product species (see reactions 7.1 and 7.2 above).

A marginal oscillator detector on an icr mass spectrometer is not normally noted for its operation in the high mass region. However, with the signal averaging capabilities of a computer controlled data acquisition system low intensity ions up to mass 400 can be probed for chemical information.

APPENDIX A BASIC PROGRAM

The subsequent text and program listing describe the BASIC program used to control the marginal oscillator detector on our icr spectrometer. Understanding of the code requires a good knowledge of the APPLESOFT II BASIC language and the DOS 3.3 disk operating system. The appropriate manuals should be consulted for the function and syntax of the various commands [121].

Due to the interpreting mechanism of the BASIC language, program execution time is shortened by placing more frequently used routines early in the program and less used code towards the end. Memory space is conserved and execution time shortened by not using remark statements in the program. To aid in deciphering of the code, Table A.1 identifies numbered sections of the BASIC routine and their purpose.

The most important part of software initialization is the defining of certain variables and an array used by the machine code programs described in Appendix B. The first four variables defined must be the data, D%, number of passes, PA%, KIM program vector, KV%, and KIM status, KE%. The names are not important but they must be integers in the order given. Next, the first array defined must be the pulse parameter integer array PP%(8,1), nine long by two wide. All variables must be as indicated to insure proper communication between the routines.

Table A.1. List of ICR-MO code sections along with line numbers and brief description of the routine.

Line Number

<u>From</u>	<u>To</u>	<u>Routine Description</u>
10	30	Pulse parameter set up
50	54	Data plotting
100	110	Get data and key command check
200	250	Continuous scan experiment
260	370	Detect delay sweep experiments
400	420	Signal average scan experiment
800	840	String input and evaluation
900	910	Key command input
920	1080	Print experiment parameters
1300	1320	Print experiment numerical values
1500	1680	Key command interpreter
1700	1920	Experiment parameter alteration
2000	2170	Print experiment conditions
2200	2230	Print condition numerical values
2405	2490	Condition change command interpreter
2500	2680	Experiment condition alteration
4000	4180	Experiment parameter limit check
5000	5070	Store data on disk
5100	5140	Print hardcopy of parameters and conditions
5400	5500	Load parameter file from disk
5505	5550	Save parameter file on disk
5800	5830	Disk error handler
5900	5910	Disk catalog
6000	6200	Mass calculation
6500	6597	Rate constant calculation
7000	7040	Print data hardcopy
7400	7430	Load KIM's control program
7500	7900	Cursor movement routine
8000	9000	Numbered command display and interpreter
10000	10040	Initialize arrays, variables, and parameters

The plot data routine takes X,Y pairs, checks for Y value under- and overflows, then displays them as points on the high resolution graphics screen. The routine which activates the Apple machine code also checks for key commands pressed during the machine code execution. When a key is pressed the machine code routine is left and the key command interpreted and executed. The program then reenters the machine code, waiting for data from the KIM or another key. The string input and evaluation routine accepts characters during experiment parameter or condition changes and returns the numerical value of the expression in the variable PAR. If the string cannot be evaluated the error flag, ER, is set to one, otherwise it is zero. Disk errors handled by the designated routine result in the display of the error number and sounding of the bell, then program control returns to the numbered command display and input routine. The code for printing hardcopy of the parameters and conditions assumes that the printer interface card is in slot 1.

The following is a listing of the BASIC program ICR-MO.

```

1  GOTO 10000
10 PP%(2,0) = TD * TW:PP%(2,1) = (TD + DW) * TW:PP%(1,0) =
   PP%(2,0):PP%(1,1) = PP%(1,0) + 1:PP%(3,0) = PP%(2,1):PP%(3,1)
   = PP%(2,1) + 1: RETURN
20 PP%(4,0) = WD * TW:PP%(4,1) = (WD + WW) * TW: RETURN
30 PP%(7,0) = QD * TW:PP%(7,1) = (QD + QW) * TW:PP%(8,0) = DC
   * TW:PP%(0,1) = GW * TW: RETURN
50 YV = 159 - INT (YV * FE + .5): IF YV > 159 THEN YV = 159:
   GOTO 54
52 IF YV < 0 THEN YV = 0
54 HPLOT XV,YV: RETURN
100 CALL 2048: IF KE% < > 0 THEN A = PEEK ( - 16384) - 128:
   POKE - 16368,0: GOSUB 1500: GOTO 100
110 RETURN
200 TD = DD: GOSUB 10: HGR :KV% = - 23912
210 CALL 62450:ME = 0: FOR I = 0 TO 279
240 GOSUB 100:DA(I,0) = D%:N = I + 1:XV = I:YV = D%: GOSUB 50
250 NEXT : GOTO 210
260 POKE - 16304,0:N = 0:XS = 279 / DD: IF DD / DS > 280

```

```

THEN EX = 0: PRINT BE$: GOTO 900
270 KV% = - 23854:TD = 0: GOSUB 10:XV = 0:PP%(0,1) = 0:Z = 1:
  GOSUB 100: FOR TD = 0 TO DD STEP DS: GOSUB 10:PP%(0,1) = GW *
  TW: GOSUB 100:DV = D%:DA(N,Z) = DV / PA%
280 YV = DA(N,Z): GOSUB 50:Z = 0:XV = INT (XS * TD + .5): IF
  MD% = 4 THEN PP%(0,1) = 0: GOSUB 100:DV = D%:DA(N,Z) = DV /
  PA%:YV = DA(N,Z): GOSUB 50:Z = 1:
290 IF TD = 0 AND Z = 0 THEN NEXT
295 N = N + 1: NEXT
300 KV% = - 23912:PP%(0,1) = GW * TW: GOSUB 100:DV =
  D%:DA(N,Z) = DV / PA%:YV = DA(N,Z): GOSUB 50
305 IF MD% = 3 THEN N = N + 1: GOTO 370
310 C = 0:T = 0:U = 0:V = 0:W = 0: FOR I = 1 TO N:X = I - 1:Y
  = DA(I,1):C = C + X:T = T + Y:U = U + X * X:V = V + Y * Y:W =
  W + X * Y: NEXT
320 B = (N * W - C * T) / (N * U - C * C):AA = (T - B * C) / N
325 XV = 0:YV = AA: GOSUB 50:YL = YV:XV = 279:YV = AA + B * (N
  - 1): GOSUB 50: HPLLOT TO 0,YL
360 FOR I = 0 TO N - 1:DA(I,0) = DA(I,0) - (AA + B * I): NEXT
370 EX = 0: GOTO 900
400 POKE - 16304,0:KV% = - 23854:TD = DD: GOSUB 10:PP%(0,1)
  = GW * TW: GOSUB 100
410 FOR I = 0 TO 278: GOSUB 100:DV = D%:DA(I,0) = DV / PA%:YV
  = DA(I,0):XV = I: GOSUB 50:N = I + 1: NEXT
420 KV% = - 23912: GOSUB 100:DV = D%:DA(N,0) = DV / PA%:YV =
  DA(N,0):XV = N: GOSUB 50:N = N + 1:EX = 0: GOTO 900
800 ER = 0:B$ = CHR$ (32)
810 GET A$: IF A$ < > CHR$ (13) THEN B$ = B$ + A$: PRINT
  A$;: GOTO 810
820 IF LEN (B$) < 2 THEN ER = 1: RETURN
830 A$ = MID$ (B$,2,1): IF A$ = "0" THEN PAR = 0: RETURN
840 PAR = VAL (B$): RETURN
900 GOSUB 920
910 GOSUB 1680: VTAB PV%: GET A$:A = ASC (A$): GOSUB 1500:
  GOTO 910
920 TEXT : HOME
930 PRINT "MO EXPERIMENT PARAMETERS": PRINT
940 PRINT "GRID PULSE WIDTH"; TAB( 27);GW; TAB( 36);"MSEC"
950 PRINT "DETECT PULSE DELAY"; TAB( 27);DD; TAB( 36);"MSEC"
960 PRINT TAB( 14);"STEP"; TAB( 27);DS; TAB( 36);"MSEC"
970 PRINT TAB( 14);"WIDTH"; TAB( 27);DW; TAB( 36);"MSEC"
980 PRINT "W2 PULSE DELAY"; TAB( 27);WD; TAB( 36);"MSEC"
990 PRINT TAB( 10);"WIDTH"; TAB( 27);WW; TAB( 36);"MSEC"
1000 PRINT "QUENCH PULSE DELAY"; TAB( 27);QD; TAB( 36);"MSEC"
1010 PRINT TAB( 14);"WIDTH"; TAB( 27);QW; TAB( 36);"MSEC"
1020 PRINT "DUTY CYCLE TIME"; TAB( 27);DC; TAB( 36);"MSEC"
1060 PRINT "SCAN MODE"; TAB( 27);MD%
1070 PRINT "NUMBER OF PASSES"; TAB( 27);PA%
1080 RETURN
1300 POKE 33,9: POKE 32,26: POKE 34,2: HOME
1310 PRINT GW: PRINT DD: PRINT DS: PRINT DW: PRINT WD: PRINT
  WW: PRINT QD: PRINT QW: PRINT DC: PRINT MD%: PRINT PA%
1320 RETURN
1500 IF EX = 1 GOTO 1540

```

```

1505 IF A = 3 THEN GOSUB 7500: RETURN
1510 IF A = 17 THEN POP : GOTO 9000
1515 IF A = 11 THEN GOSUB 6500: RETURN
1520 IF A = 27 THEN POP : GOTO 8000
1530 IF A = 16 THEN POP : EX = 1: ON MD% GOTO 200,400,260,260
1540 IF A = 1 AND EX < > 0 THEN POP : PP%(0,1) = GW *
    TW:TD = DD:KV% = - 23912: CALL 2048:EX = 0: GOTO 900
1545 IF A = 18 THEN GOSUB 100: GOSUB 1300: RETURN
1570 IF A = 5 THEN CALL 62450:ME = 0: RETURN
1580 IF A = 7 THEN POKE - 16304,0: RETURN
1590 IF A = 20 THEN POKE - 16303,0: RETURN
1610 IF A = 13 THEN GOSUB 1700: RETURN
1620 IF A = 43 THEN SD = 1: GOSUB 4000: GOSUB 1300: RETURN
1630 IF A = 45 THEN SD = - 1: GOSUB 4000: GOSUB 1300: RETURN
1640 IF A = 8 THEN PV% = PV% - 1
1650 IF A = 21 THEN PV% = PV% + 1
1660 IF PV% < 3 THEN PV% = 13
1670 IF PV% > 13 THEN PV% = 3
1680 POKE 32,25: POKE 33,1: POKE 34,2: HOME : VTAB PV%: PRINT
    ">": VTAB PV%: RETURN
1700 POKE 32,26: POKE 33,9: VTAB PV%: HTAB 1: GOSUB 800
1710 IF ER = 1 THEN RETURN
1720 IF PAR < 0 THEN RETURN
1730 TP% = TW * PAR:PAR = TP% / TW
1740 ON PV% - 2 GOTO 1780,1790,1800,1810,20,1830,1840,1850,
    1860,1900,1910
1770 GOTO 1500
1780 GW = PAR: GOTO 1920
1790 DD = PAR: GOTO 1920
1800 DS = PAR: GOTO 1920
1810 DW = PAR: GOTO 1920
1820 WD = PAR: GOTO 1920
1830 WW = PAR: GOTO 1920
1840 QD = PAR: GOTO 1920
1850 QW = PAR: GOTO 1920
1860 DC = PAR: GOTO 1920
1900 IF EX = 0 THEN MD% = PAR: GOTO 1920
1905 PRINT BE$: GOSUB 1300: RETURN
1910 PA% = PAR: GOTO 1920
1920 SD = 0: GOSUB 4000: GOSUB 1300: RETURN
2000 TEXT : HOME
2010 PRINT "MO EXPERMENT CONDITIONS"
2020 PRINT : PRINT "ELECTRON BEAM :"
2030 HTAB 5: PRINT "GRID POTENTIAL"; TAB( 27);GV; TAB(
    36);"VOLT"
2040 HTAB 5: PRINT "FILAMENT POTENTIAL"; TAB( 27);FV; TAB(
    36);"VOLT"
2050 HTAB 5: PRINT "COLLECTOR POTENTIAL"; TAB( 27);CV; TAB(
    36);"VOLT"
2070 HTAB 5: PRINT "COLLECTOR CURRENT"; TAB( 27);CC; TAB(
    36);"NAMP"
2080 PRINT "CELL POTENTIALS: UPPER"; TAB( 27);UV; TAB(
    36);"VOLT"
2090 HTAB 18: PRINT "LOWER"; TAB( 27);LV; TAB( 36);"VOLT"

```

```

2100 HTAB 18: PRINT "SIDE(F)"; TAB( 27);SF; TAB( 36);"VOLT"
2105 HTAB 18: PRINT "SIDE(C)"; TAB( 27);SC; TAB( 36);"VOLT"
2110 HTAB 18: PRINT "END1"; TAB( 27);E1; TAB( 36);"VOLT"
2115 HTAB 18: PRINT "END2"; TAB( 27);E2; TAB( 36);"VOLT"
2120 PRINT "MAGNETIC FIELD STRENGTH"; TAB( 27);MF; TAB(
36);"KG"
2130 PRINT "TEMPERATURE"; TAB( 27);TC; TAB( 36);"C"
2140 PRINT "R.F. LEVEL"; TAB( 27);EP; TAB( 36);"MV"
2150 PRINT "W1 FREQUENCY"; TAB( 27);W1; TAB( 36);"KHZ"
2160 PRINT "W2 FREQUENCY"; TAB( 27);WF; TAB( 36);"KHZ"
2165 PRINT "PRESSURE"; TAB( 27);PR; TAB( 36);"TORR"
2170 RETURN
2200 POKE 33,9: POKE 32,26: POKE 34,3: HOME
2210 PRINT GV: PRINT FV: PRINT CV: PRINT CC: PRINT UV: PRINT
LV: PRINT SF: PRINT SC: PRINT E1: PRINT E2: PRINT MF: PRINT
TC: PRINT EP: PRINT W1: PRINT WF: PRINT PR
2230 RETURN
2405 GOSUB 2000
2410 GOSUB 2200
2415 POKE 32,25: VTAB TV%: HTAB 1
2420 GET A$:A = ASC (A$)
2430 IF A = 8 THEN TV% = TV% - 1: GOTO 2470
2440 IF A = 21 THEN TV% = TV% + 1: GOTO 2470
2450 IF A = 27 THEN TEXT : VTAB 20: GOTO 8000
2460 IF A = 13 THEN 2500
2470 IF TV% < 4 THEN TV% = 19: GOTO 2415
2480 IF TV% > 19 THEN TV% = 4: GOTO 2415
2490 GOTO 2415
2500 POKE 32,26: VTAB TV%: HTAB 1: GOSUB 800
2510 IF ER = 1 GOTO 2410
2520 ON TV% - 3 GOTO 2540,2550,2560,2580,2590,2600,2610,2615,
2620,2625,2630,2640,2650,2660,2670,2680
2530 GOTO 2410
2540 GV = PAR: GOTO 2410
2550 FV = PAR: GOTO 2410
2560 CV = PAR: GOTO 2410
2580 CC = PAR: GOTO 2410
2590 UV = PAR: GOTO 2410
2600 LV = PAR: GOTO 2410
2610 SF = PAR: GOTO 2410
2615 SC = PAR: GOTO 2410
2620 E1 = PAR: GOTO 2410
2625 E2 = PAR: GOTO 2410
2630 MF = PAR: GOTO 2410
2640 TC = PAR: GOTO 2410
2650 EP = PAR: GOTO 2410
2660 W1 = PAR: GOTO 2410
2670 WF = PAR: GOTO 2410
2680 PR = PAR: GOTO 2410
4000 ON PV% - 2 GOTO 4020,4030,4040,4050,4060,4070,4080,4090,
4100,4140,4150
4010 RETURN
4020 UL = 25:LL = 0:S = SD * .5:V = GW: GOSUB 4160:GW = V:
GOSUB 30: RETURN

```

```

4030 UL = QD - DW:LL = 0:S = SD * DS:V = DD: GOSUB 4160:DD =
      V:TD = DD: GOSUB 10: RETURN
4040 UL = 100:LL = 0:S = SD * 5:V = DS: GOSUB 4160:DS = V:
      RETURN
4050 UL = 25:LL = 1.5:S = SD * .5:V = DW: GOSUB 4160:DW = V:
      GOSUB 10: RETURN
4060 UL = 16000:LL = 0:S = SD * 10:V = WD: GOSUB 4160:WD = V:
      GOSUB 20: RETURN
4070 UL = 16000:LL = 0:S = SD * 10:V = WW: GOSUB 4160:WW =
      V:SW = WW: GOSUB 20: RETURN
4080 UL = DC - QW:LL = 0:S = SD * 100:V = QD: GOSUB 4160:QD =
      V: GOSUB 30: RETURN
4090 UL = 10:LL = 0:S = SD * 1:V = QW: GOSUB 4160:QW = V:
      GOSUB 30: RETURN
4100 UL = 16000:LL = QD + QW:S = SD * 100:V = DC: GOSUB
4160:DC = V: GOSUB 30: RETURN
4140 IF EX = 0 THEN UL = 4:LL = 1:S = SD * 1:V = MD$: GOSUB
4160:MD$ = V: RETURN
4145 PRINT BE$: RETURN
4150 UL = 256:LL = 1:S = SD * 1:V = PA$: GOSUB 4160:PA$ = V:
      RETURN
4160 V = V + S: IF V > UL THEN V = UL: PRINT BE$: RETURN
4170 IF V < LL THEN V = LL: PRINT BE$
4180 RETURN
5000 TEXT : PRINT : FLASH : PRINT "INSERT DATA DISK": NORMAL
5010 INPUT "ENTER FILENAME : ";DN$
5020 ONERR GOTO 5800
5030 PRINT D$;"VERIFY";DN$
5040 POKE 216,0: PRINT : PRINT "FILE ALREADY EXISTS!!!";BE$:
      PRINT "RE";
5045 GOTO 5010
5050 ONERR GOTO 5810
5060 PRINT D$;"OPEN";DN$: PRINT D$;"WRITE";DN$: PRINT TW * N:
      FOR I = 0 TO N - 1: ON MD$ GOTO 5061,5061,5062,5062
5061 PRINT I: GOTO 5064
5062 PRINT I * DS: GOTO 5064
5064 PRINT DA(I,0): NEXT : PRINT D$;"CLOSE";DN$: PRINT
      D$;"VERIFY";DN$
5070 POKE 216,0
5100 PRINT : PRINT "PARAMETER HARDCOPY (Y/N)? ";
5110 INPUT A$: IF A$ = "N" GOTO 8000
5120 IF A$ < > "Y" GOTO 5100
5122 GOSUB 5125: PRINT CHR$ (12);D$;"PR#0": GOTO 8000
5125 PRINT : INPUT "DESCRIPTION: ";DS$
5130 PRINT D$;"PR#1": PRINT CHR$ (29);D$;"IN#1": PRINT CHR$
      (23);"CS": PRINT D$;"PR#0": INPUT T$: PRINT D$;"IN#0":DA$ =
      MID$ (T$,3,8):T$ = MID$ (T$,12,8)
5135 PRINT D$;"PR#1": PRINT CHR$ (9);"T"
5140 PRINT : PRINT "FILENAME: ";DN$: PRINT : PRINT
      "DESCRIPTION: ";DS$: PRINT : PRINT "DATE: ";DA$: PRINT :
      PRINT "TIME: ";T$: PRINT : GOSUB 930: PRINT : GOSUB 2010:
      RETURN
5400 GOSUB 5405: GOTO 8000
5405 TEXT : HOME : INPUT "ENTER PARAMETER FILENAME: ";PN$: IF

```

```

LEN (PN$) = 0 THEN PN$ = "EXP PARAMETERS"
5410 ONERR GOTO 5150
5420 PRINT D$;"OPEN";PN$;"D1";D$;"READ";PN$
5430 INPUT GW: INPUT DD: INPUT DS: INPUT DW: INPUT WD: INPUT
    WW: INPUT QD: INPUT QW: INPUT DC: INPUT MD$: INPUT PA%
5440 INPUT GV: INPUT FV: INPUT CV: INPUT CC: INPUT UV: INPUT
    LV: INPUT SF: INPUT SC: INPUT E1: INPUT E2: INPUT MF: INPUT
    PR: INPUT EP: INPUT W1: INPUT WF: INPUT TC
5450 PRINT D$;"CLOSE";PN$: POKE 216,0: RETURN
5500 GOSUB 5505: GOTO 8000
5505 TEXT : HOME : INPUT "ENTER PARAMETER FILENAME: ";PN$: IF
    LEN (PN$) = 0 THEN PN$ = "EXP PARAMETERS"
5510 ONERR GOTO 5150
5520 PRINT D$;"OPEN";PN$;"D1";D$;"WRITE";PN$
5530 PRINT GW: PRINT DD: PRINT DS: PRINT DW: PRINT WD: PRINT
    WW: PRINT QD: PRINT QW: PRINT DC: PRINT MD$: PRINT PA%
5540 PRINT GV: PRINT FV: PRINT CV: PRINT CC: PRINT UV: PRINT
    LV: PRINT SF: PRINT SC: PRINT E1: PRINT E2: PRINT MF: PRINT
    PR: PRINT EP: PRINT W1: PRINT WF: PRINT TC
5550 PRINT D$;"CLOSE";PN$: POKE 216,0: RETURN
5800 IF PEEK (222) = 6 GOTO 5050
5810 PRINT : PRINT "DISK ERROR! ERROR NUMBER = "; PEEK
    (222);BE$
5820 PRINT : PRINT "PRESS ANY KEY TO CONTINUE": GET A$
5830 POKE 216,0: GOTO 8000
5900 TEXT : PRINT D$;"CATALOG": PRINT : PRINT "PRESS ANY KEY
    TO CONTINUE";
5910 GET A$: GOTO 8000
6000 TEXT : HOME
6005 PRINT "ENTER A ZERO FOR THE UNKNOWN PARAMETER": PRINT
6010 INPUT "ION MASS (G/M) ? ";MI
6020 INPUT "MAGNETIC FIELD STRENGTH (TESLA) ? ";M
6030 INPUT "CYCLOTRON FREQUENCY (KHZ) ? ";CF
6050 IF MI < = 0 THEN MI = MF * 1.53575E7 / (CF * 1000):
    GOTO 6100
6060 IF M < = 0 THEN M = CF * 1000 * MI / 1.5357E7: GOTO
    6100
6070 CF = M * 1.5357E7 / (MI * 1000)
6100 PRINT : PRINT "ION MASS (G/M) ";MI
6105 PRINT "MAGNETIC FIELD (TESLA) ";M
6110 PRINT "CYCLOTRON FREQ. (KHZ) ";CF
6150 PRINT : PRINT "PRESS ANY KEY TO CONTINUE": GET A$
6200 GOTO 8000
6500 TEXT : HOME : IF MD% = 4 OR MD% = 3 GOTO 6507
6502 PRINT : PRINT "SCAN MODE ERROR";BE$: GOTO 6590
6507 INPUT "FIRST, LAST POINTS: ";FP,LP
6508 INPUT "OFFSET: ";KS
6510 IF FP < 1 OR LP > N THEN PRINT "LIMIT ERROR";BE$: GOTO
    6590
6520 IF FP > = LP THEN PRINT "RANGE ERROR";BE$: GOTO 6590
6530 PRINT : TK = 0: NK = 0: FOR I = FP TO LP - 1: PRINT I;"",
    "I + 1; TAB( 15); "I/IO = ";
6533 IF DA(I - 1,0) = 0 THEN R = 0: GOTO 6537
6535 R = (DA(I,0) - KS) / (DA(I - 1,0) - KS): TK = TK + R

```

```

6537 PRINT R:NK = NK + 1: NEXT
6538 AK = TK / NK: PRINT : PRINT "AVERAGE I/IO = ";AK
6540 PK = - LOG (AK) * (TC + 273) * 1000 / (DS * 3.53539E16
      * 273): PRINT : PRINT "PRELIMINARY K = ";PK
6590 PRINT : INPUT "SATISFACTORY (Y:N) ? ";A$: IF A$ = "Y"
      THEN GOSUB 920: RETURN
6595 IF A$ = "N" GOTO 6507
6597 GOTO 6590
7000 DN$ = "NONE": GOSUB 5125: PRINT : ON MD$ GOTO
      7010,7010,7020,7020,7030,7030,7030
7010 PRINT "POINT"; TAB( 10);"INTENSITY": FOR I = 0 TO N - 1:
      PRINT TAB( 2);I + 1; TAB( 10);DA(I,0): NEXT : GOTO 7040
7020 PRINT "POINT"; TAB( 10);"TIME"; TAB( 20);"INTENSITY":
      FOR I = 0 TO N - 1: PRINT TAB( 2);I + 1; TAB( 10);I * DS;
      TAB( 20);DA(I,0): NEXT
7040 PRINT CHR$( 12);D$;"PR#0": GOTO 8000
7400 POKE 49360,0: POKE 49362,0: PRINT D$;"BLOAD KIM MO
      CODE": POKE 49361,0
7410 FLASH : PRINT : PRINT "KIM INITIALIZATION INSTRUCTIONS
      ": NORMAL
7420 PRINT : PRINT "ENTER KIM KEYBOARD INSTRUCTIONS ": PRINT
      : PRINT " RS": PRINT " AD 00F1": PRINT " DA 04": PRINT
      " AD 17FA": PRINT " DA 8E": PRINT " + A2"
7430 PRINT : PRINT "PRESS ANY KEY TO CONTINUE": GET A$:A =
      PEEK (49362) + PEEK (49363): GOTO 8000
7500 GOSUB 7800: POKE - 16304,0
7510 CP = INT ( PDL (1) * 4 + PDL (0) / 8):A = PEEK ( -
      16384): IF A > 127 THEN POKE - 16368,0: POKE - 16303,0:
      RETURN
7525 NX = INT (CP * (N - 1) / 1031 + .5)
7528 IF NL = NX GOTO 7510
7529 IF ME < > 0 THEN XDRAW 1 AT XL,YL
7530 ON MD$ GOTO 7540,7540,7560,7570
7540 XV = NX:YV = DA(NX,0):DV = NX:CI = YV: GOTO 7600
7560 XV = INT (NX * DS * XS + .5):YV = DA(NX,0):CI = YV:DV =
      NX * DS: GOTO 7600
7570 XV = INT (NX * DS * XS + .5):YV = DA(NX,0) + (AA + B *
      NX):CI = DA(NX,0):DV = NX * DS
7600 GOSUB 50: XDRAW 1 AT XV,YV:ME = 1:XL = XV:YL = YV
7700 GOSUB 7900:NL = NX: GOTO 7510
7800 POKE 32,0: POKE 33,40: POKE 34,20: HOME : PRINT
      "POINT": PRINT "X VALUE": PRINT "INTENSITY": GOSUB 7900:
      RETURN
7900 POKE 32,11: POKE 33,20: POKE 34,20: HOME : PRINT NX + 1:
      PRINT DV: PRINT CI: RETURN
8000 F$ = FRE (0):EX = 0: POKE - 16254,0:: POKE - 16297,0
8010 TEXT : HOME : HTAB 15: FLASH : PRINT "MO PROGRAM":
      NORMAL
8020 PRINT : PRINT
8030 PRINT "COMMANDS : "
8040 PRINT "1...EXIT PROGRAM"
8050 PRINT "2...STORE DATA ON DISK"
8060 PRINT "3...CATALOG DISK"
8070 PRINT "4...UPDATE EXPERIMENTAL CONDITIONS"

```

```

8080 PRINT "5...CHANGE PARAMETERS"
8090 PRINT "6...MASS CALCULATION"
8100 PRINT "7...LOAD PARAMETER FILE"
8110 PRINT "8...SAVE PARAMETER FILE"
8120 PRINT "9...PRINT DATA"
8130 PRINT "10...LOAD KIM PROGRAM"
8310 PRINT : INPUT "COMMAND ? ";CMD$
8320 ON CMD$ GOTO 9000,5000,5900,2405,900,6000,5400,5500,
      7000,7400
8330 PRINT : PRINT "ILLEGAL COMMAND !";BE$
8340 GOTO 8310
9000 TEXT : END
10000 D% = 0:PA% = 0:KV% = 0:KE% = 00
10010 DIM PP$(8,1),DA(279,1)
10020 TW = 2:WN = 1:PV% = 3:TV% = 4:FE = .625:EX = 0: ROT= 0:
      SCALE= 2:ME = 0:BE$ = CHR$(7) + CHR$(7) + CHR$(7):D$ =
      CHR$(13) + CHR$(4)
10030 PN$ = "EXP PARAMETERS": GOSUB 5410:TD = DD: GOSUB 10:
      GOSUB 20: GOSUB 30
10040 HGR : HCOLOR= 3: TEXT : GOTO 7400

```


APPENDIX B ASSEMBLY LANGUAGE PROGRAMS

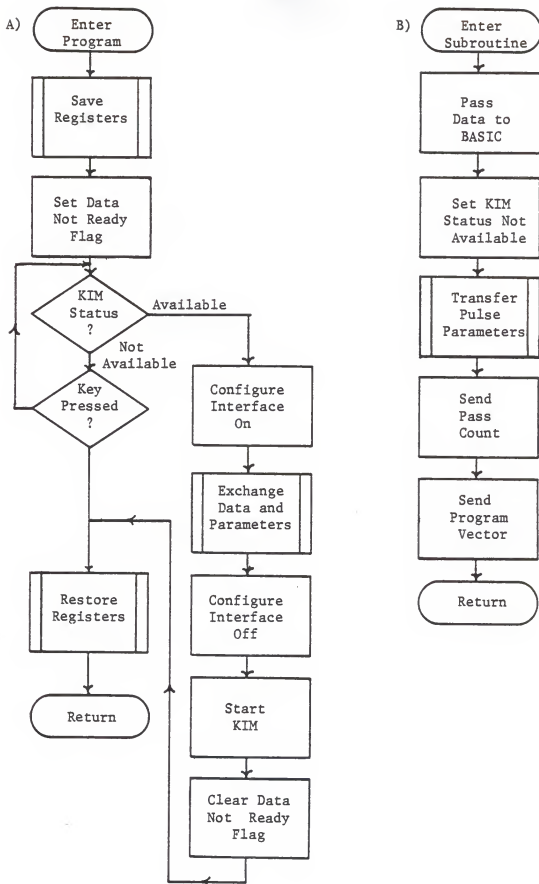
The three assembly language programs used to run the icr experiment are detailed in this section. All programs were prepared as text files with a text editor, PIE, then converted to machine code by an interactive assembler, LISA [122]. The manuals should be consulted for language syntax and operation of the assembler and editor. Source text listings for the three programs end with the word "TEXT" in their filenames, while the corresponding assembled code are stored as binary files ending in "CODE".

Apple Program

The program execution sequence for the Apple machine code is shown in Figure B.1. As explained in the previous appendix, the program expects the first BASIC variable to be the data, the second the pass count, the third the program vector, and the fourth the KIM availability status. Again, the pulse parameter array must be the first one declared. The program code begins at 800 hex or 2048 in decimal, thus, the program is started by the BASIC statement "CALL 2048" in line number 100 of the program listed in Appendix A.

Upon entering the routine, the system registers are saved and the data not ready flag is set. Monitor routines in ROM, IOSAV and IOREST, save and restore the Apple registers, respectively. This allows the program to be called at any time without disturbing BASIC or any other

Figure B.1. Flowchart of the assembly language program APPLE ICR-MO showing the main program execution sequence (part A) and the data transfer subroutine (part B) which passes data and parameters between the Apple and KIM.



routine. Next the KIM's availability status is examined, and if the KIM is not available the Apple keyboard status port is checked for the pressed key flag (bit 7). If a key has been pressed, the system registers are restored and program execution returns to BASIC with the data not ready flag set.

When the KIM is available, the interface is configured for the S-100 memory "on" and the S-100 bus requested. The data and KIM program parameters are exchanged and then the interface is configured "off" by releasing the S-100 bus and switching the Apple memory "on". Next a NMI request is sent to the KIM to start program execution. Now the data not ready flag is cleared, registers are restored, and the program returns to BASIC control. Since data and program parameters are passed at the same time, each run through the code supplies the Apple with data from the last experiment while sending the KIM pulse parameters for the next.

Dual microcomputer timing coordination is maintained through the KIM's status port. Two situations are possible and communicated through bit 7 of the port. A one indicates the KIM is busy with a pulse sequence and should not be disturbed. A zero signifies the KIM has completed a task and is available for service without interfering with an experiment.

The APPLE ICR-MO TEXT Listing follows. When the program is assembled, it occupies memory locations 800 to 869 hex made available by the initialization procedure described in Chapter 4.

```

INS
;
;DEFINE VARIABLES AND ADDRESSES
;
INT      EPZ $69          ;BASIC INTEGER VARIABLE ADDRESS
ARVEC    EPZ $6B          ;APPLE ARRAY ADDRESS
TIMON    EQU $A000        ;PULSE PARAMETER ADDRESS
PRGVEC   EQU $A030        ;KIM PROGRAM VECTOR
NPASS    EQU $A032        ;KIM NUMBER OF PASSES
DATA     EQU $A033        ;KIM DATA ADDRESS
KYBD     EQU $C000        ;APPLE KEYBOARD STATUS
S1BUS    EQU $C0D0        ;S-100 BUS REQUEST ADDRESS
S1MEM    EQU $C0D2        ;S-100 MEMORY ENABLE ADDRESS
APMEM    EQU $C0D6        ;APPLE MEMORY ENABLE ADDRESS
KSTAT    EQU $C0D1        ;KIM STATUS PORT READ ADDRESS
KRES     EQU $C0D2        ;KIM RESET ADDRESS
KNMI     EQU $C0D3        ;KIM NMI ADDRESS
KSPORT   EQU $C51F        ;KIM STATUS PORT WRITE ADDRESS
IOSAV    EQU $FF4A        ;APPLE REGISTER SAVE PROGRAM
IOREST   EQU $FF3F        ;APPLE REGISTER RESTORE PROGRAM
;
      ORG $800            ;ICR EXP. ENTRY POINT
;
; THIS ROUTINE WILL SET THE INITIAL PARAMETERS
; REQUIRED TO OPERATE THE MO PULSE ROUTINE
; AND COMMUNICATE WITH THE KIM.
; THE PROGRAM IS TOTALLY RELOCATABLE.
; ALL REGISTERS ARE RESTORED.
;
ICRMO    JSR IOSAV        ;SAVE ALL REGISTERS
      LDY #$18            ;SET DATA NOT READY FLAG
      LDA #$01
      STA (INT),Y        ;PASS TO APPLESOFT
;
KWAIT    BIT KSTAT        ;CHECK KIM STATUS
      BPL KRDY            ;BRANCH IF KIM READY
      BIT KYBD            ;CHECK KEYBOARD STATUS
      BPL KWAIT          ;KEEP CHECKING
      CLC                ;EXIT FOR ABORT
      BCC EXIT
;
KRDY     STA S1BUS        ;REQUEST S-100 BUS
      STA S1MEM          ;ENABLE S-100 MEMORY
      JSR COMM            ;TRANSFER DATA WITH KIM
;
      STA S1BUS+1        ;RELEASE S-100 BUS
      STA APMEM          ;ENABLE APPLE MEMORY

```

```

        LDA KNMI             ;START KIM
;
        LDY #$18             ;CLEAR DATA NOT READY FLAG
        LDA #$00
        STA (INT),Y          ;PASS TO APPLESOFT
;
EXIT    JSR IOREST           ;RESTORE ALL REGISTERS
        RTS                  ;RETURN
;
; THIS ROUTINE TRANSFERS THE NECESSARY PARAMETERS
; BETWEEN THE KIM AND APPLE.
;
COMM    LDA DATA            ;GET LOW BYTE
        LDY #$03             ;PASS DATA TO APPLESOFT
        STA (INT),Y
        LDA DATA+1          ;GET HIGH BYTE
        DEY                  ;SET TO STORE HIGH BYTE
        STA (INT),Y
;
        LDA #$80             ;SET KIM NOT AVAILABLE
        STA KSPORT
;
        JSR XFER             ;TRANSFER PULSE PARAMETERS
        LDY #$0A             ;SET FOR PASS COUNT
        LDA (INT),Y          ;GET PASS COUNT
        STA NPASS            ;SEND TO KIM
        LDY #$11             ;SET FOR PROGRAM VECTOR
        LDA (INT),Y          ;GET LOW BYTE
        STA PRGVEC           ;SEND TO KIM
        DEY                  ;SET FOR HIGH BYTE
        LDA (INT),Y          ;GET HIGH BYTE
        STA PRGVEC+1         ;SEND TO KIM
        RTS                  ;RETURN
;
; THIS ROUTINE TRANSFERS 17 DOUBLE PRECISION VALUES
; FROM THE FIRST BASIC ARRAY TO THE S-100 MEMORY.
;
XFER    LDX #133             ;INITIALIZE COUNTER
        LDY #142             ;INITIALIZE POINTER
NEXT    LDA (ARVEC),Y        ;GET ARRAY BYTE
        STA TIMON            ;SEND BYTE
        DEY                  ;DECREMENT COUNTERS
        DEX
        BPL NEXT            ;REPEAT TILL DONE
        RTS                  ;RETURN
;
FINADD EQU *                 ;END OF PROGRAM ADDRESS
;
        PAG
        END

```

KIM Programs

The operation of the KIM requires two assembly language programs, the slave controller and pulse generator. The two routines are assembled separately then combined, along with default timing and control parameters, to form the load time package of KIM MO CODE. For instruction timing considerations and KIM operating procedures, one should consult the manuals [123].

Slave Control

The program KIM ICR-MO performs slave control tasks which run the pulsed icr experiment, collect and average the data, and light up the KIM's display. The program execution sequence can be traced in Figure B.2. The routine is entered when a NMI request is serviced by the KIM's CPU. After receiving the NMI the computer is initialized: the processor's interrupt request line is disabled, the decimal mode cleared, and the KIM's status set not available. An indirect jump command, directed by the KIM's program vector, places the KIM in either the continuous run or signal averaging mode.

The continuous run mode of operation, detailed in the upper half of Figure B.2, first initializes the display parameters, zeroes the data, initializes the Biomation and pulse port hardware, then transfers the duty cycle, pulse "on", and "off" times from the common memory to page zero to satisfy the 8-bit pulse routine. After all initialization procedures have been completed, the experiment is performed with the specified timing parameters. The data from each pass is fetched from the Biomation and placed in the low byte of the double precision data address. The program repeats until another NMI command is received by the KIM's CPU. Periodic flickering of the KIM's display each pass indicates the code is functioning properly.

Signal averaging is accomplished through the sequence shown in the lower half of Figure B.2. During initialization the number of passes is set and execution continues similar to the continuous run mode. Next, the KIM's status is set not available and the pulse sequence is repeated the number of times specified in NPASS. The data from each pass is added to the previous sum and stored. When all passes have been completed, the KIM's status is set available and the program enters a display loop while it waits for service. The resulting data is a total; therefore, it must be divided by the number of passes for the average. The program remains in the display loop until the next NMI request is received.

The following is a listing of the assembly language program KIM ICR-MO TEXT. When assembled, the program occupies memory locations A28E to A38E hex in the S-100 memory.

```

INS
;
; DEFINE VARIABLES AND ADDRESSES
;
DISD   EPZ $F9           ;KIM DISPLAY DATA BYTE
DISLA  EPZ $FA           ;KIM DISPLAY LOW ADDRESS
DISHA  EPZ $FB           ;KIM DISPLAY HIGH ADDRESS
PAD     EQU $1700        ;KIM PORT A DATA
PADD    EQU $1701        ;KIM PORT A DATA DIRECTION
PBD     EQU $1702        ;KIM PORT B DATA
PBDD    EQU $1703        ;KIM PORT B DATA DIRECTION
PULSER  EQU $A100        ;8 BIT PULSE ROUTINE ADDRESS
SPAD    EQU $F004        ;S-100 PARALLEL PORT A DATA
SPBD    EQU $F005        ;S-100 PARALLEL PORT B DATA
KSTAT   EQU $F01F        ;KIM STATUS ADDRESS
EXPB    EQU $F026        ;EXP. PARALLEL I/O PORT B
KIMDP   EQU $1F1F        ;KIM KEYBOARD DISPLAY ROUTINE
;
          ORG $A000      ;SET PULSE PARAMETERS
          OBJ *-$9800
TIMON    EQU *           ;PULSE BIT ON TABLE
DUTCYL   EQU *+$10       ;DUTY CYCLE DURATION TIME
TIMOFF   EQU *+$12       ;PULSE BIT OFF TABLE
;
          ORG $A030      ;SET PARAMETER TABLE

```

```

      OBJ *-$9800
PRGVEC ADR CRUN          ;PROGRAM EXECUTION VECTOR
NPASS  BYT $01          ;NUMBER OF PASSES
DATA   HEX 0000         ;DOUBLE PRECISION DATA
RDATA  BYT $00          ;RAW DATA STORAGE
      PAG
;
      ORG $A28E          ;PROGRAM BEGINNING
      OBJ *-$9800
;
; THIS ROUTINE IS ENTERED BY A NON-MASKABLE
; INTERRUPT REQUEST, INITIALIZES THE KIM AND INTERFACE,
; THEN JUMPS TO THE DESIGNATED ROUTINE.
;
      SEI                ;DISABLE INTERRUPT
      CLD                ;CLEAR DECIMAL MODE
      LDA #$80           ;KIM STATUS: BUSY
      STA KSTAT
      JMP (PRGVEC)
;
; THIS ROUTINE SETS THE KIM FOR CONTINUOUS RUN
; OF THE ICR-MO PULSE ROUTINE.
;
CRUN   LDA #$1           ;SET OPERATION MODE
      STA DISHA          ;AND UPDATE DISPLAY
      LDA RDATA          ;DISPLAY LAST POINT
      STA DISD
      LDA #$00           ;ZERO THE DATA
      STA DATA
      STA DATA+1
      JSR INIT           ;INITIALIZE THE PARAMETERS
      JSR SETPUL         ;SET PULSE PARAMETERS
;
CONT   LDA #$80           ;KIM STATUS: BUSY
      STA KSTAT
      JSR KIMDP          ;DELAY AND DISPLAY
;
      JSR BIOARM         ;ARM THE BIOMATION
      JSR PULSER         ;RUN EXPERIMENT
;
      JSR BIODAT         ;GET DATA FROM BIOMATION
      STA DATA          ;SAVE DATA
      STA DISD           ;DISPLAY DATA
;
      LDA #$00           ;KIM STATUS: AVAILABLE
      STA KSTAT
      INC DISLA          ;INCREMENT COUNTER
      JSR KIMDP          ;DEALY AND DISPLAY
      CLC                ;CONTINUE RUNNING
      BCC CONT
      PAG
;
; THIS ROUTINE SETS THE KIM UP FOR DATA COLLECTION
; SIGNAL AVERAGING. WHEN THE SPECIFIED NUMBER OF PASSES

```

```

; HAVE BEEN TAKEN THE KIM EXECUTES A DISPLAY LOOP.
;
DATAVG LDA NPASS          ;SET THE NO. OF PASSES
      STA DISLA          ;SAVE WORKING PASS COUNT
      LDA #$02          ;SET OPERATION MODE
      STA DISHA          ;DISPLAY THE MODE
      LDA #$00          ;ZERO THE DATA
      STA DATA
      STA DATA+1
      JSR INIT          ;INITIALIZE THE PARAMETERS
      JSR SETPUL        ;SET PULSE PARAMETERS
      LDA #$80          ;KIM STATUS: BUSY
      STA KSTAT
;
;NEXTP JSR KIMDP          ;DISPLAY
      JSR BIOARM        ;ARM THE BIOMATION
      JSR PULSER        ;EXECUTE A PASS
      JSR BIODAT        ;GET DATA FROM BIOMATION
      STA DISD          ;DISPLAY RAW DATA
;
      CLC              ;CLEAR FOR SIGNAL AVERAGING
      ADC DATA          ;AVERAGE SIGNAL
      STA DATA          ;STORE IT
      LDA DATA+1        ;HIGH BYTE
      ADC #$00
      STA DATA+1
;
      DEC DISLA          ;DECREMENT PASS COUNT
      BNE NEXTP          ;CONTINUE AVERAGING
      LDA #$00          ;KIM STATUS: AVAILABLE
      STA KSTAT
      LDA #$00          ;SET OPERATION MODE
      STA DISHA          ;DISPLAY IT
WAITLP JSR KIMDP          ;DISPLAY VITAL SIGNS
      JMP WAITLP         ;CONTINUE DISPLAYING
;
; THIS SUBROUTINE WILL SET THE INITIAL PARAMETERS
; REQUIRED TO OPERATE THE ICR-MO PULSE ROUTINE,
; BIOMATION, AND PULSE OUTPUT PORT.
; THE PROGRAM IS TOTALLY RELOCATABLE.
; ALL REGISTERS ARE RESTORED.
;
INIT  PHA              ;SAVE THE ACCUMULATOR
      LDA #$FF          ;SET PARALLEL PORT A TO ALL OUTPUTS
      STA PADD
      LDA #$07          ;KIM PBO,1,2 ARE OUTPUTS
      STA PBDD
      LDA #$87          ;INITIALIZE THE BIOMATION
      STA SPBD
;
      LDA #$00          ;ACCESS PIA DATA DIRECTION
      STA EXPB+1        ;EXP. PARALELL PORT B
      LDA #$FF          ;SET FOR 8 OUTPUT LINES
      STA EXPB

```

```

        LDA #$04                ;ACCESS DATA PORT
        STA EXPB+1

;

        PLA                    ;RESTORE ACCUMULATOR
        RTS                    ;RETURN
        PAG

;
; SUBROUTINE SETPUL TRANSFERS THE PULSE PARAMETERS IN
; THE COMMON MEMORY TO PAGE ZERO FOR USE BY THE KIM.
;
SETPUL LDX #$21                ;INITIALIZE COUNTER
NEXTV  LDA $A000,X             ;GET PULSE PARAMETER
        STA $0000,X            ;TRANSFER TO ZERO PAGE
        DEX                    ;DECREMENT COUNTER
        BPL NEXTV              ;REPEAT TILL DONE
        RTS                    ;RETURN
        PAG

;
; SUBROUTINE BREQ SENDS AN OUTPUT COMMAND TO THE
; BIOMATION THEN WAITS FOR THE OPT FLAG.
; ALL REGISTERS ARE RESTORED.
;
BREQ   PHA                    ;SAVE ACC
        LDA #$85                ;SEND OPT COMMAND
        STA SPAD

WFLG   LDA #$01                ;CHECK OPT FLAG
        AND SPBD                ;READ STATUS PORT
        BEQ WFLG                ;WAIT FOR OPT FLG
        PLA                    ;RESTORE ACC
        RTS                    ;RETURN

;
; SUBROUTINE GETB READS A DATA POINT FROM THE BIOMATION
; THEN TOGGLES WDC FOR THE NEXT POINT.
; THE DATA POINT IS IN THE ACCUMULATOR UPON
; EXIT FROM THE ROUTINE.
;
GETB   LDA SPAD                ;GET DATA
        PHA                    ;SAVE IT
        LDA #$84                ;TOGGLE WDC LOW
        STA SPAD                ;FOR NEXT POINT
        LDA #$85
        STA SPAD
        PLA                    ;RESTORE ACC
        RTS                    ;RETURN

;
; THIS SUBROUTINE INTERROGATES THE BIOMATION FOR DATA
; AND STORES THE RESULT IN RDATA.
; THE ACCUMULATOR CONTAINS THE DATA UPON EXIT FROM
; THE ROUTINE.
;
BIODAT BIT SPBD                ;WAIT FOR RECORD DONE FLAG
        BMI BIODAT

;

        JSR BREQ                ;REQUEST BIOMATION OUTPUT

```

```

        JSR GETB           ;SKIP FIRST POINT
        JSR GETB           ;GET DATA
        STA RDATA          ;STORE AS RAW DATA
        PHA                ;SAVE THE DATA
        LDA #$87           ;RELEASE BIOMATION
        STA SPAD
        PLA                ;RESTORE THE DATA
        RTS                ;RETURN
;
; THIS ROUTINE ARMS THE BIOMATION.
;  ALL REGISTERS ARE RESTORED.
;
BIOARM PHA                ;SAVE THE ACCUMULATOR
        LDA #$07          ;ARM BIOMATION
        STA SPAD
        LDA #$87
        STA SPAD
        PLA                ;RESTORE THE ACCUMULATOR
        RTS                ;RETURN
;
FINADD EQU *              ;END OF PROGRAM ADDRESS
;
        PAG
        END

```

Pulse generator

Pulse timing is controlled by executing a series of computer instructions of known length such that the total execution time is constant. Since each instruction takes from two to four computer clock cycles to execute and the computer clock runs at a constant frequency, the execution time of each instruction is known. Even though conditional branch statements vary the code executed each time the program runs, the number of clock cycles is constant for every possible execution path.

The program execution sequence is outlined in Figure B.3. Upon entering the routine, the program expects the duty cycle time, "on", and "off" times to be in page zero. The program first zeroes the pulse master clock, next the pulse port value is set to zero. Now each bit's "on" and "off" time is compared to the pulse master clock by double precision subtraction. If the clock is greater than or equal to the "on"/"off" time, the carry is set and the appropriate bit set or cleared in the pulse port value. When all eight bits are configured, the pulse port value is sent to the pulse port hardware. It is at this time that all bits seen by the detection electronics change synchronously. The pulse master clock is then compared to the duty cycle time. If they are equal, program execution is returned back to the calling program; if not, the pulse master clock is incremented and the program is delayed before repeating the code.

This code can be used on either the Apple or KIM microcomputers with the appropriate modification. The CPU phase zero clock frequency is 1.00000 MHz for the KIM; consequently, each instruction cycle lasts one microsecond. Thus, 500 instruction cycles are needed for a 0.5 msec

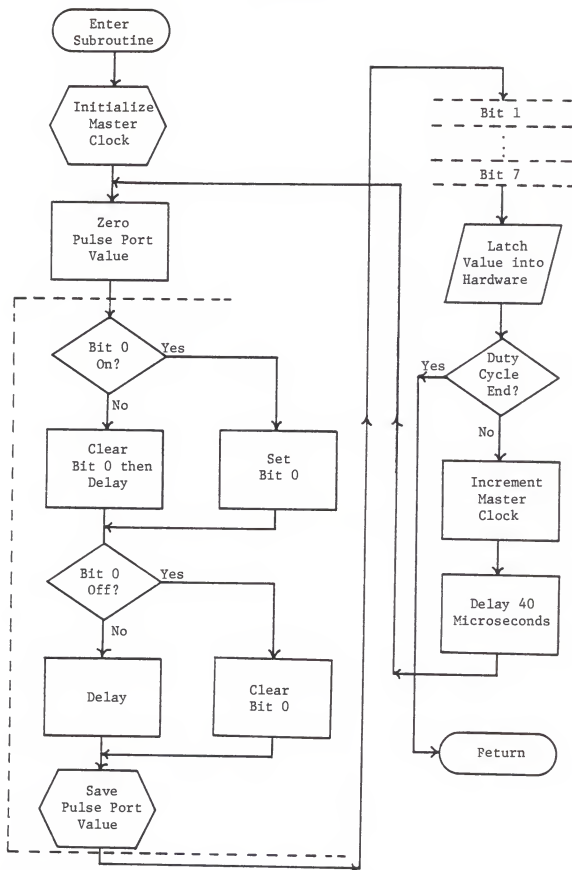


Figure B.3. Flowchart of the 8-bit pulse generator subroutine.

program cycle time. This dictates the 40 CPU cycle delay after incrementing the pulse master clock. However, the Apple phase zero clock frequency is 1.02050 MHz; thus, 510 CPU clock cycles approximate the 510.25 clock cycles needed for a 0.5 msec program cycle time. The 50 CPU clock cycle delay at the end of the routine introduces a timing error of only 0.05%.

The code used to generate the pulse sequences, KIM PULSE 8 TEXT, follows. When assembled, it occupies memory locations A100 to A28D hex in the S-100 memory.

```

INS
;
;DEFINE VARIABLES AND ADDRESSES.
;
; ALL THE FOLLOWING VARIABLES ARE 16 BITS LONG.
; HIGH ORDER BYTES ARE FIRST.
;
TIMON  EPZ $00          ;PULSE BIT ON TABLE
DUTCYL EPZ $10          ;DUTY CYCLE TIME
TIMOFF EPZ $12          ;PULSE BIT OFF TABLE
PCLK   EPZ $22          ;PULSE MASTER CLOCK
;
; THE FOLLOWING LOCATIONS ARE 8 BITS IN LENGTH.
;
BASE2  EQU $F026        ;PIA B ADDRESS
PLSVAL EQU $2FF         ;PULSE PORT VALUE
;
        ORG $A100        ;8 BIT PULSE ROUTINE ENTRY
        OBJ *-$9900      ;STORE AT $800
;
;8 BIT PULSE ROUTINE
;
PULSER LDA #$00          ;ZERO PULSE MASTER CLOCK
        STA PCLK+1       ; LOW BYTE
        STA PCLK         ; HIGH BYTE
;
PULSE  LDA #$00          ;ZERO PULSE PORT VALUE
        STA PLSVAL
;
BO     SEC               ;CHECK FOR BIT 0 ON
        LDA PCLK+1       ; LOW BYTE
        SBC TIMON+1
        LDA PCLK         ; HIGH BYTE
        SBC TIMON
        BCC BODELA       ;BRANCH IF NOT ON

```



```

        LDX #$01                ;SET BIT 0 ON
        JMP BOOFF
BODELA  LDX #$00                ;SET BIT 0 NOT ON
        NOP                    ;DELAY
BOOFF   SEC                    ;CHECK FOR BIT 0 OFF
        LDA PCLK+1              ; LOW BYTE
        SBC TIMOFF+1
        LDA PCLK                ; HIGH BYTE
        SBC TIMOFF
        BCC BODELB              ;BRANCH IF BIT 0 NOT OFF
        LDX #$00                ;CLEAR BIT 0
        JMP BOSET
BODELB  NOP                    ;DELAY
        NOP
BOSET   TXA                    ;SET PULSE PORT VALUE
        ORA PLSVAL
        STA PLSVAL              ;STORE IT
;
B1      SEC                    ;CHECK FOR BIT 1 ON
        LDA PCLK+1              ; LOW BYTE
        SBC TIMON+3
        LDA PCLK                ; HIGH BYTE
        SBC TIMON+2
        BCC B1DELA              ;BRANCH IF NOT ON
        LDX #$02                ;SET BIT 1 ON
        JMP B1OFF
B1DELA  LDX #$00                ;SET BIT 1 NOT ON
        NOP                    ;DELAY
B1OFF   SEC                    ;CHECK FOR BIT 1 OFF
        LDA PCLK+1              ; LOW BYTE
        SBC TIMOFF+3
        LDA PCLK                ; HIGH BYTE
        SBC TIMOFF+2
        BCC B1DELB              ;BRANCH IF BIT 1 NOT OFF
        LDX #$00                ;CLEAR BIT 1
        JMP B1SET
B1DELB  NOP                    ;DELAY
        NOP
B1SET   TXA                    ;SET PULSE PORT VALUE
        ORA PLSVAL
        STA PLSVAL              ;STORE IT
;
B2      SEC                    ;CHECK FOR BIT 2 ON
        LDA PCLK+1              ; LOW BYTE
        SBC TIMON+5
        LDA PCLK                ; HIGH BYTE
        SBC TIMON+4
        BCC B2DELA              ;BRANCH IF NOT ON
        LDX #$04                ;SET BIT 2 ON
        JMP B2OFF
B2DELA  LDX #$00                ;SET BIT 2 NOT ON
        NOP                    ;DELAY
B2OFF   SEC                    ;CHECK FOR BIT 2 OFF
        LDA PCLK+1              ; LOW BYTE

```

```

        SBC TIMOFF+5
        LDA PCLK                      ; HIGH BYTE
        SBC TIMOFF+4
        BCC B2DELB                    ;BRANCH IF BIT 2 NOT OFF
        LDX #$00                      ;CLEAR BIT 2
        JMP B2SET
B2DELB  NOP                          ;DELAY
        NOP
B2SET   TXA                          ;SET PULSE PORT VALUE
        ORA PLSVAL
        STA PLSVAL                    ;STORE IT
;
B3      SEC                          ;CHECK FOR BIT 3 ON
        LDA PCLK+1                    ; LOW BYTE
        SBC TIMON+7
        LDA PCLK                      ; HIGH BYTE
        SBC TIMON+6
        BCC B3DELA                    ;BRANCH IF NOT ON
        LDX #$08                      ;SET BIT 3 ON
        JMP B3OFF
B3DELA  LDX #$00                      ;SET BIT 3 NOT ON
        NOP                          ;DELAY
B3OFF   SEC                          ;CHECK FOR BIT 3 OFF
        LDA PCLK+1                    ; LOW BYTE
        SBC TIMOFF+7
        LDA PCLK                      ; HIGH BYTE
        SBC TIMOFF+6
        BCC B3DELB                    ;BRANCH IF BIT 3 NOT OFF
        LDX #$00                      ;CLEAR BIT 3
        JMP B3SET
B3DELB  NOP                          ;DELAY
        NOP
B3SET   TXA                          ;SET PULSE PORT VALUE
        ORA PLSVAL
        STA PLSVAL                    ;STORE IT
;
B4      SEC                          ;CHECK FOR BIT 4 ON
        LDA PCLK+1                    ; LOW BYTE
        SBC TIMON+19
        LDA PCLK                      ; HIGH BYTE
        SBC TIMON+18
        BCC B4DELA                    ;BRANCH IF NOT ON
        LDX #$10                      ;SET BIT 4 ON
        JMP B4OFF
B4DELA  LDX #$00                      ;SET BIT 4 NOT ON
        NOP                          ;DELAY
B4OFF   SEC                          ;CHECK FOR BIT 4 OFF
        LDA PCLK+1                    ; LOW BYTE
        SBC TIMOFF+19
        LDA PCLK                      ; HIGH BYTE
        SBC TIMOFF+18
        BCC B4DELB                    ;BRANCH IF BIT 4 NOT OFF
        LDX #$00                      ;CLEAR BIT 4
        JMP B4SET

```

```

B4DELB NOP                ;DELAY
NOP
B4SET  TXA                ;SET PULSE PORT VALUE
ORA PLSVAL
STA PLSVAL                ;STORE IT
;
B5     SEC                ;CHECK FOR BIT 5 ON
LDA PCLK+1                ; LOW BYTE
SBC TIMON+!11
LDA PCLK                  ; HIGH BYTE
SBC TIMON+!10
BCC B5DELA                ;BRANCH IF NOT ON
LDX #$20                  ;SET BIT 5 ON
JMP B5OFF
B5DELA LDX #$00            ;SET BIT 5 NOT ON
NOP                        ;DELAY
B5OFF  SEC                ;CHECK FOR BIT 5 OFF
LDA PCLK+1                ; LOW BYTE
SBC TIMOFF+!11
LDA PCLK                  ; HIGH BYTE
SBC TIMOFF+!10
BCC B5DELB                ;BRANCH IF BIT 5 NOT OFF
LDX #$00                  ;CLEAR BIT 5
JMP B5SET
B5DELB NOP                ;DELAY
NOP
B5SET  TXA                ;SET PULSE PORT VALUE
ORA PLSVAL
STA PLSVAL                ;STORE IT
;
B6     SEC                ;CHECK FOR BIT 6 ON
LDA PCLK+1                ; LOW BYTE
SBC TIMON+!13
LDA PCLK                  ; HIGH BYTE
SBC TIMON+!12
BCC B6DELA                ;BRANCH IF NOT ON
LDX #$40                  ;SET BIT 6 ON
JMP B6OFF
B6DELA LDX #$00            ;SET BIT 6 NOT ON
NOP                        ;DELAY
B6OFF  SEC                ;CHECK FOR BIT 6 OFF
LDA PCLK+1                ; LOW BYTE
SBC TIMOFF+!13
LDA PCLK                  ; HIGH BYTE
SBC TIMOFF+!12
BCC B6DELB                ;BRANCH IF BIT 6 NOT OFF
LDX #$00                  ;CLEAR BIT 6
JMP B6SET
B6DELB NOP                ;DELAY
NOP
B6SET  TXA                ;SET PULSE PORT VALUE
ORA PLSVAL
STA PLSVAL                ;STORE IT
;

```

```

B7      SEC                      ;CHECK FOR BIT 7 ON
        LDA PCLK+1              ; LOW BYTE
        SBC TIMON+115
        LDA PCLK                ; HIGH BYTE
        SBC TIMON+114
        BCC B7DELA              ;BRANCH IF NOT ON
        LDX #$80                ;SET BIT 7 ON
        JMP B7OFF
B7DELA  LDX #$00                ;SET BIT 7 NOT ON
        NOP                    ;DELAY
B7OFF   SEC                    ;CHECK FOR BIT 7 OFF
        LDA PCLK+1              ; LOW BYTE
        SBC TIMOFF+115
        LDA PCLK                ; HIGH BYTE
        SBC TIMOFF+114
        BCC B7DELB              ;BRANCH IF BIT 7 NOT OFF
        LDX #$00                ;CLEAR BIT 7
        JMP B7SET
B7DELB  NOP                    ;DELAY
        NOP
B7SET   TXA                    ;SET PULSE PORT VALUE
        ORA PLSVAL
        STA BASE2              ;SEND PULSE VALUE OUT HARDWARE
;
        SEC                    ;CHECK FOR DUTY CYCLE END
        LDA PCLK+1              ; LOW BYTE
        SBC DUTCYL+1
        LDA PCLK                ; HIGH BYTE
        SBC DUTCYL
        BCC CLOCK              ;BRANCH IF NO DONE
        RTS                    ;EXIT, END OF DUTY CYCLE
;
CLOCK   CLC                    ;INCREMENT PULSE MASTER CLOCK
        LDA PCLK+1              ; LOW BYTE
        ADC #$01
        STA PCLK+1              ; SAVE IT
        LDA PCLK                ; HIGH BYTE
        ADC #$00
        STA PCLK                ; SAVE IT
;
        LDX #17                ;START 40 CYCLE DELAY
DEL      DEX                    ; DELAY LOOP
        BNE DEL
        NOP
        NOP
;
        JMP PULSE              ; NEXT PASS
;
FINADD  EQU *                  ;END OF PROGRAM ADDRESS
        PAG
        END

```

REFERENCES

1. H. Hartmann, Topics Curr. Chem. 43, 57 (1973).
2. K.-P. Wanczek, "Dynamic Mass Spectrometry", eds. D. Price and J.F.J. Todd, Vol. 6, Chapter 2 (Heyden, Philadelphia, 1981).
3. J.L. Beauchamp, Annu. Rev. Phys. Chem. 22, 527 (1971).
4. J.A. Hipple, H. Sommer, and H.A. Thomas, Phys. Rev. 76, 1877 (1949).
5. E.B. Ledford, Jr. and R.T. McIver, Jr., Int. J. Mass Spectrom. and Ion Phys. 22, 399 (1976).
6. D. Wobschall, J.R. Graham, and D.P. Malone, Phys. Rev. 131, 1565 (1963).
7. M.S. Henis and W. Frasure, Rev. Sci. Instrum. 39, 1771 (1968).
8. R.T. McIver, Jr., Rev. Sci. Instrum. 41, 126 (1970).
9. J.L. Beauchamp and J.T. Armstrong, Rev. Sci. Instrum. 40, 123 (1969).
10. J.L. Beauchamp, L.R. Anders, and J.D. Baldeschweiler J. Am. Chem. Soc. 89, 4569 (1967).
11. R.T. McIver, Jr., Rev. Sci. Instrum. 41, 555 (1970).
12. J.E. Bartmess and G. Caldwell, Int. J. Mass Spectrom. and Ion Phys. 41, 125 (1981).
13. R.T. McIver, Jr. and R.C. Dunbar, Int. J. Mass Spectrom. and Ion Phys. 7, 471 (1971).
14. R.T. McIver, Rev. Sci. Instrum. 44, 1071 (1973).
15. J.W. Cooley and J.W. Tukey, Math. Comput. 19, 297 (1965).
16. A.G. Marshall, Anal. Chem. 51, 1710 (1979).
17. M.B. Comisarow and A.G. Marshall, Chem. Phys. Lett. 25, 282 (1974).

18. A.G. Marshall and D.C. Roe, J. Mag. Res. 33, 551 (1979).
19. M.B. Comisarow and J.D. Melka, Anal. Chem. 51, 2198 (1979).
20. A.G. Marshall and D.C. Roe, J. Chem. Phys. 73, 1581 (1982).
21. A.G. Marshall, Chem. Phys. Letters 63, 515 (1979).
22. E.B. Ledford, Jr., R.L. White, M.L. Gross, and C.L. Wilkins, Anal. Chem. 52, 1090 (1980).
23. M.B. Comisarow and A.G. Marshall, J. Chem. Phys. 64, 110 (1976).
24. A.G. Marshall, M.B. Comisarow, and G. Parisod, J. Chem. Phys. 71, 4434 (1979).
25. R.L. White, E.B. Ledford, Jr., S. Ghaderi, C.L. Wilkins, and M.L. Gross, Anal. Chem. 52, 1525 (1980).
26. M. Allemann, H. Kellerhals, and K.-P. Wanczek, Chem. Phys. Letters 75, 328 (1980).
27. C.L. Wilkins and M.L. Gross, Anal. Chem. 53, 1661A (1981).
28. E.B. Ledford, Jr., S. Ghaderi, R.L. White, R.B. Spencer, P.S. Kulkarni, C.L. Wilkins, and M.L. Gross, Anal. Chem. 52, 463 (1980).
29. E.B. Ledford, Jr., R.L. White, S. Ghaderi, C.L. Wilkins, and M.L. Gross, Anal. Chem. 52, 2450 (1980).
30. S. Ghaderi, M.L. Gross, E.B. Ledford, and C.L. Wilkins, Anal. Chem. 58, 428 (1981).
31. R.B. Cody and B.S. Freiser, Int. J. Mass Spectrom. and Ion Phys. 41, 199 (1982).
32. R.L. Hunter, Ph.D. Dissertation, University of California, Irvine (1979).
33. G. Parisod and T. Gaumann, Chimia 34, 271 (1980).
34. R.T. McIver, Jr., R.L. Hunter, E.B. Ledford, Jr., M.L. Locke, and T.J. Franci, Int. J. Mass Spectrom. and Ion Phys. 39, 65 (1981).
35. J. Wronka and D.P. Ridge, Rev. Sci. Instrum. 53, 491 (1981).
36. D. Wobschall, Rev. Sci. Instrum. 36, 466 (1965).
37. E.G. Voigtman, Jr., Ph.D. Dissertation, University of Florida (1979).

38. L.N. Morgenthaller, Ph.D. Dissertation, University of Florida (1979).
39. R.J. Doyle, Master Thesis, University of Florida (1981).
40. T.J. Buckley, R.J. Doyle, and J.R. Eyler, "Lecture Notes in Chemistry; Proceedings of the 2nd International Ion Cyclotron Resonance Conference" (Springer, Berlin, 1982).
41. S.C. Crumpton, M.S. Alder, J.E. Ramirez, and R.J. Hanrahan, "Personal Computers in Chemistry", ed. P. Lykes, Chapter 2 (John Wiley and Sons, N.Y. 1981).
42. A. Braithwaite and K. Henthorn, "Dynamic Mass Spectrometry", eds. D. Price and J.F.J. Todd, Vol. 6, Chapter 12 (Heyden, Philadelphia, 1981).
43. T.R. Mueller, J.R. Sites, and L.K. Bertram, Chem., Biomed., and Environ. Instr. 11, 197 (1981).
44. L.S. Dale, I. Liepa, P.S. Rendell, and R.N. Whittmen, Anal. Chem. 53, 2288 (1981).
45. P. Ausloos, J. Am. Chem. Soc. 104, 5259 (1982).
46. T.E. Sharp, J.R. Eyler, and E. Li, Int. J. Mass Spectrom. and Ion Phys. 2, 421 (1972).
47. R.T. McIver, Jr., and A.D. Baranyi, Int. J. Mass Spectrom. and Ion Phys. 14, 449 (1974).
48. H. Hartmann, K.-M. Chung, D. Schuch, and K.-P. Wanczek, Int. J. Mass Spectrom. and Ion Phys. 34, 303 (1980).
49. S.E. Buttrill, Jr., J. Chem. Phys. 50, 4125 (1969).
50. M.B. Comisarow, J. Chem. Phys. 69, 4097 (1978).
51. M.B. Comisarow, Int. J. Mass Spectrom. and Ion Phys. 26, 369 (1978).
52. C. Amano, Int. J. Mass Spectrom. and Ion Phys. 35, 47 (1980).
53. R.T. McIver, Jr., E.B. Ledford, Jr., and R.L. Hunter, J. Chem. Phys. 72, 2535 (1980).
54. H.V. Malmstadt, C.G. Enke, S.R. Crouch, and G. Horlik, "Instrumentation For Scientists Series", Module 4, Chapter 1 (W.A. Benjamin, Inc., Meleno Park 1974).
55. J.W. Cooper, "The Minicomputer in the Laboratory", Chapter 7 (John Wiley and Sons, N.Y. 1977).

56. S.G. Lias, J.R. Eyler, and P. Ausloos, *Int. J. Mass Spectrom. and Ion Phys.* 12, 219 (1976).
57. Apple II Microcomputer (Apple Computer Inc., Cupertino, Ca.).
58. CPS Multifunction Card (Mountain Computer Inc., Scotts Valley, Ca.).
59. ADALAB (Interactive Microware Inc., State College, Pa.).
60. IEEE 488 Controller (SSM Microcomputer Products Inc., San Jose, Ca.).
61. Frequency Synthesizer Hewlett Packard Model 3325A (Hewlett-Packard Co., Loveland, Co.).
62. Microsoft RAM Card (Microsoft Consumer Products, Bellevue, Wa.).
63. KIM-1 Microcomputer (MOS Technology Inc., Norristown, Pa.).
64. KIMSI S-100 Bus (Forethought Products, Coburg, Or.).
65. Waveform Recorder, Biomation Model 805 (Gould Inc., Cupertino, Ca.).
66. Frequency Synthesizer Model 5100 (Rockland Systems Corp., West Nyack, N.Y.).
67. Fast Floating Point Processor Board AM9511 (Computer Stations Inc., Granite City, Il.).
68. "M6800 Microcomputer System Design Data" (MOTOROLA Semiconductor Products Inc., Phoenix, Az. 1976).
69. P.K. Warne, "Scientific Plotter" (Interactive Microware Inc., State College, Pa. 1980). "Curve Fitter", *ibid.* "Vidichart", *ibid.*
70. "GRAPHTRIX Manual, Version 1.2" (Data Transforms Inc., Denver, Co. 1981).
71. W.T. Huntress, Jr., J.B. Laudenslager, and R.F. Pinizzotto, Jr., *Int. J. Mass Spectrom. and Ion Phys.* 13, 331 (1974).
72. W.T. Huntress and R.F. Pinizzotto, *J. Chem. Phys.* 59, 4742 (1973).
73. L.W. Sieck and S.G. Lias, *J. Phys. and Chem. Ref. Data* 5, 1123 (1976).
74. Barocel Model 1023 Electronic Manometer with Model 523H-15 Pressure Head and 525 Thermal Base (CGS Datametries, Watertown, Ma.).

75. Gas temperature in an icr cell is not at ambient temperature due to the heating effect of the filament near the cell. The temperature reported (323 K) is assumed to be the same as the temperature measured on a similar icr spectrometer at NBS.
76. V. Talrose, "Ion-Molecule Reactions in the Gas Phase" (Nauka Publishing House, Moscow 1979).
77. D. Holtz, J.L. Beauchamp, and J.R. Eyler, J. Am. Chem. Soc. 92, 7045 (1970).
78. P.R. LeBreton, A.D. Williamson, J.L. Beauchamp, and W.T. Huntress, J. Chem. Phys. 62, 1623 (1975).
79. J.A.D. Stockdale, J. Chem. Phys. 58, 3881 (1973).
80. F.W. Brill, Personal communication. Pressure calibration experiments on propargyl chloride were performed on the same icr spectrometer. No error limits were given.
81. P.J. Ausloos and S.G. Lias, J. Am. Chem. Soc., 103, 6505 (1981).
82. R.P. Clow and J.H. Futrell, Int. J. Mass Spectrom. and Ion Phys. 4, 165 (1970).
83. F.H. Field, P. Hamlet, and W.F. Libby, J. Am. Chem. Soc. 89, 6035 (1967).
84. H.M. Rosenstock, K. Draxl, B.W. Steiner, and J.T. Herron, J. Phys. Chem. Ref., Data Suppl. 1, 6 (1977).
85. H.F. Calcote, Comb. and Flame 42, 215 (1981).
86. T. Tanzawa and W.C. Gardiner, Jr., J. Chem. Phys. 84, 236 (1980).
87. J.C. Jachimowski, Comb. and Flame 29, 55 (1977).
88. D.B. Olson and H.F. Calcote, "Particulate Carbon: Formation during Combustion", ed. D.C. Siegla and G.W. Smith, p. 177 (Plenum Press, N.Y., 1981).
89. U. Bonne, K.H. Homann, and H.G. Wagner, Tenth Symp. (Int.) Comb., the Combustion Institute, p. 503 (1965).
90. P. Ausloos and S.G. Lias, in "Ion-Molecule Reactions", Vol. 2, ed. J.L. Franklin, p. 707 (Plenum Press, N.Y. 1972).
91. S. Tajima and T. Tsuchiya, Bull. Chem. Soc. Japan 46, 3291 (1973).
92. J.L. Occolowitz and G.L. White, Aust. J. Chem. 21, 997 (1968).
93. F.P. Lossing and J.C. Traeger, J. Am. Chem. Soc. 97, 1579 (1975).

94. S. Furyama, D.M. Golden, and S.W. Benson, *Int. J. Chem. Kin.* 3, 237 (1971).
95. D.A. McCrery and B.S. Freiser, *J. Am. Chem. Soc.* 100, 2902 (1978).
96. The error reported here assumes the reference values are exact and the observed proton affinity lies half way between them. Obviously this is not the case, thus the error limits are somewhat larger but the relative proton affinities are valid.
97. R.A. Davidson and P.S. Skell, *J. Am. Chem. Soc.* 95, 684 (1973).
98. D.H. Aue and M.T. Bowers, "Gas Phase Ion Chemistry," Vol. 2, ed. M.T. Bowers, Chapter 9 (Academic Press Inc. 1979).
99. J.F. Liebman, personal communication.
100. H.M. Rosenstock, J. Dannacher, and J.F. Liebman, *Radiation Phys. Chem.* 20, 7, (1982).
101. S.W. Benson, "Thermochemical Kinetics", 2nd ed. (John Wiley Sons, N.Y., 1976).
102. W. Hehre and W.J. Pople, *J. Am. Chem. Soc.* 97, 6441 (1975).
103. J.B. Pedley and J. Rylance, "N.P.L. Computer Analyzed Thermochemical Data: Organic and Organo-metallic Compounds", (University of Sussex, Sussex, England 1977).
104. J.M. Donovan and R.J. Hanrahan, *Radiat. Phys. Chem.* 3, 491 (1971).
105. L.H. Gevantman and R.R. Williams, Jr., *J. Phys. Chem.* 56, 569 (1952).
106. I. McAlpine and H. Sutcliffe, *J. Phys. Chem.* 73, 3215 (1969).
107. I. McAlpine and H. Sutcliffe, *J. Phys. Chem.* 74, 848 (1970).
108. P.G. Shah, D.R. Straks, and R. Cooper, *Aust. J. Chem.* 23, 253 (1970).
109. D. Teclemariam and R.J. Hanrahan, *Radiat. Phys. Chem.* 6, 443 (1982).
110. J.L. Beauchamp, D. Holtz, S.D. Woodgate, and S.L. Patt, *J. Am. Chem. Soc.* 94, 2798 (1972).
111. R.F. Pottie, R. Barker, and W.H. Hamill, *Radiat. Res.* 10, 644 (1959).

112. J.M.S. Henis, M.D. Loberg, and M.J. Welch, J. Am. Chem. Soc. 96, 1665 (1974).
113. T. Hsieh, J.R. Eyler, and R.J. Hanrahan, Int. J. Mass Spectrom. and Ion Phys. 29, 113 (1978).
114. D.W. Berman and J.L. Beauchamp, Int. J. Mass Spectrom. and Ion Phys. 39, 47 (1981).
115. L.R. Anders, J.L. Beauchamp, R.C. Dunbar, and J.D. Baldeschwieler, J. Chem. Phys. 45, 1062 (1966).
116. M.P. Langevin, Ann. Chim. Phys. 58, 245 (1905)
117. T. Su and M.T. Bowers, J. Chem. Phys. 58, 3027 (1973).
118. A.A. Maryott and F. Buckely, "Table of Dielectric Constants and Electric Dipole Moments of Substances in the Gaseous State", National Bureau of Standards Circular, 573 (1953).
119. L.W. Sieck and R. Gorden, Jr., Int. J. Chem. Kin., Vol. V, 445 (1973).
120. L.W. Sieck, J. Res. of N.B.S.- A. Phys. and Chem. 81A, 267 (1977).
121. "APPLE II Reference Manual" (Apple Computer Inc., Cupertino, California, 1981). "BASIC Programming Reference Manual", ibid. "The DOS Manual", ibid.
122. "LISA User's Guide" (Programma International, Inc., Los Angeles, Ca. 1979). "Pie User's Guide", ibid.
123. "MCS6500 Microcomputer Family Hardware Manual" (MOS Technology, Inc. 1976). "MCS Microcomputer User Manual", ibid. "KIM-1 Microcomputer Module User Manual", ibid.

BIOGRAPHICAL SKETCH

Thomas James Buckley was born on January 19, 1955, in Lorain, Ohio, the third of seven children. During his childhood he always was interested in the physical sciences and spent much of his time learning about them. Thanks to his father and neighbors he learned to use his hands as a carpenter, mechanic, and other useful trades. His high school days served him well in learning about chemistry, physics, mathematics, and computer science. He graduated from Lorain High School in June of 1973.

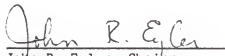
He accepted an appointment to the U.S. Air Force Academy where he was trained in chemistry, mathematics, engineering, and self discipline for two years. In May of 1975, he resigned his appointment "due to changes in career goals."

He entered the Ohio State University where he majored in chemistry and graduated with a degree of Bachelor of Science in June, 1977.

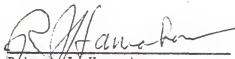
Chilled by the winter of '77, he accepted a teaching assistantship at the University of Florida. Figuring a tan would look better than a pair of snow shoes, he decided he might as well have some fun in the sun while attending graduate school. Later, as he sat writing his dissertation and peeling burnt skin off his body, he contemplated the wisdom of his decision.

After graduation, he accepted a job with the National Bureau of Standards, moved to Washington, D.C., and lived happily ever after.

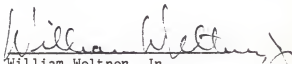
I certify that I have read this study and in my opinion it conforms to acceptable standards of scholarly presentation and is fully adequate, in scope and quality, as a dissertation for the degree of Doctor of Philosophy.


John R. Eyler, Chairman
Associate Professor of
Chemistry


I certify that I have read this study and in my opinion it conforms to acceptable standards of scholarly presentation and is fully adequate, in scope and quality, as a dissertation for the degree of Doctor of Philosophy.


Robert J. Hanrahan
Professor of Chemistry

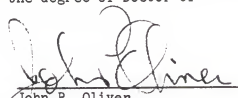
I certify that I have read this study and in my opinion it conforms to acceptable standards of scholarly presentation and is fully adequate, in scope and quality, as a dissertation for the degree of Doctor of Philosophy.


William Weltner, Jr.
Professor of Chemistry

I certify that I have read this study and in my opinion it conforms to acceptable standards of scholarly presentation and is fully adequate, in scope and quality, as a dissertation for the degree of Doctor of Philosophy.


Eric V. Dose
Assistant Professor of
Chemistry

I certify that I have read this study and in my opinion it conforms to acceptable standards of scholarly presentation and is fully adequate, in scope and quality, as a dissertation for the degree of Doctor of Philosophy.



John P. Oliver
Associate Professor of
Astronomy

This dissertation was submitted to the Graduate Faculty of the Department of Chemistry in the college of Liberal Arts and Sciences and to the Graduate Council, and was accepted as partial fulfillment of the requirments for the degree of Doctor of Philosophy.

December 1982

Dean for Graduate Studies
and Research